National Technical University of Athens

School of Naval Architecture and Marine Engineering

Evaluation of the efficiency of a Mewis duct by performance monitoring

Anastasios Zalachoris

Diploma Thesis

Supervisor: Nikolaos Themelis, Assistant Professor

Athens, July 2020

Abstract

The current diploma thesis estimates the efficiency of a Mewis propeller duct utilizing a performance monitoring system. The analysis includes operational data of a three-year period for two sister vessels, Vessel 1 and Vessel 2, with the former being the one that has the duct installed during dry-dock. Once the collected data are processed and corrected, three Key Performance Indicators (KPIs) are calculated to monitor the performance of the vessels for different operational periods, such as pre-dry-dock and post-dry-dock, as well as for different loading conditions (ballast and laden). The KPI analysis aims at evaluating the duct's efficiency through the indicators' fluctuations over time as well as through a comparison between the two vessels' performances. Finally, a multiple linear regression model is developed in order estimate the fuel oil consumption based on weather and sea travel related variables, such as the wind speed, the ship's speed, her draft, trim and rudder angle. The occurring model offers a prediction for the fuel consumption, which is used in different scenarios in order to provide an alternative estimate of performance and, thus, an evaluation of the duct's efficiency.

[This page is intentionally left blanc]

Acknowledgements

I gratefully acknowledge the guidance and support of my supervisor, Assistant Professor Nikolaos Themelis whose dedication, knowledge and advice played a fundamental role in the realization of the current diploma thesis. I would like to sincerely thank him for our excellent cooperation, his patience and his insights.

I would also like to acknowledge the contribution of Prisma Electronics to this thesis. The data provided by the company's LAROS system constituted the foundation of this study.

Last but not least, I own special thanks to my family, my friends and fellow students for their incredible support not only during the realization of this diploma thesis but also throughout my studies. I am especially grateful to my girlfriend and fellow student, Georgina, for working with me, side by side, on the short-term and long-term challenges and helping me to face them.

[This page is intentionally left blanc]

Contents

List of Figures

List of Tables

[This page is intentionally left blanc]

1 Introduction

Ships are complicated energy systems whose operations require the harmonic and effective cooperation of various subsystems. They are able to produce great amounts of "work", whether that is measured in produced kW (power) or tons of cargo (transportation ability), but also consume a lot of energy to achieve that. The shipping industry has been trying for a long time to tip the balance of this "give and take" relationship in favor of the produced work, which represents the financial income when the economics' aspect of the system is brought to the equation.

The term of "efficiency" has been introduced to better describe the aforementioned relationship. Efficiency can be defined as a fraction; its numerator expresses the produced result and its denominator is the total "sacrifices" made for that particular result to be achieved. For example, the efficiency of an engine is its produced work over the total energy consumption while the efficiency of a financial investment is the value of the gains over the value of the invested capital. Consequently, a vessel's propulsive efficiency could be defined as the total travelled distance over the consumed energy or, alternatively, as the effective propulsive power over the overall power consumption. When the propulsive efficiency is examined over time, then another term is introduced; the ship's performance.

The performance of a vessel is an operational parameter that the industry aims to improve. By achieving that, a vessel can reach the same results with less effort or improved results with the same effort. Reducing the amount of consumed fuel needed to reach a certain speed is an example of improved performance. Since performance is an operational parameter, a popular method to increase it is through the installation of various appliances and machinery designed to improve certain operational aspects and activities. One category of these energy-saving appliances involves installations that are positioned at the area of the ship's propeller, aiming to increase its efficiency and, thus, the vessel's overall propulsive performance. Such upgrades include the Kort nozzle, the wake-equalizing duct, the Mewis duct, the Schneekluth wake equalizing duct, the pre-swirl stator, the propeller boss cap fin and other.

Two main problems arise when examining the potential installation of an energy device. The first one is about selecting the most suitable of the available technologies, the one that offers an optimal solution to the problem under consideration. The second one is the evaluation of the benefits of the device and its effect on performance. In the constantly evolving and competitive global shipping market, ship performance is measured by financial units rather than physical ones. As a result, the installation of an energy-saving appliance may be considered redundant despite its positive impact on propulsion, simply because the magnitude of the improvement weights less than the financial investment or the time required. Therefore, the most important question concerning energy-saving devices is not whether it helps but rather how much it does and whether its installation is a profitable investment.

1.1 Mewis duct

Of the aforementioned propeller-related energy-saving devices, the one examined in the particular study is the Mewis duct. The Mewis duct is a hull appendage with an integrated fin system located forward of the propeller, mounted in its inflow region. It is usually used in tankers and high block coefficient ships. It manages to improve the propeller's efficiency due to its three main operation principles [1]:

- Wake field equalization: The duct strengthens and accelerates the hull's wake into the propeller and also produces a net forward thrust.
- Reduction of propeller hub vortex: An improved slipstream behind the duct significantly reduces the hub vortex with corresponding thrust deduction, leading to improved thrust and better inflow to the rudder.
- Contra-rotating swirl: Due individually placed fins a pre-swirl in counter direction is generated, recovering the rotational energy from the slipstream and reducing the rotational flow losses of the propeller.

The Mewis duct provides with a better streamlined and directed flow into the propeller, reducing its losses and therefore improving its efficiency. The power savings offered vary from 3%, for multipurpose vessels, up to 8%, for tankers and bulk carriers, with an average value of 6.5%. However, its true efficiency relies on a variety of factors and is ship-specific.

Additional advantages of the Mewis duct include the low installation time (approximately 4 days), the reduction of cavitation and vibrations as well as that it requires no service

Figure 1: The Mewis duct.

1.2 Purpose and study structure

The Mewis duct was introduced in the market in 2010 as a propulsive, energy-saving device promising energy savings of up to 8%. However, its potential is subject to various factors that constitute the ship's hydrodynamic profile and, therefore, each vessel should perform individual hydrodynamic analysis and/or model tests before installing the Mewis duct in order to evaluate its actual efficiency. The purpose of this study is to suggest an alternative method of evaluating the duct's efficiency. Performance monitoring involves measuring various physical quantities that affect a vessel's performance by onboard sensors with pre-arranged frequency and for a defined amount of time. As a result, a database that characterizes the vessel and its operation under different scenarios and conditions is created. The real-time data describe the vessel's behavior under various circumstances and can, thus, be used to evaluate the effect of these circumstances or events on the vessel's performance. As suggested by *Hasselaar (2010)* [2], performance monitoring offers multiple benefits as it facilitates the assessment of the hull and engine condition, it evaluates the ship's design by comparing the true operational parameters with the designed ones and it optimizes the sailing performance as the true, optimal and ship-specific operation point can be found. The current study utilizes vessel data gathered before and after the installation of a Mewis duct in order to assess its actual, real-operation impact on the propulsive performance. Furthermore, a sister vessel that did not had a duct installed is also monitored for the same period, in order to provide with a solid comparison that underlines the long-term effect of the Mewis duct.

An overview of the proposed procedure for the evaluation of the Mewis duct efficiency is presented in Figure 2. Firstly, real-time operational data are collected, by a variety of sensors and measuring devices, and corrected by sets of filters. The data processing procedure, described in the Data analysis chapter, is fundamental for the study as it eliminates outliers that distort the relationships among the physical quantities, eventually creating the final dataset that is the basis of the performance analysis. Once the operational data are filtered, Key Performance Indicators are calculated to quantify the vessels' performance. The study of the KPIs, conducted in the Key performance indicators chapter, is crucial as it reveals the effect of the Mewis duct on performance. Finally, a regression model is produced in the Regression analysis chapter to fit the available operational data and provide with predictions about the fuel oil consumption (FOC) for different operational scenarios. The regression analysis is a different approach for evaluating the duct's efficiency, utilizing the FOC performance-related variable.

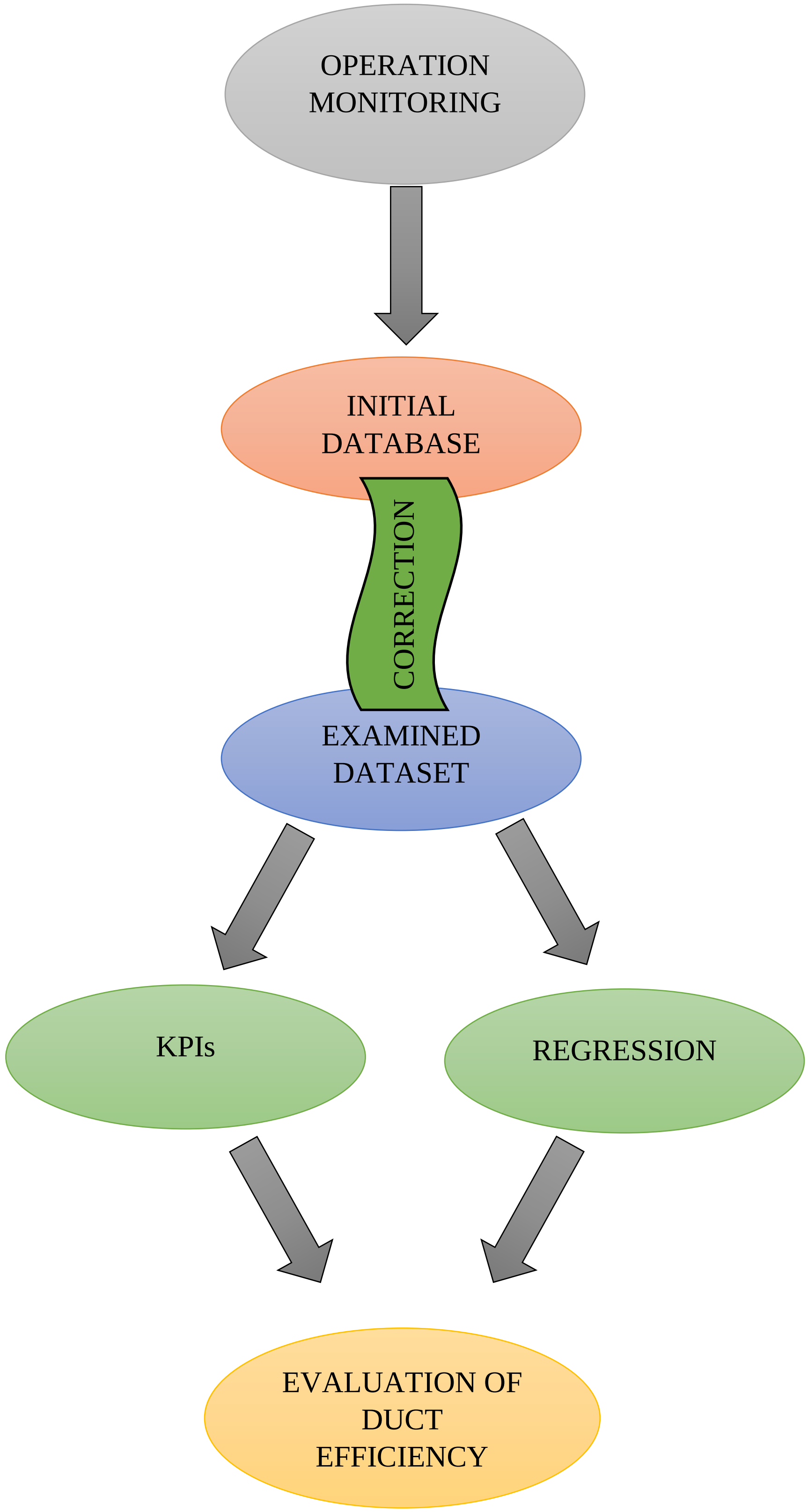

Figure 2: Study structure scheme.

2 Data analysis

The monitored physical quantities, which constitute the variables of the problem under study, are presented along with the onboard devices that are responsible for their measuring. The acquired data are shortly analyzed with the help of some parameter vs parameter scatter plots that visualize the expected relationships among the physical quantities. The initial data analysis includes the identification of these relationships.

As it can be observed, the measured data are not entirely aligned with the relationships among the physical quantities that occur from the general scientific understanding. For the analysis to be more accurate and solid, the initial data, once plotted and accessed, need to be properly processed in order to cause a reduction in bias. By omitting values that are not in accordance with the scientific theory a reliable dataset can be created and used as the basis of the regression model whose aim is to provide a realistic approximation of the real-life situations occurring in sea travel.

The data correction can be achieved by the application of certain filters that accurately identify and reject the “undesirable” parameter values. Due to the analysis being time-bound, it should be noted that in case a single parameter value is considered “undesirable” then all the other parameter values measured at the same moment will be automatically omitted. Despite disregarding possibly “desirable” values, the proposed method allows for an examination of the parameters through time without causing a significant distortion of the dataset mainly because of its big size (over 100,000 points for each vessel).

The first part of the filtering process aims to create a general framework of the analysis by setting threshold values for some parameters. All measurements below the threshold values are discarded, thus reducing the dataset. By these simple preliminary filters, values with no physical meaning, such as negative ship speeds or negative fuel consumptions, are excluded from the new dataset. Furthermore, data, such as low water speeds or low engine power, considered to be measured during port procedures and cargo handling are effectively omitted through this procedure. The data points associated with port operations cannot accurately represent the relationships among the physical quantities, and thus create outlier regions in the graphs. By excluding the lower speed and engine-related values the “in port” data are not taken into consideration in the new dataset, limiting the amount of distortion.

The second part of the filtering process aims to further reduce the dataset by identifying and omitting outlying data points. To achieve that, the relationships among the physical quantities are utilized. Firstly, the correlations among the variables are calculated, resulting in a better understanding of the level of co-dependency among them. Afterwards, highly correlated variables are paired and filtered through a process that omits values of one parameter, called “primary”, based on the outliers of the other, called “secondary”. The process, which is explained analytically in the respective chapter, effectively pairs highly correlated parameters and manages to significantly reduce the outlying data points, creating a final filtered dataset that sets the standards for an accurate regression analysis.

2.1 Data collection

Measured parameters

The evaluation of the efficiency of the Mewis duct relies on the operational data of the two sister vessels provided by the LAROS platform. The collected data concern an operational period of three years, beginning in June 2014 and ending in June 2017. The measuring period covers both the pre-duct and the after-duct periods, allowing the conduction a comparative analysis between the two periods as well as between the two sister vessels.

The physical quantities monitored by the LAROS platform are presented in Table 1.

Measured physical quantity	Parameter name	Units
Speed over ground	SOG	knots (kn)
Speed through water	STW	knots (kn)
Main engine power	EP	kilowatts (kW)
Mean draft	TM	meters (m)
Shaft's revolutions	RPM	revolutions per minute (rpm)
Wind speed	WS	meters per second (m/s)
Main engine's fuel oil consumption	FOC	tons/day
Aft draft	TA	meters (m)
Fore draft	TF	meters (m)
Rudder angle	RA	degrees (deg)

Table 1: Monitoring parameters.

FOC values should not be mistakenly considered to represent the overall fuel consumption for one operational day. Instead, as the rest of the parameters, FOC is measured every 15 minutes in *tons per day* units.

The trim of the vessel is also calculated: $\mathrm{TRIM} = \mathrm{TA} - \mathrm{TF}$.

The measured data are to serve as the basis of the KPI analysis that will help in the estimation of the duct's efficiency as well as of the regression model that will be developed to estimate the fuel oil consumption. For that to be achieved, the initial data need to be filtered for outliers, data points that do not correspond with the relationships among the physical quantities or that do not have a physical meaning (i.e. negative speed values). In order to visualize the outlier data points the following graphs are plotted for the initial data points: SOG – STW, EP – STW, EP – RPM, EP – FOC, FOC – RPM, TM – TRIM. The graphs and the occurring outlier data are discussed in the Initial data analysis chapter.

2.1.1 Measuring devices

The measuring devices that are required onboard for the monitoring of the above parameters are summarized in Table 2.

Device	Parameter
Global Positioning System (GPS)	SOG
Speed log	STW
Shaft torque meter	EP, RPM
Mass flow meter	FOC
Anemometer	WS
Pressure sensor	TM, TA, TF
Rudder angle indicator	RA

Table 2: Onboard measuring devices.

Global Positioning System (GPS)

The GPS retrieves information about the ship's position in global coordinates (longitude, latitude). The vessel's speed over ground (SOG) is obtained from the arithmetical derivation of the vessel's position. The GPS's operation requires constant communication with a system of satellites, for the location of the ship's position, and has an accuracy of a few meters.

Speed logs

Two popular sensors are utilized for the measurement of the vessel's speed through water.

a) Doppler log: An acoustic speed log based on the Doppler effect in which the wave lengths of moving objects appear to shift in relation to the observer. This shift can be converted to speed, thereby producing a very accurate result. The Dual Axis Doppler Speed Log utilizes the Doppler shifted returns from high frequency acoustic energy transmitted into water to provide precise speed data, distance travelled, and water depth below the transducer. The transmitted signal is scattered back from the sea bottom and/or scatters in the water mass. The system amplifies the received signals and processes them to determine the Doppler shift.

b) Electromagnetic log: The electromagnetic log works by generating a small alternating current in a transducer producing an electromagnetic field in the adjacent water. As the vessel moves through the water, the voltage proportional to the speed is generated at 90 degrees to the direction of travel. This signal voltage is detected by the probes and transmitted to the master electronic unit where it is amplified and processed digitally before being passed to the speed and distance displays.

Shaft torque meter

The shaft torque meter is a piece of equipment the measures the torque and the rotational speed of the shaft, and multiplies them to estimate the transmitted power's value. The instrument consists of strain gauges, arranged on a ring and mounted directly on the shaft for the continuous monitoring and logging the aforementioned values. The basic principal of operation is that any deformations of the strain gauges are transferred into voltages deviations which determine the strain of the shaft.

Mass flow meter

The most reliable way to measure the fuel consumption in a ship is to use mass flow meters, also known as Coriolis mass flow meters, because they eliminate the need for converting the volumetric flow into a mass flow, according to the fuel's density estimations. The reason is that the Coriolis acceleration induces oscillations to the tubes of the device that depend on the mass flow in them. As a result, the magnitude and the frequency of these oscillations help determine the fuel mass flow through the tubes.

Anemometer

The wind anemometer is a device that measures both, the relative speed and direction of the wind with respect to the ship's orientation. It consists of a helicoid propeller and a vane the measure the wind's speed and direction, respectively. The angular displacement of the vane helps estimate the wind's relative direction, while the rotational speed of the helicoid propeller helps estimate the wind speed.

Pressure sensor

The draft of the ship can be estimated by the hydrostatic pressure on the hulls bottom surface. Sensors that measure the pressure are placed on the outer surface of hull's bottom and can deduce the instantaneous draft of the hull at the position in which they are installed. From the measurement of the draft in two different longitudinal positions of the hull, the ship's trim can be calculated.

Rudder angle indicator

The rudder angle indicator is an electrical device that measures the actual angle of the rudder. It consists of the two parts, the transmitter which is mounted on the steering system of the ship (steering gear room) and the receiver which is placed in the wheelhouse and displays the transmitter's signal. The measuring accuracy is usually below the range of $\pm 0.5°$ for common angles and $\pm 1.5°$ for hard over rudder.

2.1.2 Initial data analysis

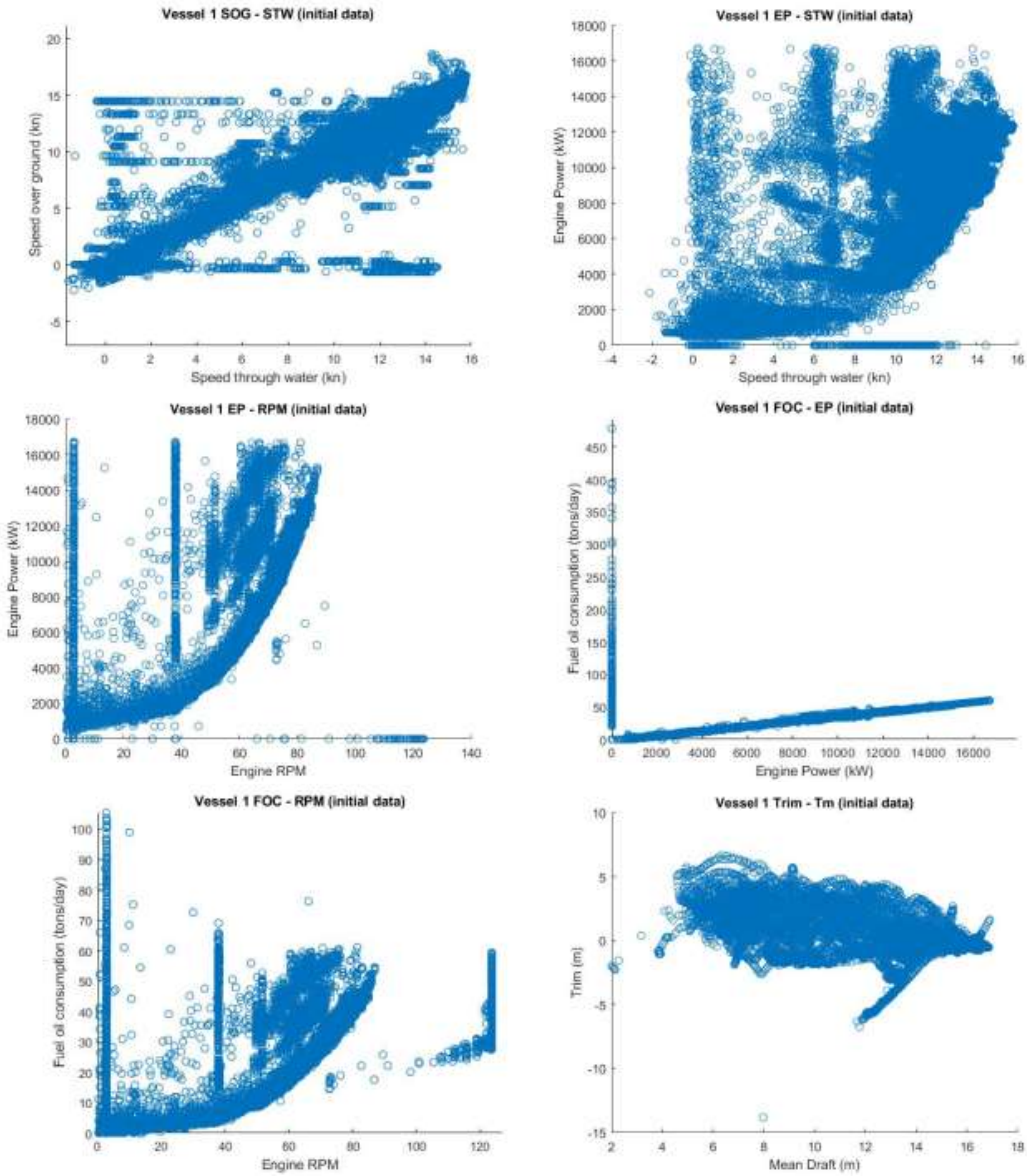

Figure 3: Initial data – scatter plots (Vessel 1).

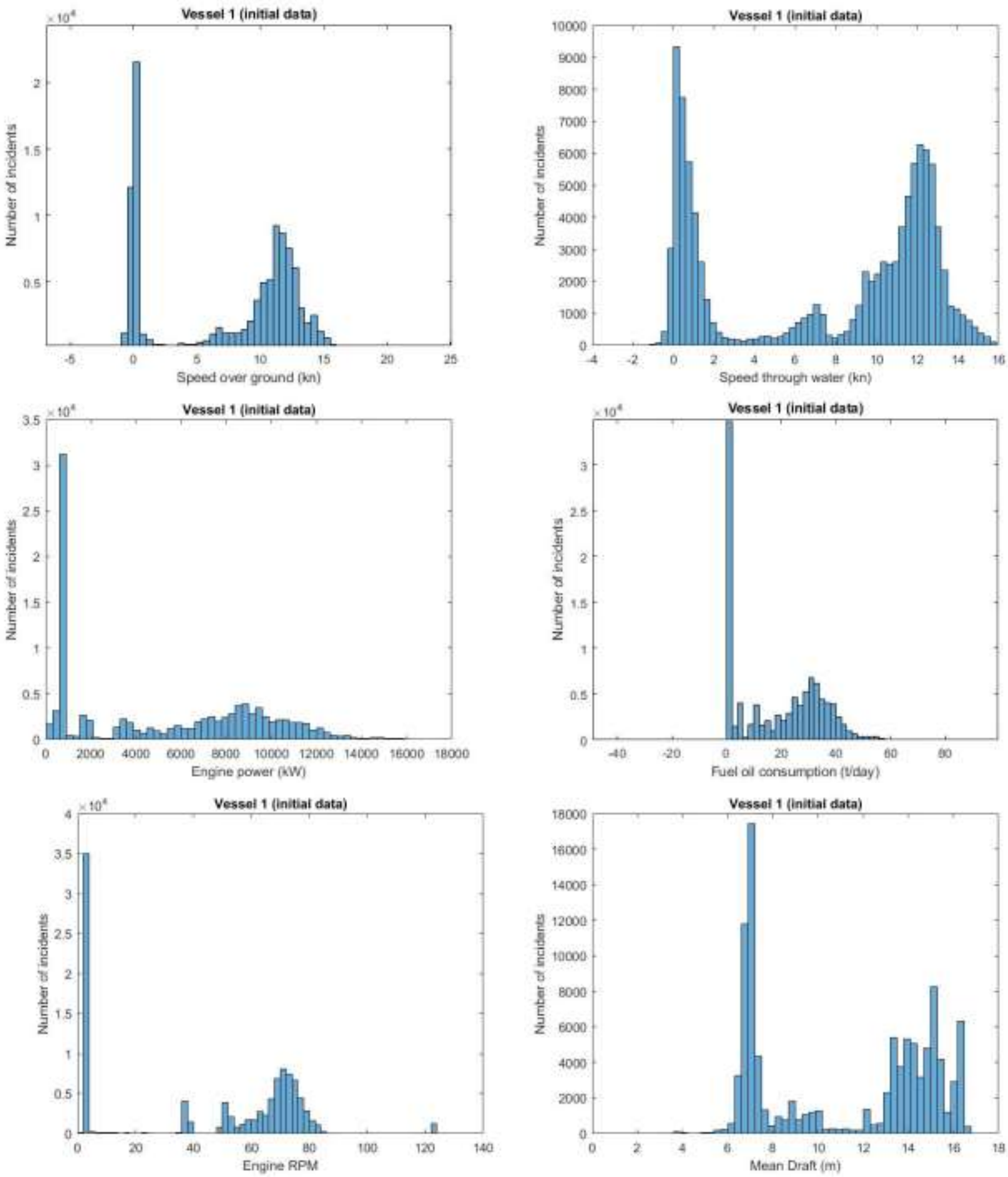

Figure 4: Initial data – histograms (Vessel 1).

As it can be observed above, the SOG – STW graph depicts the linear relationship between the two speed variables (over ground and through water). However, there are points that deviate from the main diagonal of the graph, forming the following outlier regions:

- $\mathrm{SOG} \approx 0$ & $\mathrm{STW} > 2$
- $5 < \mathrm{SOG} < 10$ & $11 < \mathrm{STW} < 14$
- $10 < \mathrm{SOG} < 15$ & $8 < \mathrm{STW} < 10$
- $\mathrm{SOG} > 2$ & $\mathrm{STW} < 2$
- $\mathrm{SOG} > 5$ & $2 < \mathrm{STW} < 4$
- $\mathrm{SOG} < 0$ (speed cannot be negative)
- $\mathrm{STW} < 0$ (speed cannot be negative)

The EP – STW is a curve that expresses the power-speed relationship. However, the two vertical regions of data points ("columns") for $0 < \mathrm{STW} < 2$ and $4 < \mathrm{STW} < 8$ should be considered outlier areas as they obviously do not correspond with the expected curve. Moreover, data points of negative speed through water values and/or negative engine power values are also outlier as they do not have any physical meaning. Finally, the horizontal line associated with very low engine speed values ($\mathrm{EP} \approx 0$) clearly deviates from the main plot area and must therefore be omitted.

The EP – RPM and FOC – RPM graphs are very similar, a fact that is verified by the strongly linear relationship developed between the fuel oil consumption and the engine power (FOC – EP graph). The EP/FOC variables are connected with the shaft's revolutions (RPM) through a relationship that expresses the propeller law: $\mathrm{P} = \mathrm{c} \cdot \mathrm{n}^{\mathrm{a}}, 3 \leq \mathrm{a} \leq 4$. The graphs reveal the presence of three $\mathrm{P} = \mathrm{c} \cdot \mathrm{n}^{\mathrm{a}}$ curves, each associated with different propulsion conditions (weather conditions and level of hull fouling). The upward displacement of a propeller curve expresses the increased resistance of the vessel due to severer weather conditions and/or increased hull fouling. As it can be understood, these curves contain valuable information of the vessel's performance and shall not be eliminated during the data correction process. On the other hand, the vertical "columns" of data at $\mathrm{RPM} \approx 0$, $\mathrm{RPM} \approx 40$ and $\mathrm{RPM} \approx 50$, as well as the horizontal line for $\mathrm{EP} \approx 0$ (only for the EP – RPM graph) and the area of $\mathrm{RPM} > 100$ (only for the FOC – RPM graph) are all considered outlier regions and their omission is vital.

The FOC – EP graph, as mentioned above, successfully expresses the linear relationship between the two variables. The only outlier region defined is the vertical line for $\mathrm{EP} \approx 0$.

Finally, the Trim – Mean draft graph has the form of a large "cloud" of data points, which is defined within the following limits: $4 < \mathrm{T_m} < 17$ and $-5 < \mathrm{Trim} < 5$. The data correction process should effectively split the "cloud" into two smaller ones, each related with one of the two general loading conditions: Ballast – lower Tm values and Laden – greater Tm values. The middle area of the draft is, thus, considered an outlier region and has probably occurred by the constant changes of draft during the in-port operations of the vessel (loading and un-loading).

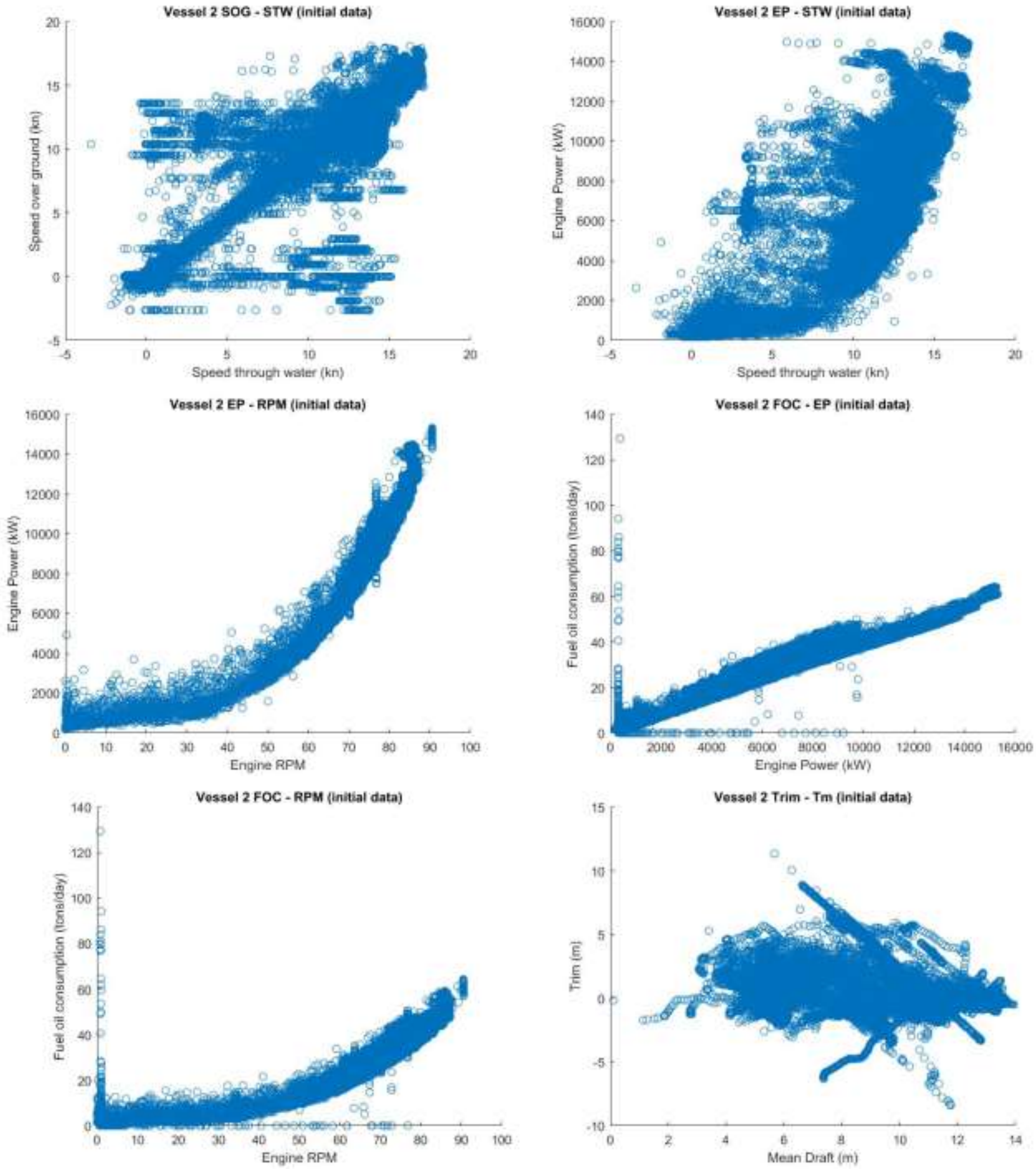

Figure 5: Initial data – scatter plots (Vessel 2).

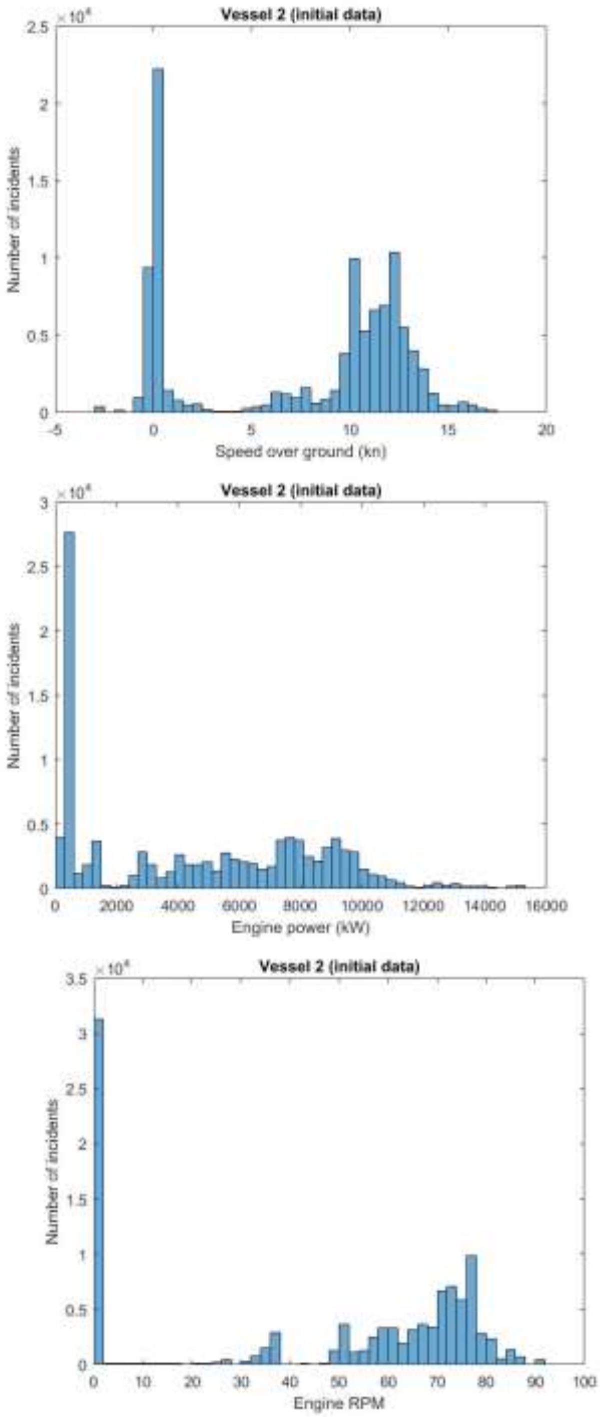

Figure 6: Initial data – histograms (Vessel 2).

As it can be observed above, the SOG – STW graph depicts the linear relationship between the two speed variables (over ground and through water). However, there are points that deviate from the main diagonal of the graph, forming the following outlier regions:

- $0 < SOG < 5$ & $STW > 2$
- $SOG > 10$ & $STW < 6$
- $SOG < 0$ (speed cannot be negative)
- $STW < 0$ (speed cannot be negative)

The EP – STW graph depicts a curve that expresses the power-speed relationship and has no significant outlier regions.

The EP – RPM and FOC – RPM graphs are very similar, a fact that is verified by the strongly linear relationship developed between the fuel oil consumption and the engine power (FOC – EP graph). The EP/FOC variables are connected with the shaft's revolutions (RPM) through a relationship that expresses the propeller law: $P = c \cdot n^a$,$3 \leq a \leq 4$. The two graphs contain few outlier data points, mostly for very low rpm values (RPM ≈ 0).

The FOC – EP graph, as mentioned above, successfully expresses the linear relationship between the two variables. The only outlier regions defined are the vertical line for EP ≈ 0 and the horizontal line for FOC ≈ 0.

Finally, the Trim – Mean draft graph has the form of a large "cloud" of data points, which is defined within the following limits: $2 < T_m < 14$ and $-10 < \text{Trim} < 10$. The data correction process should effectively split the "cloud" into two smaller ones, each related with one of the two general loading conditions: Ballast – lower Tm values and Laden – greater Tm values. The middle area of the draft is, thus, considered an outlier region and has probably occurred by the constant changes of draft during the in-port operations of the vessel (loading and un-loading).

2.2 Data correction – Part I: Threshold values

The chapter's aim is to process the initial data obtained by the LAROS platform by applying some filters according to the student's understanding of the dataset and the relationships which exist among the examined parameters. In order to allow a comparison between the two vessels in terms of performance, the exact same set of filters is applied to both of their datasets. Through this filtering process, an important step towards a smoother, corrected dataset is made as the student defines the framework of the problem under consideration. As a result, the occurring dataset expresses the relationships among the physical quantities as well as the overall nature of the problem in a more reliable and realistic manner.

2.2.1 Speed correction

Speed is one of the main parameters under examination as it is highly correlated with most of the physical quantities of the dataset. As described at the previous chapter, speed is measured through the SOG (speed over ground) and STW (speed through water) variables which should both receive non-negative values as the sensors calculate the speed's absolute values, not its vectors. Moreover, low water speeds are considered to occur at ports where the vessels may spend time waiting for berths to become available, for pilots to lead them in the port or for maneuvering. As a consequence, STW values of less than 3 knots are omitted from the dataset in order to reduce the "in port" outliers. To sum up, the following two filter were applied to the speed parameters:

i. $\text{SOG} \geq 0$ knots
ii. $\text{STW} \geq 3$ knots

2.2.2 Power correction

Engine power (EP) along with the fuel consumption (FOC) and the shaft's revolutions (RPM) are the engine-related parameters of the study. The three parameters demonstrate high correlation which is in terms with the general understanding of the co-dependency of these physical values. As explained above, the data measured during port operations should not be included in the final dataset of the analysis as bias will be caused. To achieve that, the following filters were applied to the mentioned parameters:

i. $\text{EP} \geq 1000$ kW
ii. $\text{FOC} \geq 3$ tons/day
iii. $\text{RPM} \geq 20$

2.2.3 Filters application and occurring graphs

By applying the filters analyzed in the previous page the dataset is partially corrected since outlying (e.g. port-related) or simply miscalculated data (e.g. negative values of speed) are omitted. The resulting improvement can be observed with the help of the following scatter plots. The black colored data points are the initial data points that are rejected by the set of threshold filters while the yellow ones fulfil the initial criteria.

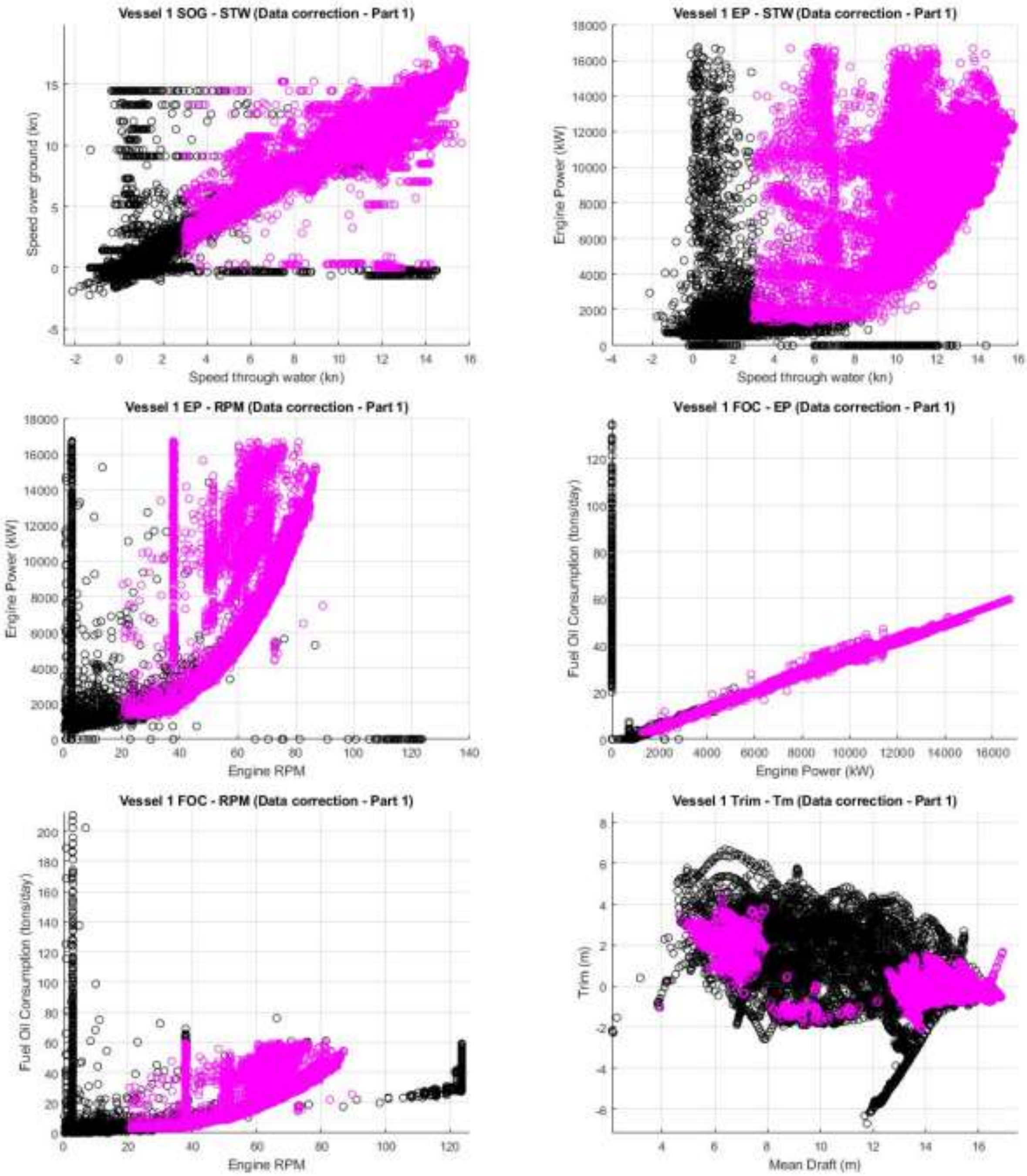

Figure 7: Scatter plots for Vessel 1 (Data correction – Part 1)

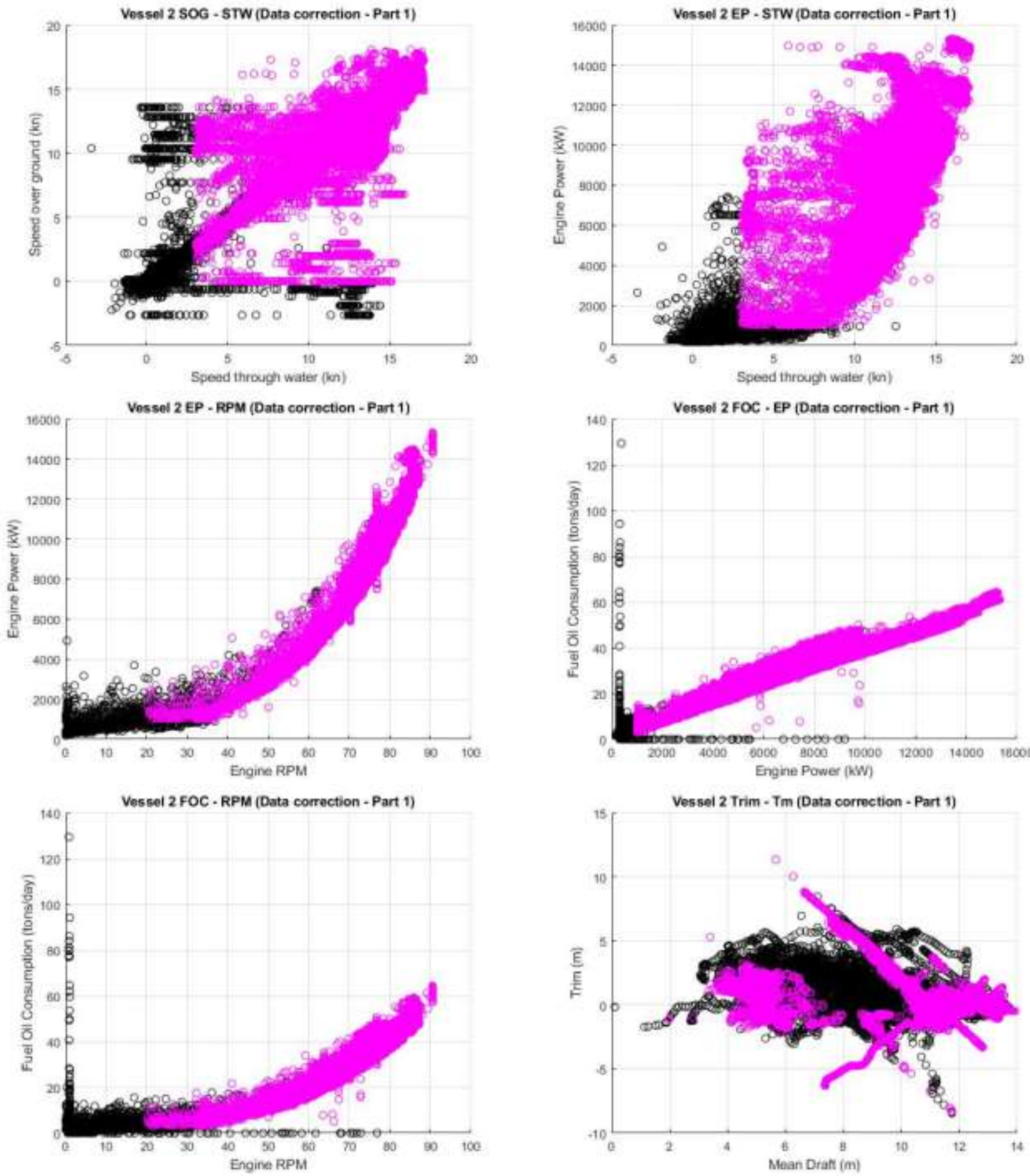

Figure 8: Scatter plots for Vessel 2 (Data correction – Part 1)

2.2.4 Graph analysis: Comparison with the initial plots

The first part of the data correction process manages to improve the dataset by omitting a significant number of outliers. However, it can be observed that further filters need to be applied for the dataset to better express the relationships among the physical quantities.

The SOG – STW linear relationship is depicted by the main diagonal line shown in the respective graphs. The threshold filter successfully eliminates some sets of horizontal outlier lines that deviate from the main diagonal. However, this elimination is limited to lower values of the two speeds and as a result the rejected points are located at the upper left and lower right areas of the plots. Further filtering shall allow the complete omission of the outlier data points which are located in following main regions:

$$\text{Vessel 1:} \begin{cases} \text{SOG} \approx 0 \text{ and STW} > 4 \\ 5 < \text{SOG} < 9 \text{ and } 11 < \text{STW} < 14 \\ \text{SOG} > 10 \text{ and } 8 < \text{STW} < 10 \end{cases}$$

$$\text{Vessel 2:} \begin{cases} 10 < \text{SOG and } 3 < \text{STW} < 6 \\ 0 < \text{SOG} < 5 \text{ and } 5 < \text{STW} \end{cases}$$

The EP – STW diagram is affected less by the preliminary filtering. The impact is greater on Vessel 1 as the left vertical column of outliers is eliminated due to omission of low water speeds. In addition, the horizontal line corresponding to near-zero engine power is rejected due to the threshold value applied on the EP parameter. However, the central column of outliers consists a region that requires further filtering to be omitted. As far as Vessel 2 is concerned, no significant improvement is noticed as the horizontal lines deviating from the power-speed curves to the left remain intact.

The EP – RPM relationship is presented by a curve that can be defined by an expression of the propeller law. While the curve presents no significant outlier regions for the dataset of Vessel 2, the case is different for Vessel 1. The graph clearly depicts three curves that express different power-revolutions relationships (different hull fouling, different weather conditions etc.) and three vertical lines that are interpreted as outlier regions. The implementation of the initial filter manages to eliminate the far-left line which is associated with near-zero RPM values. This is achieved due to the threshold value set for the shaft's revolutions. While an important improvement is made, the complete correction of the dataset requires the elimination of the remaining two vertical outlier lines ($\text{RPM} \approx 40$ & $\text{RPM} \approx 50$).

The fuel consumption is expected to be linearly connected with the engine's power, a relationship that is clearly depicted in the above graphs. The main outlier regions concern vertical lines at near-zero power values (for Vessel 1 and Vessel 2) and a horizontal line for near-zero fuel consumption values (for Vessel 2 only). Through the application of the threshold filters the outlier areas are successfully eliminated providing a graph that requires no further correction.

Similar to the EP – RPM graph, the FOC – RPM graph of Vessel 1 depicts three curves that are expressions of the propeller law for different weather conditions and hull fouling. Once again, the outliers are shown as vertical lines (RPM ≈ 0, RPM ≈ 40 & RPM ≈ 50) as well as a region locates at the far-right side of the graph (RPM > 100). The latter area along with the RPM ≈ 0 line is eliminated by the initial filters. However, the remaining two vertical lines are not identified as outliers and need to rejected by the next filtering procedure. As far as Vessel 2 is concerned, the FOC – RPM graph presents just a single outlier region at RPM ≈ 0 which is successfully eliminated.

The Trim – Mean Draft graph is expected to have data points concentrated in two main “clouds”, each representing a different loading condition (laden or ballast). The implementation of the filters on Vessel 1 leads to a dataset which is significantly closer to that expectation as in-port and maneuvering conditions, in which the draft is altered constantly, are neglected. As a result, two main clouds are formed ($5 < \mathrm{Tm} < 8$ & $12 < \mathrm{Tm} < 17$) along with a central outlier region that remains intact and shall be omitted during the next filtering process. The filters’ impact is weaker on Vessel 2 as there are two significant diagonal lines that deviate from the laden (right) cloud of drafts. Despite this fact, the formation of the two clouds is clearly depicted and the elimination of outliers is significant.

2.3 Data correction – Part II: Outlier detection

The chapter's aim is to further process the data obtained by the filtering process of the previous part by exploiting the relationships that characterize the physical quantities. As a first step, the correlations among the variables are estimated and used as a measure of their co-dependency. Through the filtering process described, some possible filters are evaluated based on their effect on the dataset, which is depicted by scatter plots. Finally, once each filter's efficiency is assessed, an optimal combination of filters is chosen and applied to the data points, thus providing the final filtered dataset to be used as the basis of the regression analysis.

2.3.1 Correlation calculation: Pearson coefficients

The correlation among the examined parameters, obtained from the first filtering process, is calculated with the help of Pearson correlation coefficients. Given two parameters x, y the Pearson correlation coefficient (PCC) of the pair (x,y) is calculated by the following formula:

$$PCC_{xy} = \frac{\sum_{i=1}^{n}(x_i - \bar{x}) \cdot (y_i - \bar{y})}{\sqrt{\sum_{i=1}^{n}(x_i - \bar{x})^2} \cdot \sqrt{\sum_{i=1}^{n}(y_i - \bar{y})^2}}$$

- x_i : the data points of parameter x.
- $\bar{x}$: the mean value of the x dataset.
- y_i : the data points of parameter y.
- $\bar{y}$: the mean value of the y dataset.
- n : the total number of datapoints.

The calculated coefficients are gathered and presented in Table 3 and Table 4.

	SOG	**STW**	**TM**	**RPM**	**WS**	**FOC**	**TA**	**TF**	**RA**	**EP**
SOG	1									
STW	0.832	1								
TM	0.137	0.277	1							
RPM	0.702	0.885	0.501	1						
WS	-0.041	0.049	0.309	0.346	1					
FOC	0.467	0.617	0.445	0.788	0.364	1				
TA	0.137	0.277	0.998	0.507	0.313	0.444	1			
TF	0.138	0.277	0.998	0.494	0.304	0.444	0.992	1		
RA	0.045	-0.006	-0.165	-0.076	-0.119	-0.037	-0.170	-0.161	1	
EP	0.466	0.616	0.437	0.787	0.366	0.999	0.436	0.436	-0.032	1

Table 3: Pearson correlation coefficients (Vessel 1).

	SOG	STW	TM	RPM	WS	FOC	TA	TF	RA	EP
SOG	1									
STW	0.460	1								
TM	0.055	0.261	1							
RPM	0.432	0.814	0.533	1						
WS	-0.236	-0.210	-0.101	-0.175	1					
FOC	0.396	0.732	0.518	0.954	-0.118	1				
TA	0.062	0.269	0.992	0.543	-0.108	0.527	1			
TF	0.049	0.250	0.993	0.515	-0.093	0.503	0.971	1		
RA	-0.012	-0.048	-0.164	-0.077	0.106	-0.096	-0.166	-0.159	1	
EP	0.400	0.742	0.525	0.960	-0.125	0.985	0.535	0.509	-0.077	1

Table 4: Pearson correlation coefficients (Vessel 2).

Not correlated — Slightly correlated — Highly correlated — Totally correlated

The Pearson coefficients have values between +1 and -1, where:

- +1 indicates a total positive linear correlation.
- -1 indicates a total negative linear correlation.
- 0 indicates no linear correlation.

The blue colored cells represent Pearson coefficients with small absolute values, indicating that the respective parameters are not correlated. On the other hand, the green cells concern highly correlated quantities with greater absolute Pearson coefficients. The orange cells contain intermediate values, which indicate a slight correlation between the physical quantities. Finally, the matrices' diagonals have a "+1" Pearson value since the correlation between a value and its self is obviously a total positive linear one.

The highly correlated values (green cells) help in identifying some possible pairs of values for the second filtering process. Although, it should be noted that high correlation is not an absolute criterion. Each pair of highly correlated values should be tested in order to safely determine whether it effectively eliminates the outlier regions of the graphs without omitting "desirable" set of data. Not correlated pairs of variables (coefficients' values close to 0) are not tested.

After careful consideration, the following pairs are chosen for evaluation:

- Speed through water (STW) ↔ Speed over ground (SOG)
- Speed through water (STW) ↔ Engine power (EP)
- Engine power (EP) ↔ Shaft's revolutions (RPM)
- Engine power (EP) ↔ Fuel oil consumption (FOC)
- Shaft's revolutions (RPM) ↔ Fuel oil consumption (FOC)
- Mean draft (TM) ↔ Trim (TF-TA)

2.3.2 Filtering procedure

The following filtering procedure is utilized for the detection and rejection of outlying data points [3]:

1. Choose a primary parameter X whose values are to be filtered.
2. Divide the parameter values into groups with range v.
3. Choose a secondary parameter Y which is correlated with the primary parameter.
4. For each group $\mathrm{G_i}$ of X calculate the mean, $\mathrm{m_{Y_i}}$, and the standard deviation, $\sigma_{\mathrm{Y_i}}$, of the respective Y values.
5. Define an "outlier threshold" k which is to be multiplied with the standard deviation σ_{Y_i}.
6. For every respective value of Y in the $\mathrm{G_i}$ group, $\mathrm{Y_{ij}}$, test if the following inequality is fulfilled:
$$\left|\mathrm{Y_{ij}} - \mathrm{m_{Y_i}}\right| \leq \mathrm{k} \cdot \sigma_{\mathrm{Y_i}}$$
7. If the inequality is not fulfilled the data point is rejected.

An example is given in order to provide a better understanding of the above method. Let the primary parameter X be the engine power (EP) and the secondary parameter Y be the shaft's revolutions (RPM). The following hypothetical dataset is examined:

	1	**2**	**3**	**4**	**5**	**6**	**7**	**8**	**9**	**10**
EP (kW)	2000	2150	2300	2730	2870	3020	3350	3680	3800	3990
RPM	51.15	52.40	53.59	56.74	65.00	58.68	60.75	62.68	50.00	64.39

Table 5: Values of the hypothetical dataset.

By plotting the EP-RPM curve two outliers are spotted: (65,2870) and (55,3800).

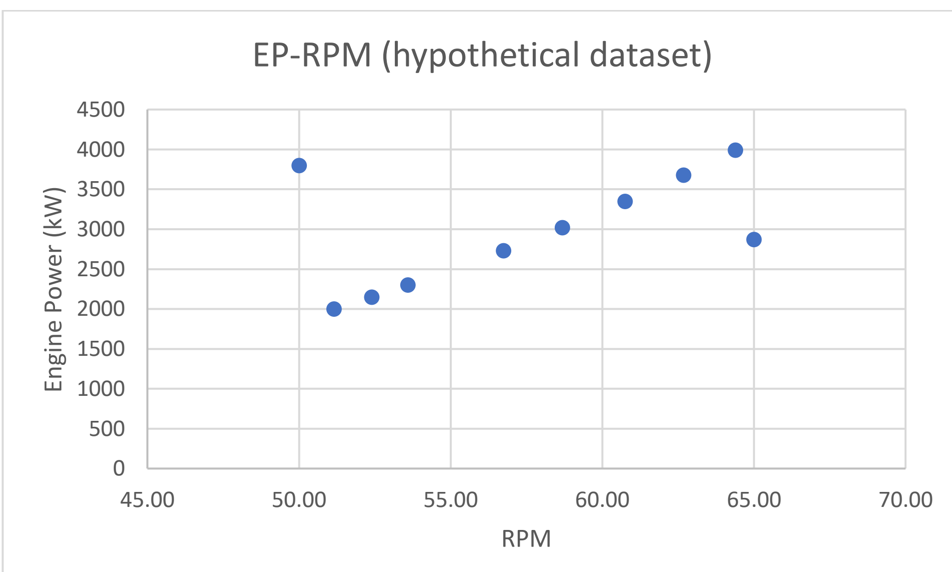

Figure 9: EP – RPM curve (hypothetical dataset).

A range v of 1000 kW is chosen so that the power values are divided into the following groups: $[2000,3000), [3000,4000)$. For each group of power values, a group of the respective RPM values is created:

- For the $[2000,3000)$ group → Y_1:$\{51.15, 52.40, 53.59, 56.74, 65\}$.
- For the $[3000,4000)$ group → Y_2:$\{58.68, 60.75, 62.68, 50, 64.39\}$.

The mean values and the standard deviations of Y_1 and Y_2 are calculated:

- $m_{Y_1} = 55.78$
- $\sigma_{Y_1} = 5.56$
- $m_{Y_2} = 59.30$
- $\sigma_{Y_2} = 5.62$

	1	2	3	4	5	6	7	8	9	10
RPM	51.15	52.40	53.59	56.74	65.00	58.68	60.75	62.68	55.00	64.39
$\mathbf{m_{Y_i}}$	55.78					59.30				
$\boldsymbol{\sigma_{Y_i}}$	5.56					5.62				
$\lvert \mathbf{Y_{ij} - m_{Y_i}} \rvert$	4.63	3.38	2.19	0.97	9.22	0.62	1.45	3.38	9.30	5.09
$\frac{\lvert \mathbf{Y_{ij} - m_{Y_i}} \rvert}{\boldsymbol{\sigma_{Y_i}}}$	0.83	0.61	0.39	0.17	1.66	0.11	0.26	0.60	1.66	0.91

Table 6: Outlier detection (hypothetical dataset).

As it can be noticed, in the particular dataset, the “desirable” points are within 1 standard deviation from the mean values. By picking a suitable value for the constant k, the outliers are omitted. The 5th and 8th data points do not fulfill the inequality $\lvert Y_{ij} - m_{Y_i} \rvert \leq k \cdot \sigma_{Y_i}$ for k values less than 1.66, and as a result a $1 \leq k \leq 1.5$ value can successfully filter these “undesirable” data points.

However, for the real examined dataset, k receives greater values ($2 \leq k \leq 3$) since there can be multiple curves representing the relationships between two values, whose data points would be falsely discarded if a low k value were applied. For example, the EP-RPM graph can have different $P = c \cdot n^a$ curves, each representing a different weather condition and/or hull fouling condition. These points-curves, despite deviating from the main EP-RPM curve, should not be omitted since they contain valuable information that provides a solid understanding of the effect of certain phenomena, such as the hull fouling, on the vessels’ performance.

The described process is applied for the 6 pairs of values that are chosen in the previous paragraph according to the correlation coefficients. For each pair, the process is applied twice by swapping the primary and secondary variables. Each of the total 12 single-filter processes is analyzed in the following paragraphs, as to the way they affect the relationships among the physical quantities, which are depicted by graphs. Once the impact of each filter is assessed, the optimal combination of filters can be found.

2.3.2.1 Speed through water – Speed over ground

The STW and SOG variables are filtered according to the process described in the "Filtering procedure" paragraph. The outlier threshold k and the range v values are shown in Table 7:

Case	Primary: STW	Primary: SOG
	Secondary: SOG	Secondary: STW
k	2	2
v	0.5 kn	0.5 kn

Table 7: Outlier threshold and range values (STW-SOG).

Both cases are analyzed with the help of graphs for both vessels. For the case in which STW is the primary parameter, the respective filter is called "*STW_SOG*" while for the one in which SOG is the primary parameter, the filter is called "*SOG_STW*". The occurring scatter plots contain data points colored in blue, red or green. The blue points are the ones that are omitted by the threshold filters that are applied during the first part of data correction. The red points are the ones that fulfill the criteria set by the first filtering procedure but are omitted due to the applied single-filter under consideration (STW_SOG, SOG_STW). Finally, the green data points are the ones that meet the standards set by the threshold filters and the applied single filter. Presented below are the graphs that are significantly affected by the application of the filter. The effect of the filter on all graphs can be found in the figures included in Appendix A: Data correction – Part II filters.

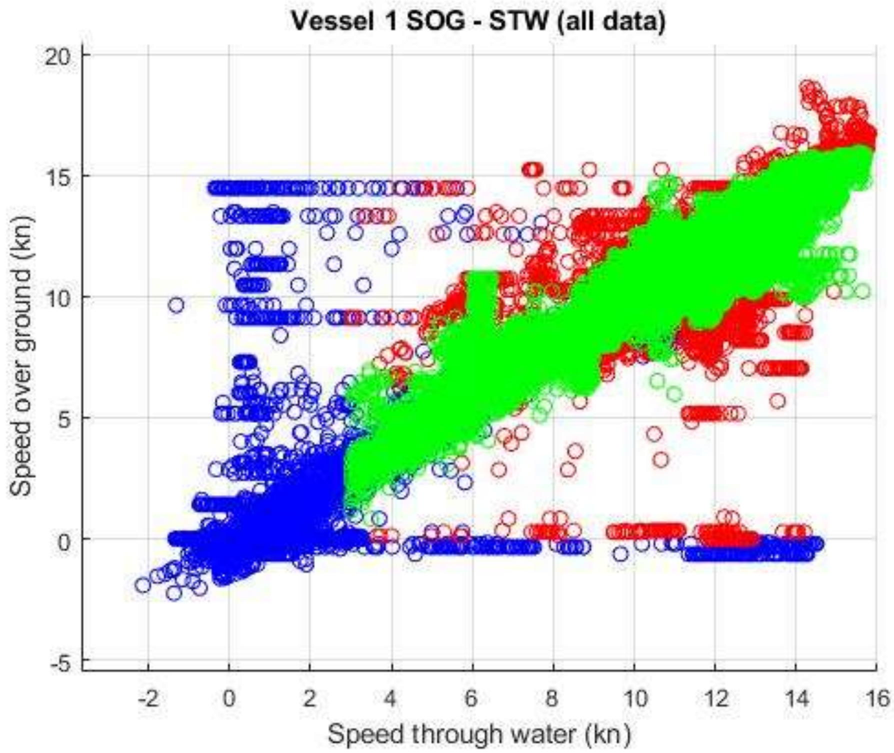

Figure 10: Filter STW_SOG – Vessel 1.

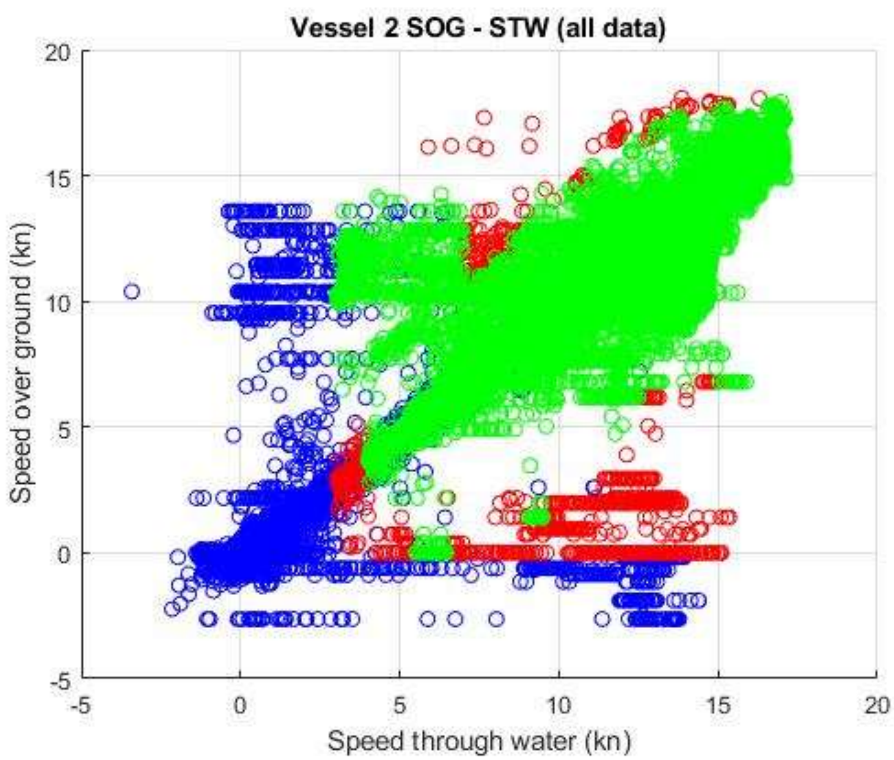

Figure 11: Filter STW_SOG – Vessel 2.

The effects of the application of the “STW_SOG” filter on the dataset can be observed with the help of the SOG – STW graphs. The filter has an insignificant effect on the other variables and the relationships that are formed among them, a conclusion that can be easily verified by the graphs’ lack of outlier points (red points).

For Vessel 1, the filter manages to eliminate some of the remaining sets of horizontal data points that deviate from the main diagonal which represents the linear relationship between the two speed variables. More specifically, data points in the following regions are successfully omitted by the filter:

- $\mathrm{SOG} \approx 0 \ \& \ \mathrm{STW} > 4$
- $5 < \mathrm{SOG} < 9 \ \& \ 11 < \mathrm{STW} < 14$
- $\mathrm{SOG} > 10 \ \& \ 8 < \mathrm{STW} < 10$

As far as Vessel 2 is concerned, the filter helps in further eliminating outliers without being able to identify all of them. The lower right area of the graph ($0 < SOG < 5 \ \& \ \mathrm{STW} > 5$) is successfully identified as an outlier region and therefore omitted by the filter. However, the upper left region ($SOG > 10 \ \& \ 3 < STW < 6$) contains sets of horizontal data points that deviate from the main diagonal line and should be considered as outliers. The filter fails to trace that outlier area.

Overall, the filter manages to identify a significant amount of outlier data points without omitting areas of desirable data points. Despite its effect being limited to the SOG – STW graphs, the filter will be used in the data correction process as it aids towards a better representation of the linear relationship that characterizes the two speeds.

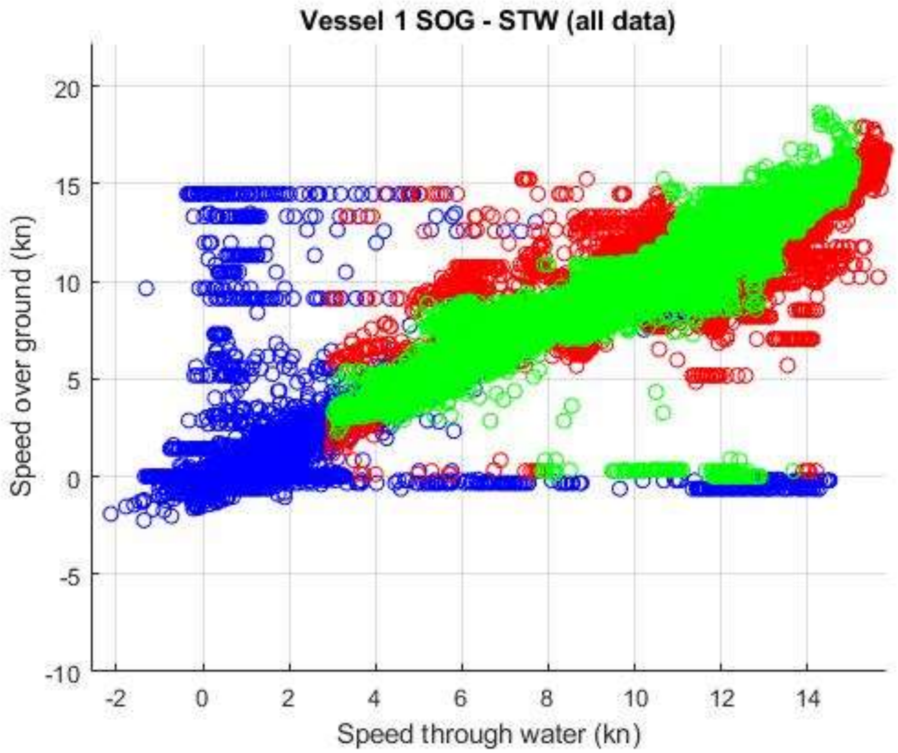

Figure 12: Filter SOG_STW – Vessel 1.

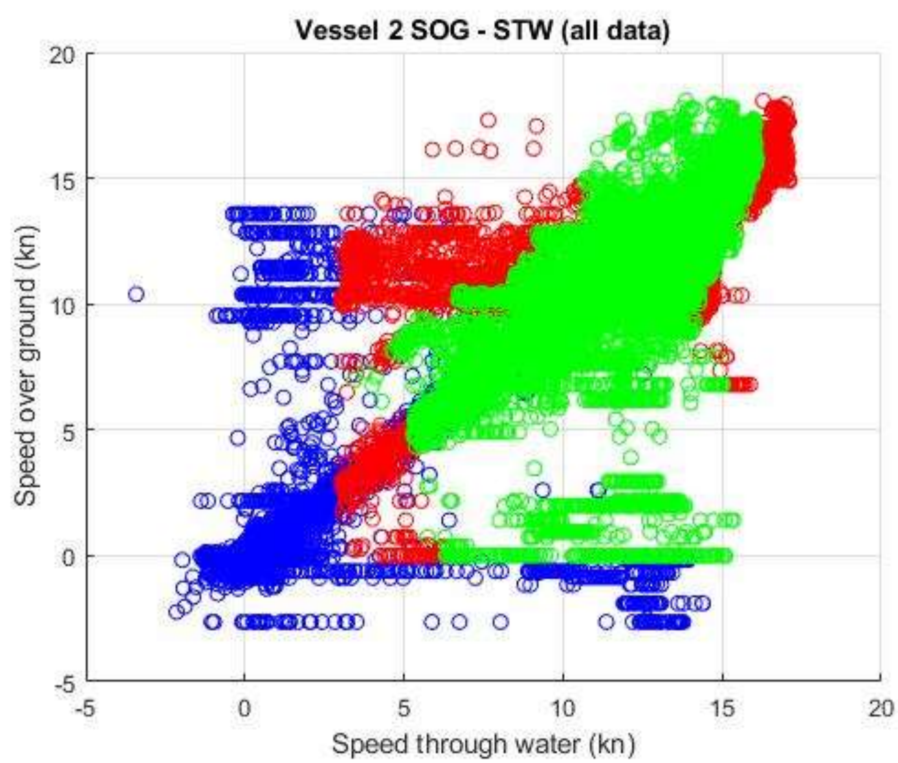

Figure 13: Filter SOG_STW – Vessel 2.

The effects of the application of the “SOG_STW” filter on the dataset can be observed with the help of the SOG – STW graphs. The filter has an insignificant effect on the other variables and the relationships that are formed among them, a conclusion that can be easily verified by the graphs’ lack of outlier points (red points).

For Vessel 1, the filter has a similar effect on the graph as the previous one. However, two significant differences can be observed. Firstly, the “SOG_STW” filter fails to eliminate the horizontal set of data points that corresponds to near zero speed over ground in contrast with the “STW_SOG” filter. On the other hand, the “SOG_STW” filter successfully identifies the upper right outlier region ($SOG > 10$ & $STW > 13$) which the previous filter neglects.

As far as Vessel 2 is concerned, the filter helps in further eliminating outliers without being able to identify all of them. In contrast with the previous filter, it manages to identify the upper left region ($SOG > 10$ & $3 < STW < 6$) as an outlier area that does not correspond with the linearly expressed relationship between the two variables. However, the filter fails to omit the lower right area of the graph ($0 < SOG < 5$ & $STW > 5$), which is successfully discarded by the previous filter.

Overall, the filter manages to identify a significant amount of outlier data points without omitting areas of desirable data points. It can be understood that the “SOG_STW” and “STW_SOG” filters complete one another in such manner that no significant outlier regions remain undetected. Thus, they should be both included in the data correction process.

2.3.2.2 Engine power – Speed through water

The EP and STW variables are filtered according to the process described in the "Filtering procedure" paragraph. The outlier threshold k and the range v values are shown in Table 8 Table 8: Outlier threshold and range values (EP-STW).:

Case	Primary: EP	Primary: STW
	Secondary: STW	Secondary: EP
k	2	2
v	100 kW	0.5 kn

Table 8: Outlier threshold and range values (EP-STW).

Both cases are analyzed with the help of graphs for both vessels. For the case in which EP is the primary parameter, the respective filter is called "*EP_STW*" while for the one in which STW is the primary parameter, the filter is called "*STW_EP*". The occurring scatter plots contain data points colored in blue, red or green. The blue points are the ones that are omitted by the threshold filters that are applied during the first part of data correction. The red points are the ones that fulfill the criteria set by the first filtering procedure but are omitted due to the applied single-filter under consideration (EP_STW, STW_EP). Finally, the green data points are the ones that meet the standards set by the threshold filters and the applied single filter. Presented below are the graphs that are significantly affected by the application of the filter. The effect of the filter on all graphs can be found in the figures included in Appendix A: Data correction – Part II filters.

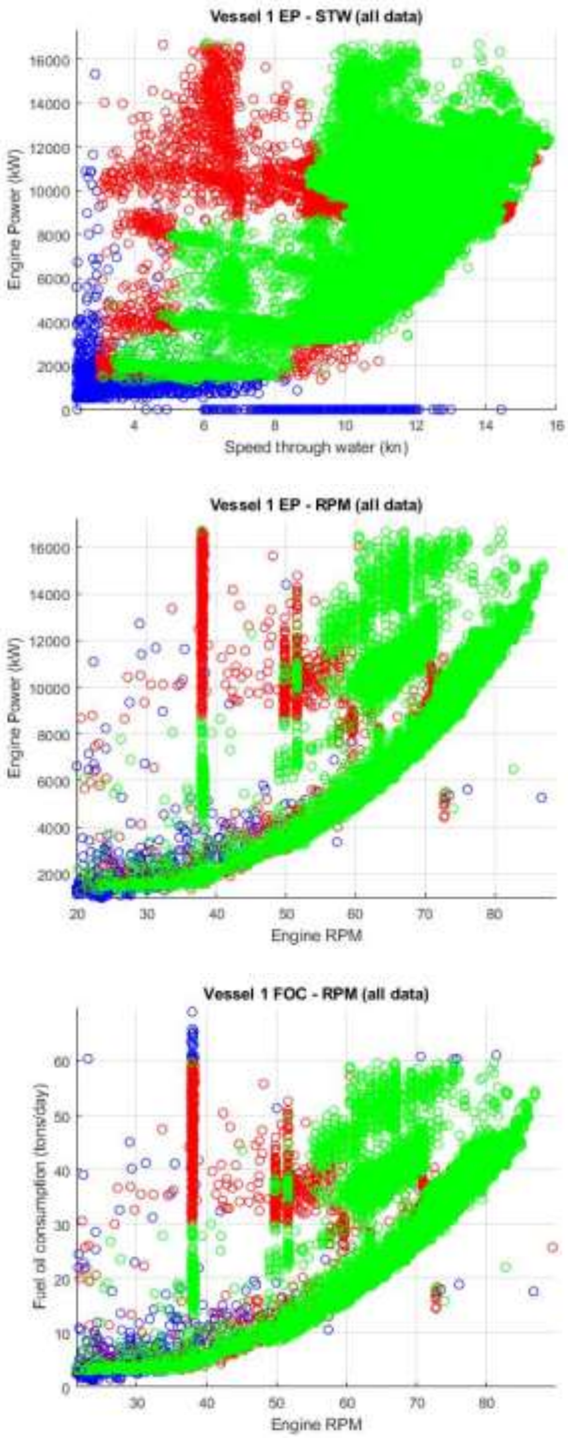

Figure 14: Filter EP_STW – Vessel 1.

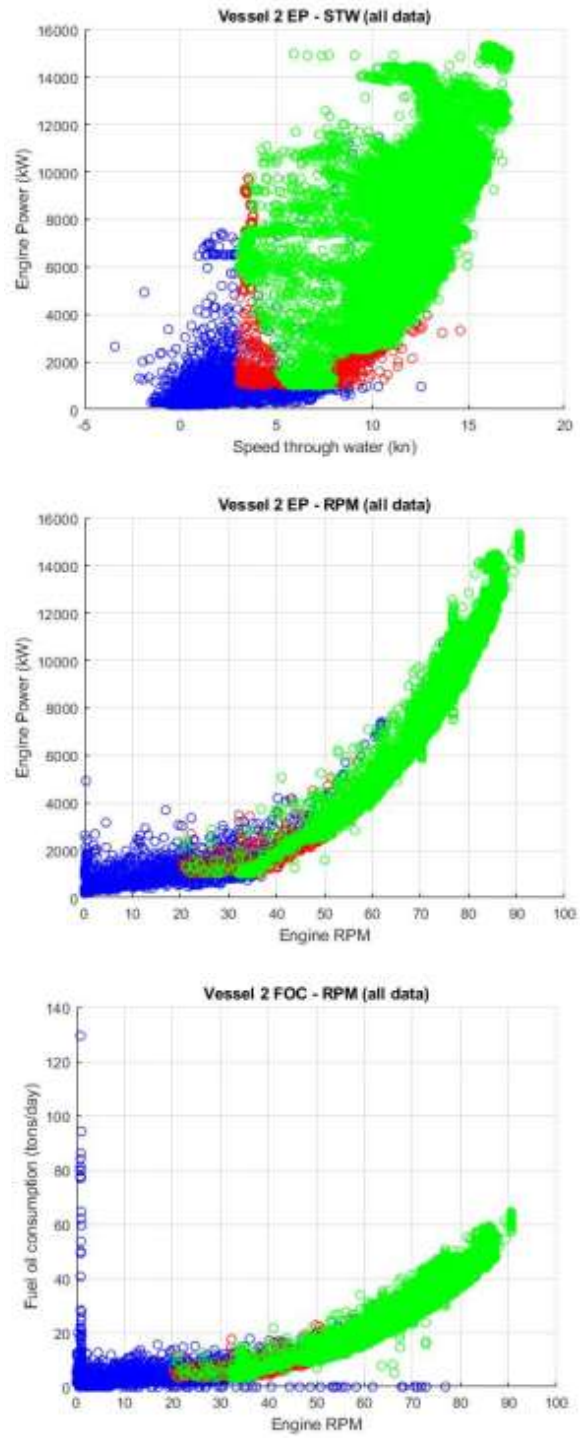

Figure 15: Filter EP_STW – Vessel 2.

The effects of the application of the “EP_STW” filter on the dataset can be observed with the help of the EP – STW, EP – RPM and FOC – RPM graphs. The filter has an insignificant effect on the other variables and the relationships that are formed among them, a conclusion that can be easily verified by the graphs’ lack of outlier points (red points).

For Vessel 1, the filter manages to eliminate the upper middle area of the EP – STW graph ($3 < \mathrm{STW} < 8$ & $\mathrm{EP} > 8{,}000$) but fails to identify outlier points of lower engine power values. Moreover, it successfully omits the data points that form a vertical line at $\mathrm{RPM} \approx 40$ but only for greater values of engine power/fuel consumption. Despite that rather positive effect, the filter falsely eliminates data points that belong to the $\mathrm{P} = \mathrm{c} \cdot \mathrm{n}^{\mathrm{a}}$ curves that correspond with fouled hull and/or bad weather conditions.

As far as Vessel 2 is concerned, the filter has limited and insignificant effect failing to further correct the dataset.

Overall, the filter manages to identify a small amount of outlier data points but also omits areas of desirable data points. Since these areas ($\mathrm{P} = \mathrm{c} \cdot \mathrm{n}^{\mathrm{a}}$ curves) are of high importance in understanding the physical relationship between the power/consumption and the shaft’s revolutions, the filter will not be used in the data correction process.

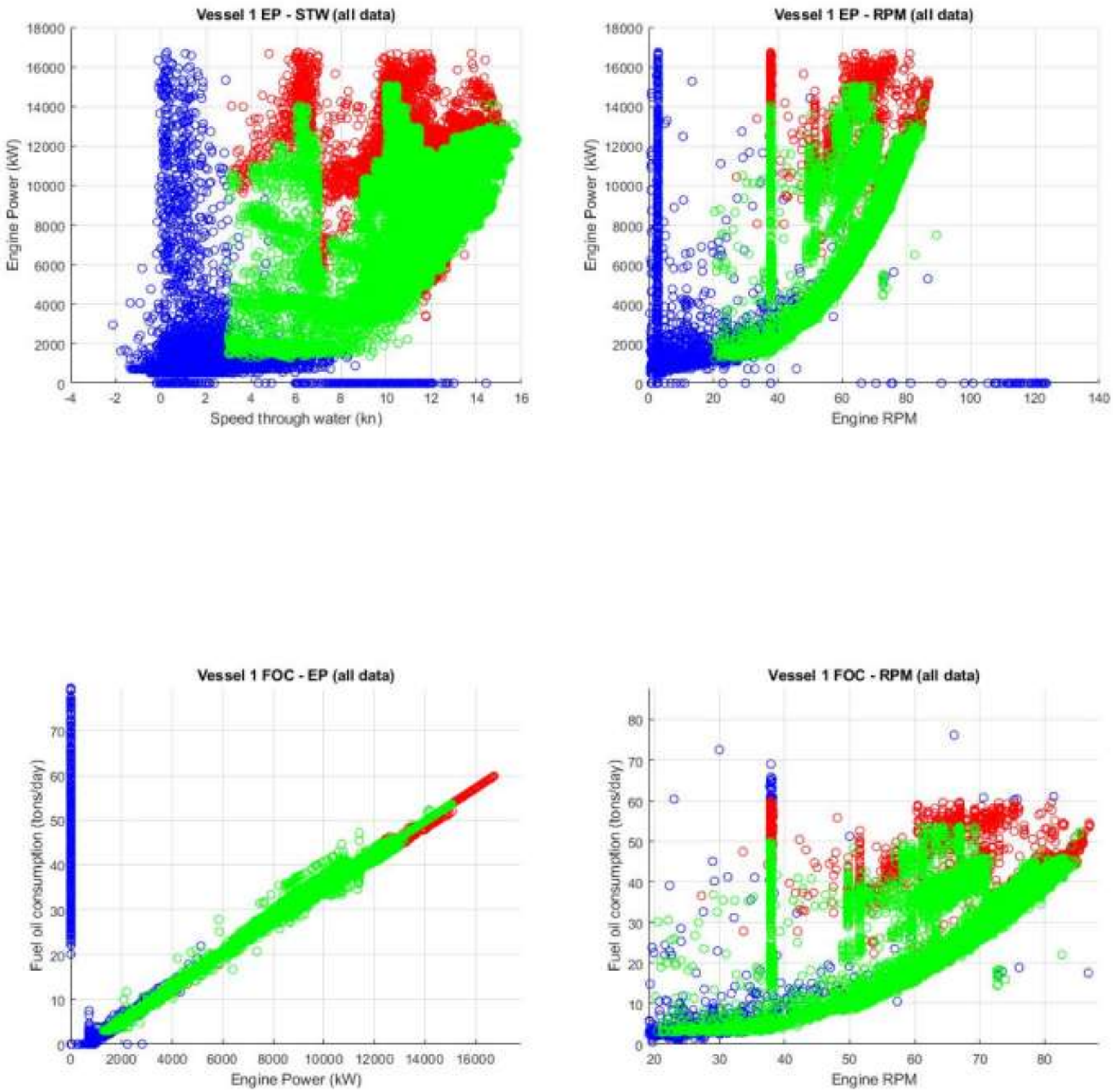

Figure 16: Filter STW_EP – Vessel 1.

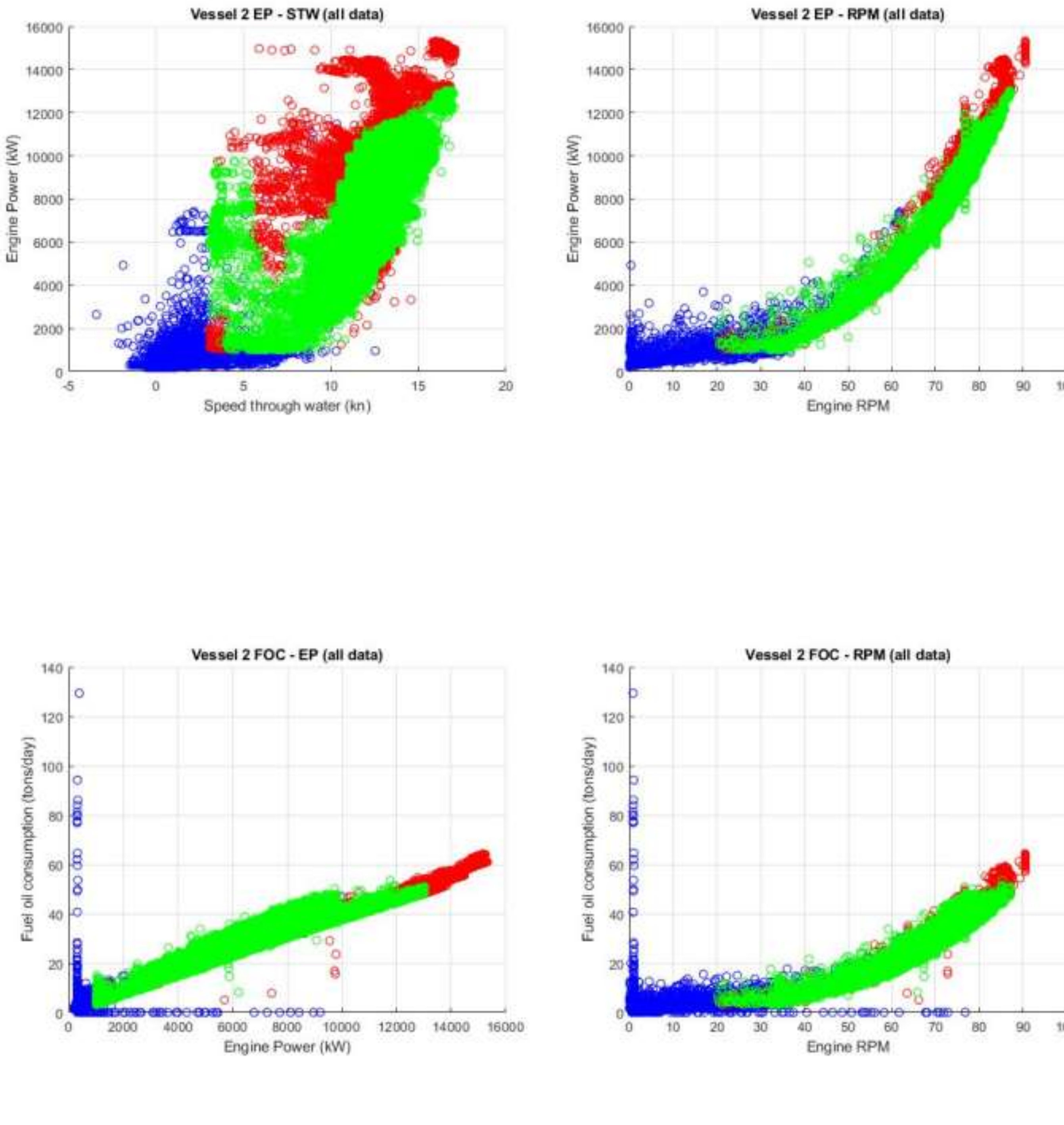

Figure 17: Filter STW_EP – Vessel 2.

The effects of the application of the “STW_EP” filter on the dataset can be observed with the help of the EP – STW, EP – RPM, FOC – RPM and FOC – EP graphs. The filter has an insignificant effect on the other variables and the relationships that are formed among them, a conclusion that can be easily verified by the graphs’ lack of outlier points (red points).

For Vessel 1, the filter manages to eliminate some outlying data points of the EP – STW graph that correspond with significantly high-power values but also falsely discards various data points that belong to higher power – speed curves, which are probably associated with greater hull fouling and/or worse weather conditions. Furthermore, the filter identifies only a small number of outliers in the EP - RPM and FOC - RPM graphs ($\text{at RPM} \approx 40$) for great values of power/consumption while it omits a far greater amount of desirable data points that belong to the power/consumption – revolutions curves. Finally, the application of the filter causes the upper right area of the FOC -EP graph to be omitted, an outcome that is considered undesirable since the graph is already sufficiently corrected.

As far as Vessel 2 is concerned, the filter manages to eliminate a significant amount of outlier data points of the EP – STW graph but also discards various data points that belong to higher power – speed curves, which are probably associated with greater hull fouling and/or worse weather conditions. The filter has a negative effect on the already sufficiently corrected power-related graphs since it omits data points associated with greater rpm and power values.

Overall, the filter, while managing to identify some outlier data point, also omits areas of desirable data points that are vital in the representation of the physical relationships among the variables. As a consequence, it will not be included in the data correction process.

2.3.2.3 Engine power – Fuel oil consumption

The EP and FOC variables are filtered according to the process described in the "Filtering procedure" paragraph. The outlier threshold k and the range v values are shown in Table 9:

Case	Primary: EP	Primary: FOC
	Secondary: FOC	Secondary: EP
k	2.5	2.5
v	100 kW	0.5 tons/day

Table 9: Outlier threshold and range values (EP-FOC).

Both cases are analyzed with the help of graphs for both vessels. For the case in which EP is the primary parameter, the respective filter is called "*EP_FOC*" while for the one in which FOC is the primary parameter, the filter is called "*FOC_EP*". The occurring scatter plots contain data points colored in blue, red or green. The blue points are the ones that are omitted by the threshold filters that are applied during the first part of data correction. The red points are the ones that fulfill the criteria set by the first filtering procedure but are omitted due to the applied single-filter under consideration (EP_FOC, FOC_EP). Finally, the green data points are the ones that meet the standards set by the threshold filters and the applied single filter. Presented below are the graphs that are significantly affected by the application of the filter. The effect of the filter on all graphs can be found in the figures included in Appendix A: Data correction – Part II filters.

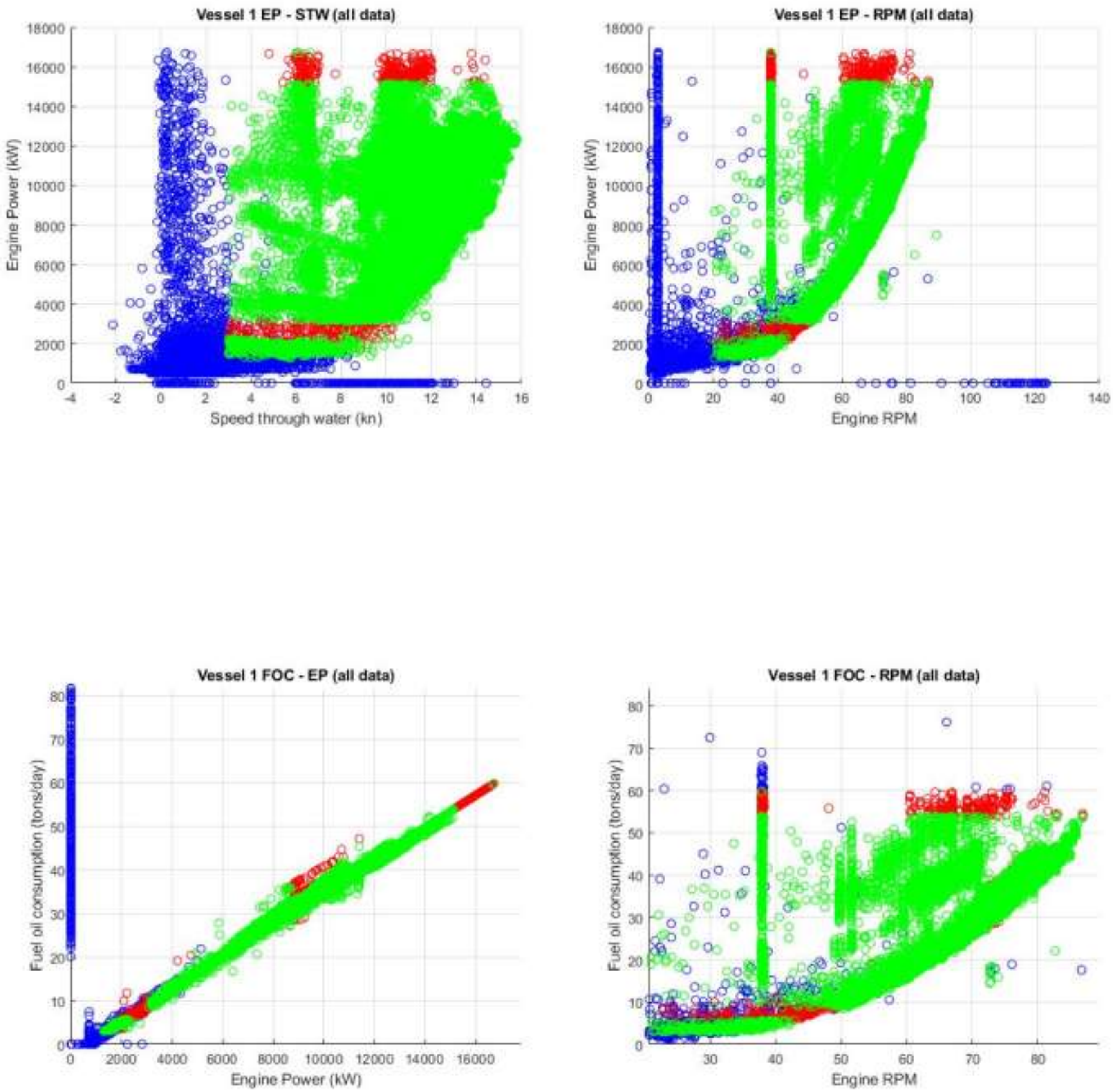

Figure 18: Filter EP_FOC – Vessel 1.

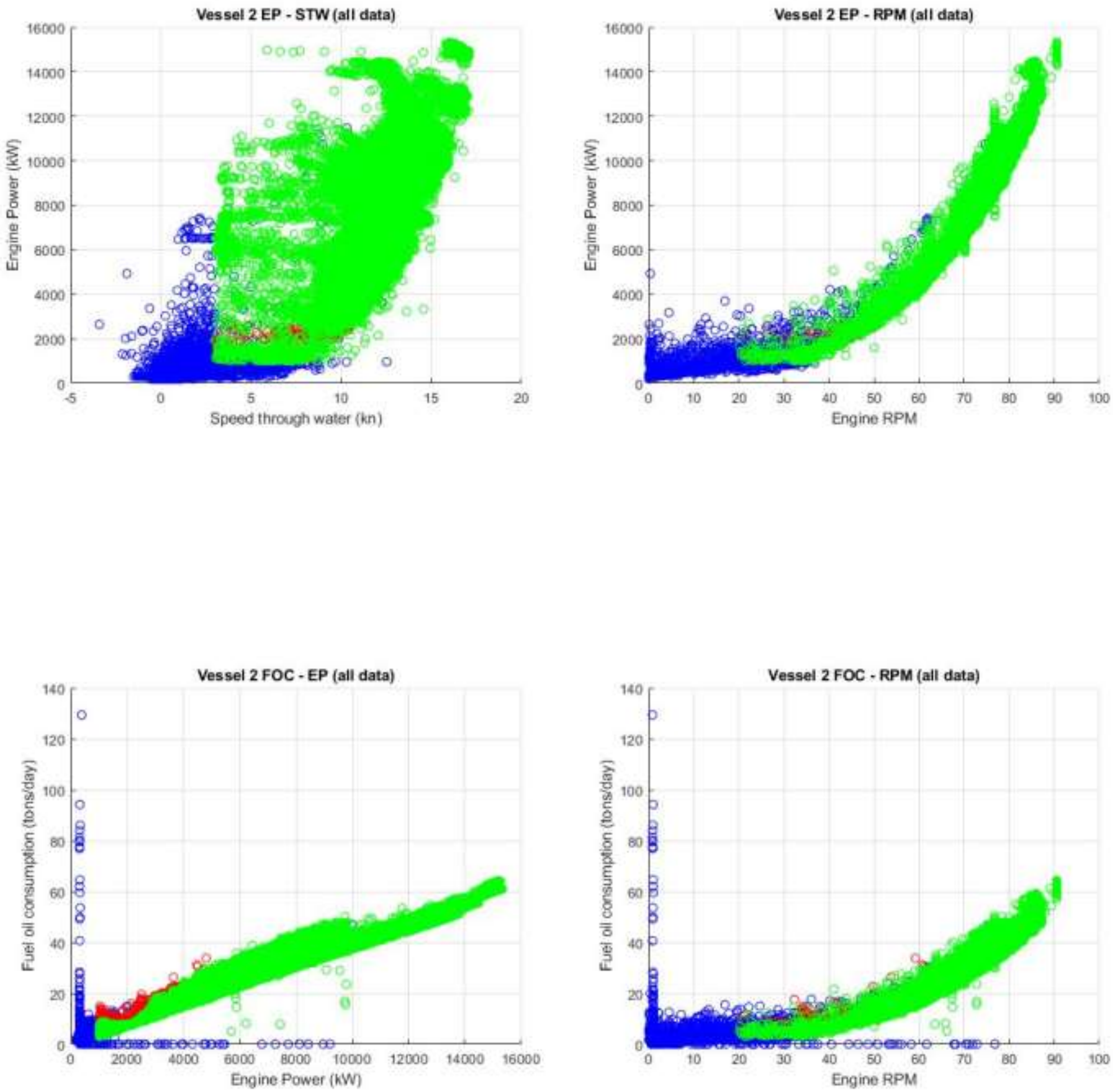

Figure 19: Filter EP_FOC – Vessel 2.

The effects of the application of the “EP_FOC” filter on the dataset can be observed with the help of the EP – STW, EP – RPM, FOC – RPM and FOC – EP graphs. The filter has an insignificant effect on the other variables and the relationships that are formed among them, a conclusion that can be easily verified by the graphs’ lack of outlier points (red points).

For Vessel 1, the filter manages to eliminate a few outlier points located at the upper middle area of the EP – STW graph ($\mathrm{STW} \approx 6$ & $\mathrm{EP} \approx 16{,}000$) but fails to identify outlier points of lower engine power values. In addition to the above, the filter falsely identifies data points that belong to the power-speed curves as outliers ($9 < \mathrm{STW} < 12$ & $15{,}000 < \mathrm{EP} < 17{,}000$). Moreover, it falsely eliminates data points that belong to the power/consumption - revolution curves ($60 < \mathrm{RPM} < 80$ & $\mathrm{FOC} > 50, \mathrm{EP} > 15{,}000$) that correspond with fouled hull and/or bad weather conditions, while managing to omit only a few true outliers ($\mathrm{RPM} \approx 40$ & $\mathrm{FOC} > 50, \mathrm{EP} > 15{,}000$). Finally, the application of the filter causes the upper right area of the FOC - EP graph to be omitted, an outcome that is considered undesirable since the graph is already sufficiently corrected.

As far as Vessel 2 is concerned, the filter has limited and insignificant effect failing to further correct the dataset.

Overall, the filter manages to identify a small amount of outlier data points while omitting significant areas of desirable data points. Therefore, it will not be utilized in the data correction process.

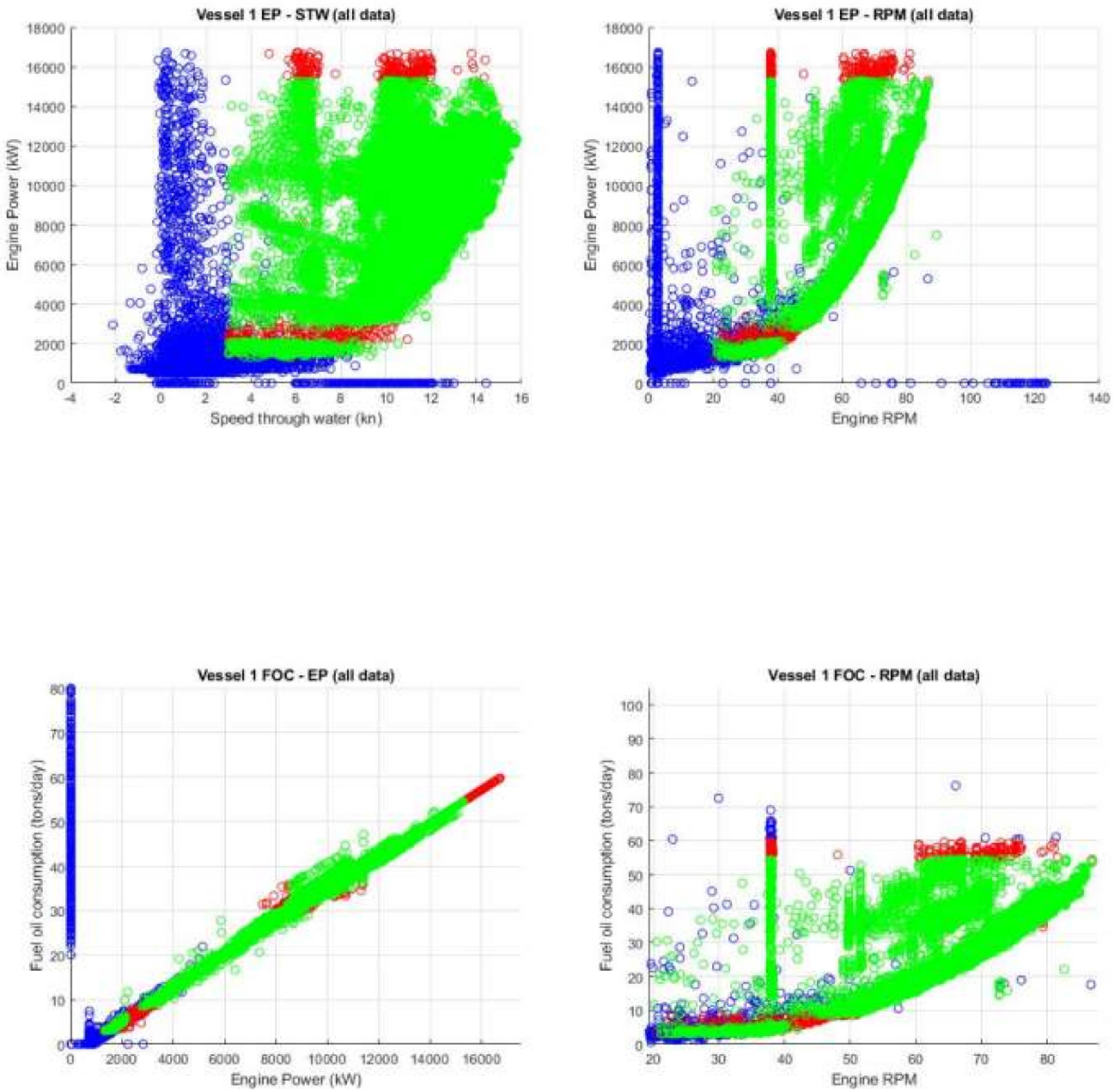

Figure 20: Filter FOC_EP – Vessel 1.

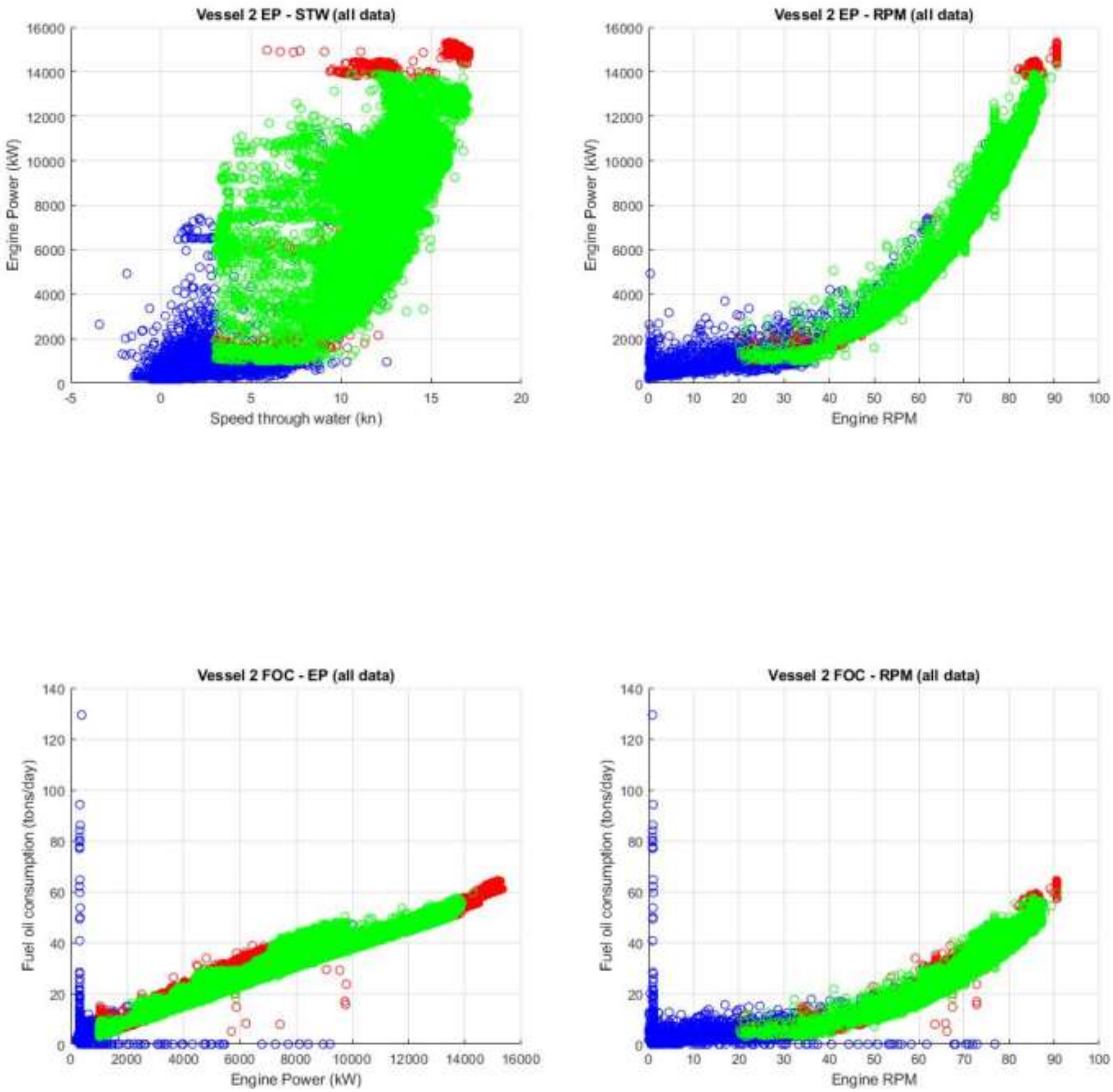

Figure 21: Filter FOC_EP – Vessel 2.

The effects of the application of the “FOC_EP” filter on the dataset can be observed with the help of the EP – STW, EP – RPM, FOC – RPM and FOC – EP graphs. The filter has an insignificant effect on the other variables and the relationships that are formed among them, a conclusion that can be easily verified by the graphs’ lack of outlier points (red points).

For Vessel 1, the filter manages to eliminate a few outlier points located at the upper middle area of the EP – STW graph ($\mathrm{STW} \approx 6$ & $\mathrm{EP} \approx 16{,}000$) but fails to identify outlier points of lower engine power values. In addition to the above, the filter falsely identifies data points that belong to the power-speed curves as outliers ($9 < \mathrm{STW} < 12$ & $15{,}000 < \mathrm{EP} < 17{,}000$). Moreover, it falsely eliminates data points that belong to the power/consumption - revolution curves ($60 < \mathrm{RPM} < 80$ & $\mathrm{FOC} > 50, \mathrm{EP} > 15{,}000$) that correspond with fouled hull and/or bad weather conditions, while managing to omit only a few true outliers ($\mathrm{RPM} \approx 40$ & $\mathrm{FOC} > 50, \mathrm{EP} > 15{,}000$). Finally, the application of the filter causes the upper right area of the FOC - EP graph to be omitted, an outcome that is considered undesirable since the graph is already sufficiently corrected.

As far as Vessel 2 is concerned, while the filter manages to eliminate a few outlier data points associated with high values of shaft’s revolutions ($\mathrm{RPM} \approx 90$) it also discards a far greater amount of data points that characterize the linear relationship between the fuel consumption and the engine power.

Overall, the filter has an almost similar effect with the previous on, managing to identify a small amount of outlier data points while omitting significant areas of desirable data points. Therefore, it will not be utilized in the data correction process.

2.3.2.4 Engine power – Shaft's revolutions

The EP and RPM variables are filtered according to the process described in the "Filtering procedure" paragraph. The outlier threshold k and the range v values are shown in Table 10:

Case	Primary: EP	Primary: RPM
	Secondary: RPM	Secondary: EP
k	2.5	2.5
v	100 kW	0.5 rpm

Table 10: Outlier threshold and range values (EP-RPM).

Both cases are analyzed with the help of graphs for both vessels. For the case in which EP is the primary parameter, the respective filter is called "*EP_RPM*" while for the one in which RPM is the primary parameter, the filter is called "*RPM_EP*". The occurring scatter plots contain data points colored in blue, red or green. The blue points are the ones that are omitted by the threshold filters that are applied during the first part of data correction. The red points are the ones that fulfill the criteria set by the first filtering procedure but are omitted due to the applied single-filter under consideration (EP_RPM, RPM_EP). Finally, the green data points are the ones that meet the standards set by the threshold filters and the applied single filter. Presented below are the graphs that are significantly affected by the application of the filter. The effect of the filter on all graphs can be found in the figures included in Appendix A: Data correction – Part II filters.

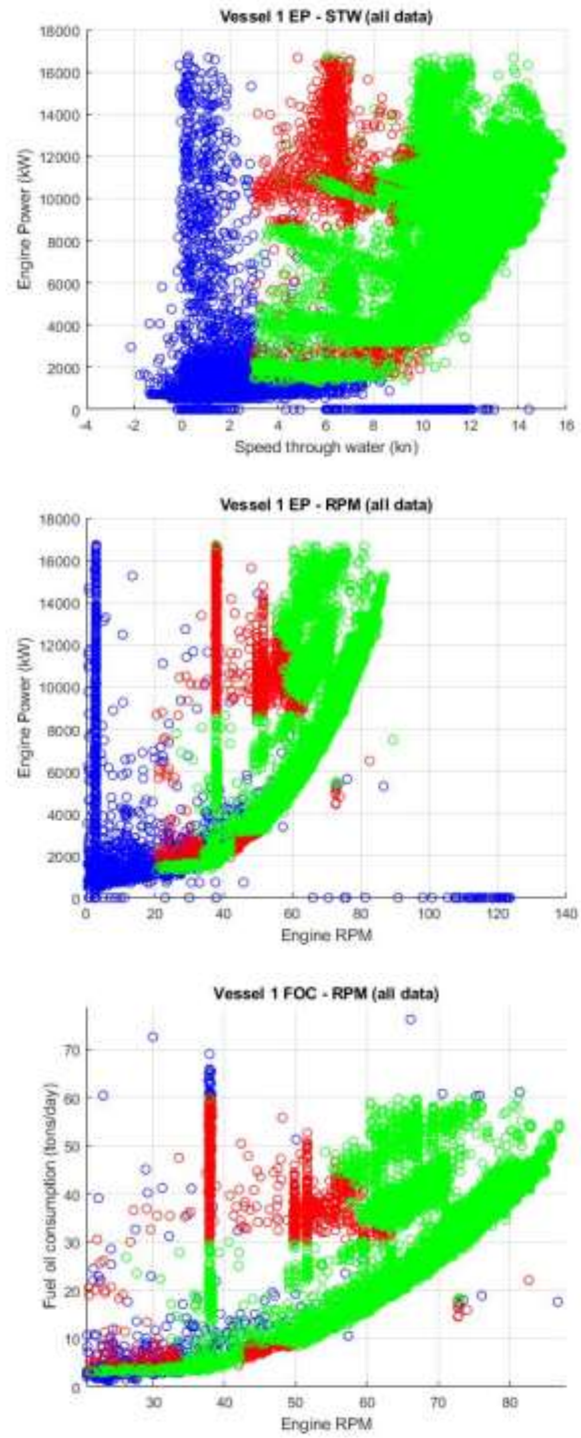

Figure 22: Filter EP_RPM – Vessel 1.

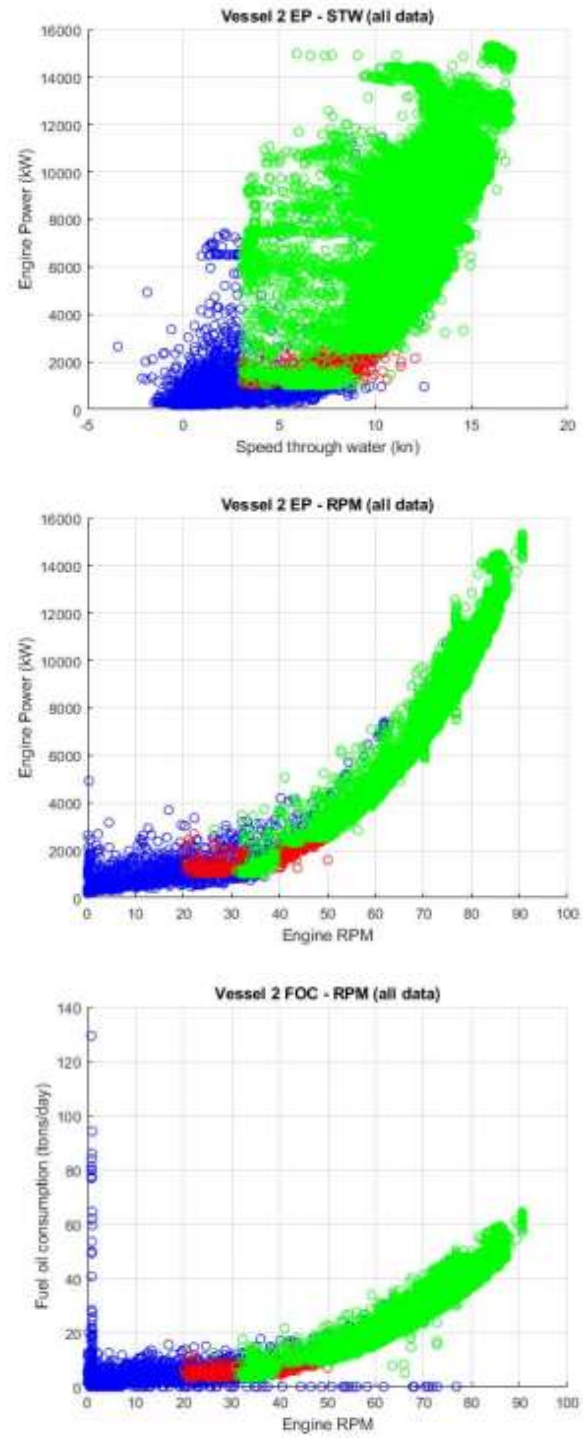

Figure 23: Filter EP_RPM – Vessel 2.

The effects of the application of the “EP_RPM” filter on the dataset can be observed with the help of the EP – STW, EP – RPM and FOC – RPM graphs. The filter has an insignificant effect on the other variables and the relationships that are formed among them, a conclusion that can be easily verified by the graphs’ lack of outlier points (red points).

For Vessel 1, the filter successfully eliminates the outlier points located at the upper middle area of the EP – STW graph $(3 < \mathrm{STW} < 8 \,\&\, \mathrm{EP} > 9{,}000)$ without omitting any group of desirable data points. Moreover, it manages to identify the outlier points that form the 3 vertical lines on the EP – RPM and FOC – RPM graphs $(\mathrm{RPM} \approx 40, \mathrm{RPM} \approx 50 \text{ and } \mathrm{RPM} \approx 52)$. The 3 vertical lines are the main outlier regions in the two graphs and their omission is crucial for the correction of the dataset. The filter successfully eliminates them for $\mathrm{FOC} > 30, \mathrm{EP} > 8{,}000$. However, it fails to identify the remaining lower parts of the vertical lines.

As far as Vessel 2 is concerned, the filter has limited and insignificant effect failing to further correct the dataset.

Overall, the filter manages to identify a significant amount of outlier data points without omitting any desirable areas. Despite the fact that its effect on the Vessel 2 dataset is limited, it greatly aids at the identification of outliers concerning Vessel 1. Therefore, it shall be applied at the data correction procedure.

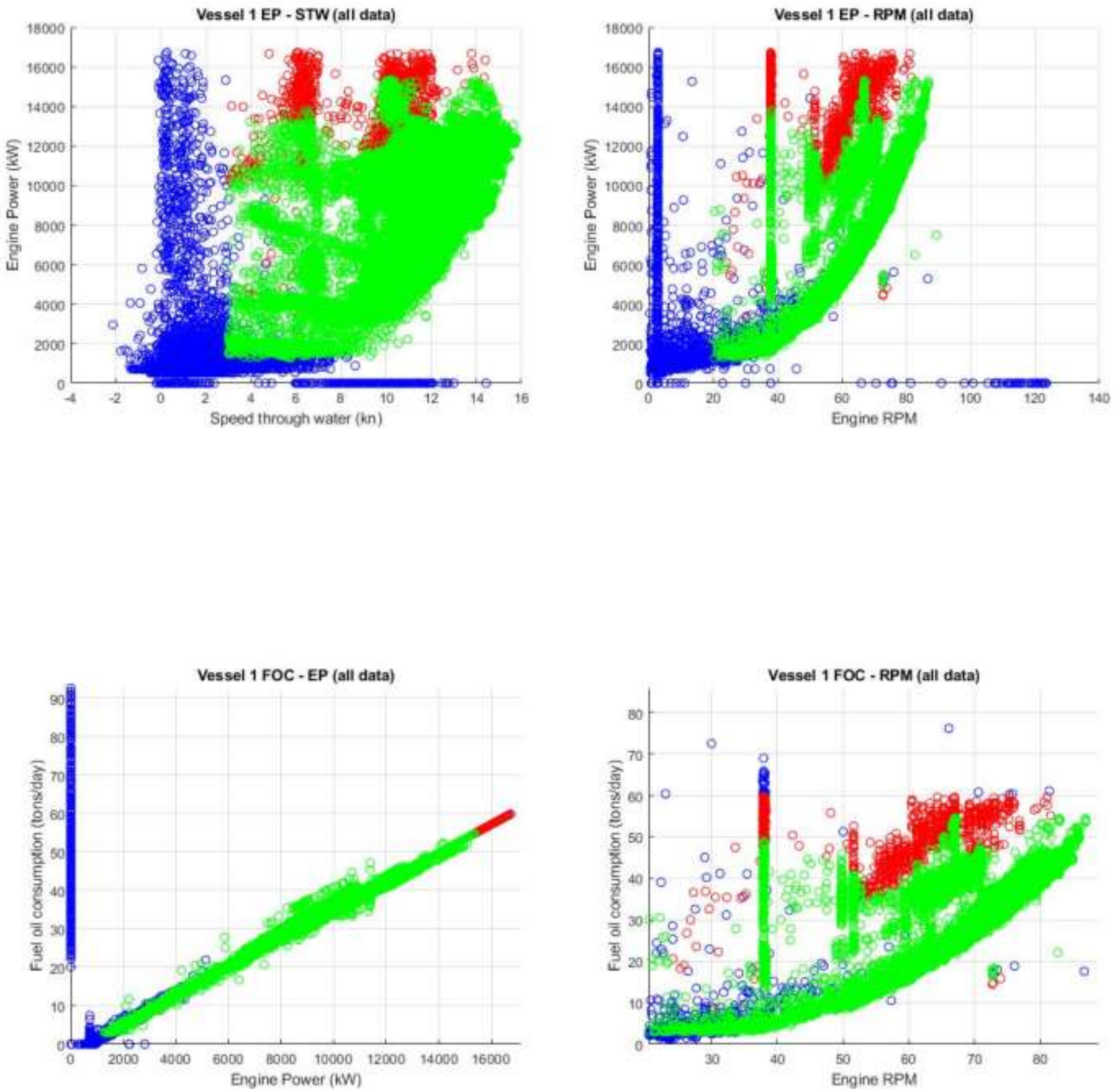

Figure 24: Filter RPM_EP – Vessel 1.

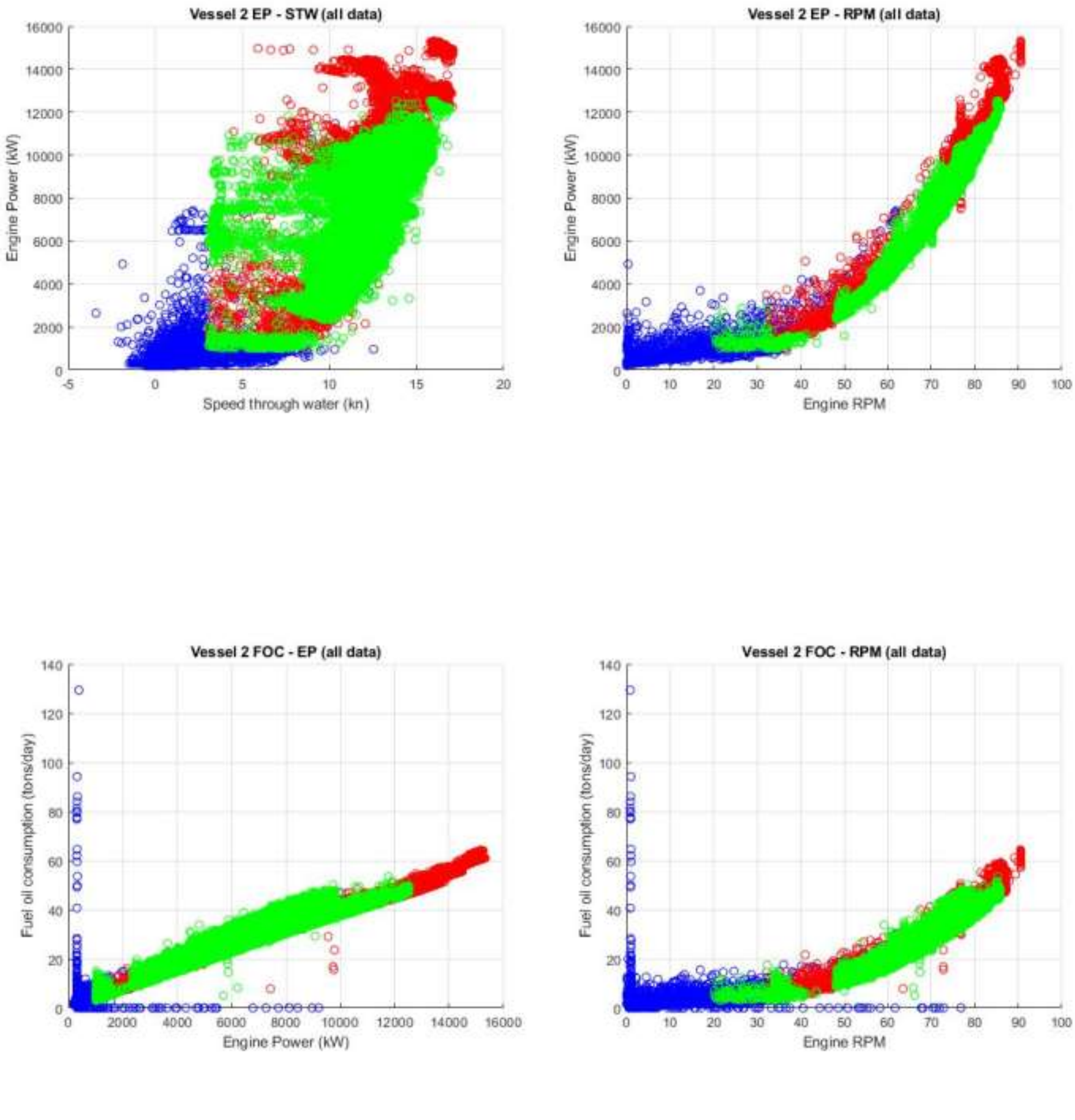

Figure 25: Filter RPM_EP – Vessel 2.

The effects of the application of the “RPM_EP” filter on the dataset can be observed with the help of the EP – STW, EP – RPM, FOC – RPM and FOC – EP graphs. The filter has an insignificant effect on the other variables and the relationships that are formed among them, a conclusion that can be easily verified by the graphs’ lack of outlier points (red points).

For Vessel 1, the filter eliminates two regions of the EP – STW graph. The first region ($4 < \mathrm{STW} < 8$ & $\mathrm{EP} > 13{,}000$) is successfully identified as an outlier area, however the second region ($8 < \mathrm{STW} < 12$ & $\mathrm{EP} > 12{,}000$) should be considered as a part of the power – speed curves which are associated with greater hull fouling and/or worse weather conditions and thus, its elimination is not correct. Furthermore, the filter identifies only a small number of outliers in the EP - RPM and FOC - RPM graphs ($\mathrm{RPM} \approx 40$ & $\mathrm{FOC} > 50, \mathrm{EP} > 14{,}000$) for great values of power/consumption while it omits a far greater amount of desirable data points that belong to the 3rd power/consumption – revolutions curve ($50 < \mathrm{RPM} < 70$ & $40 < \mathrm{FOC} < 60, 10{,}000 < \mathrm{EP} < 16{,}000$). Finally, the application of the filter causes the upper right area of the FOC -EP graph to be omitted, an outcome that is considered undesirable since the graph is already sufficiently corrected.

As far as Vessel 2 is concerned, the filter manages to eliminate a significant amount of outlier data points of the EP – STW graph but also discards various data points that belong to higher power – speed curves, which are probably associated with greater hull fouling and/or worse weather conditions. The filter has a negative effect on the already sufficiently corrected power-related graphs since it omits data points associated with greater rpm and power values. In addition to the above, it completely discards the graphs’ areas for $40 < \mathrm{RPM} < 50$ causing an important loss of information concerning the relationship between the power/consumption and the shaft’s revolutions

Overall, the filter manages to identify just a few outlier points for Vessel 1 while omitting a far greater amount of desirable data and thus distorting the dataset. Since the filter impedes the formation of the dataset that better expresses the relationships among the physical quantities rather than facilitating it, it will not be applied in the data correction process.

2.3.2.5 Fuel oil consumption – Shaft's revolutions

The FOC and RPM variables are filtered according to the process described in the "Filtering procedure" paragraph. The outlier threshold k and the range v values are shown in Table 11:

Case	Primary: FOC	Primary: RPM
	Secondary: RPM	Secondary: FOC
k	2.5	2.5
v	0.5 tons/day	0.5 rpm

Table 11: Outlier threshold and range values (FOC-RPM).

Both cases are analyzed with the help of graphs for both vessels. For the case in which FOC is the primary parameter, the respective filter is called "*FOC_RPM*" while for the one in which RPM is the primary parameter, the filter is called "*RPM_FOC*". The occurring scatter plots contain data points colored in blue, red or green. The blue points are the ones that are omitted by the threshold filters that are applied during the first part of data correction. The red points are the ones that fulfill the criteria set by the first filtering procedure but are omitted due to the applied single-filter under consideration (FOC_RPM, RPM_FOC). Finally, the green data points are the ones that meet the standards set by the threshold filters and the applied single filter. Presented below are the graphs that are significantly affected by the application of the filter. The effect of the filter on all graphs can be found in the figures included in Appendix A: Data correction – Part II filters.

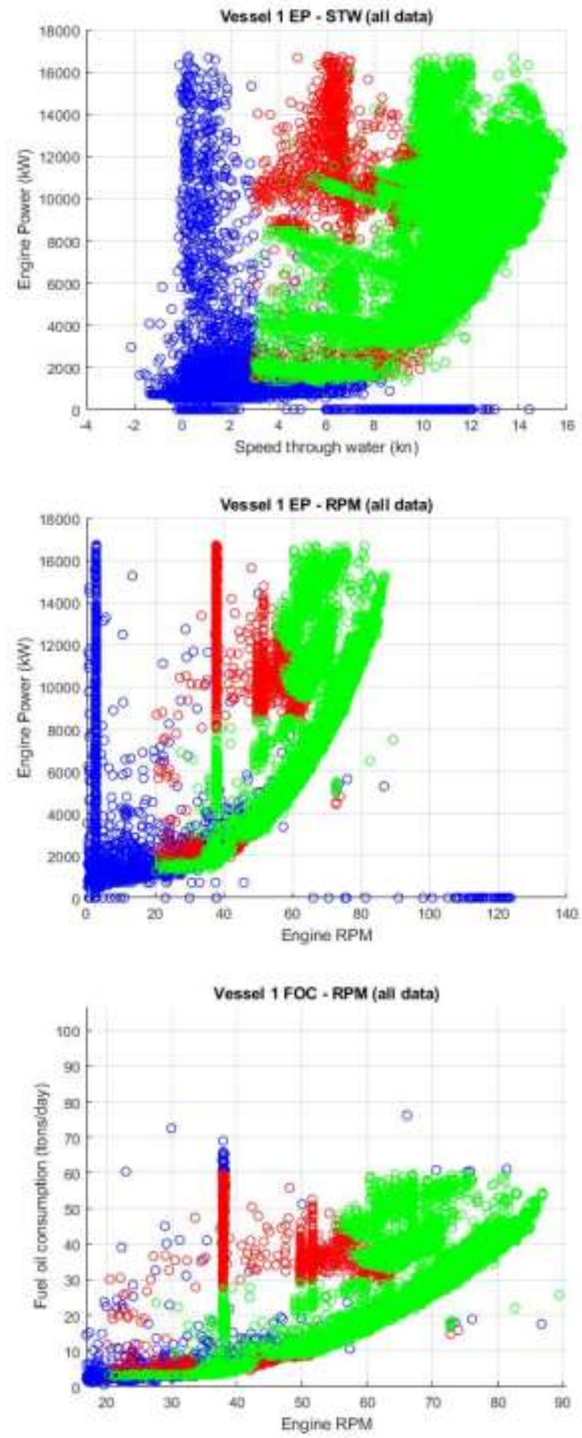

Figure 26: Filter FOC_RPM – Vessel 1.

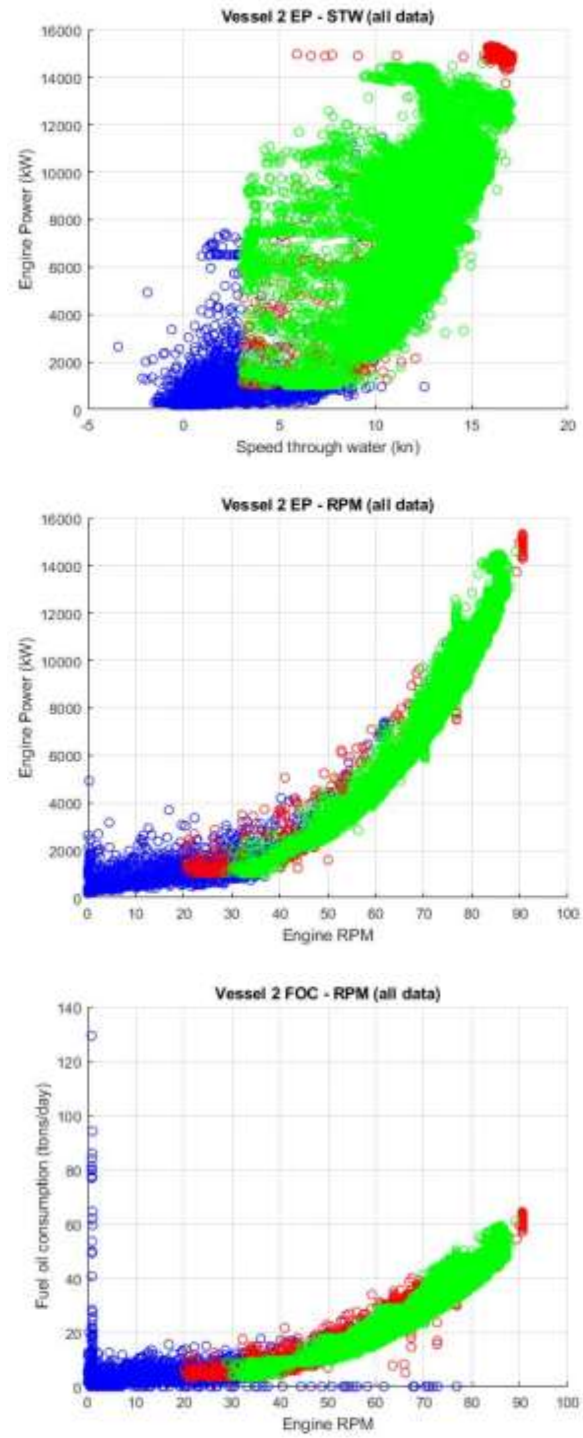

Figure 27: Filter FOC_RPM – Vessel 2.

The effects of the application of the "FOC_RPM" filter on the dataset can be observed with the help of the EP – STW, EP – RPM and FOC – RPM graphs. The filter has an insignificant effect on the other variables and the relationships that are formed among them, a conclusion that can be easily verified by the graphs' lack of outlier points (red points).

For Vessel 1, the filter successfully eliminates the outlier points located at the upper middle area of the EP – STW graph $(3 < \text{STW} < 8 \,\&\, \text{EP} > 9{,}000)$ without omitting any group of desirable data points. Moreover, it manages to identify the outlier points that form the 3 vertical lines on the EP – RPM and FOC – RPM graphs $(\text{RPM} \approx 40, \text{RPM} \approx 50 \text{ and } \text{RPM} \approx 52)$. The 3 vertical lines are the main outlier regions in the two graphs and their omission is crucial for the correction of the dataset. The filter successfully eliminates them for $\text{FOC} > 30, \text{EP} > 8{,}000$. However, it fails to identify the remaining lower parts of the vertical lines.

As far as Vessel 2 is concerned, the filter omits a significant amount of data concerning the power/consumption-related graphs, which are already sufficiently corrected and require no further filtering.

Overall, the filter achieves a similar result for Vessel 1 data points as the "EP_RPM" filter, without managing to overcome its inability to eliminate the lower parts of the vertical lines of the EP – RPM and FOC – RPM graphs. Despite its successful treatment of the Vessel 1 dataset, the filter falsely eliminates desirable data points of the power related graphs of Vessel 2. The graphs are already sufficiently corrected and require no further filtering. It can be understood that since the "EP_RPM" achieves similar results without affecting the Vessel 2 dataset, it is preferred over the "FOC_RPM" filter.

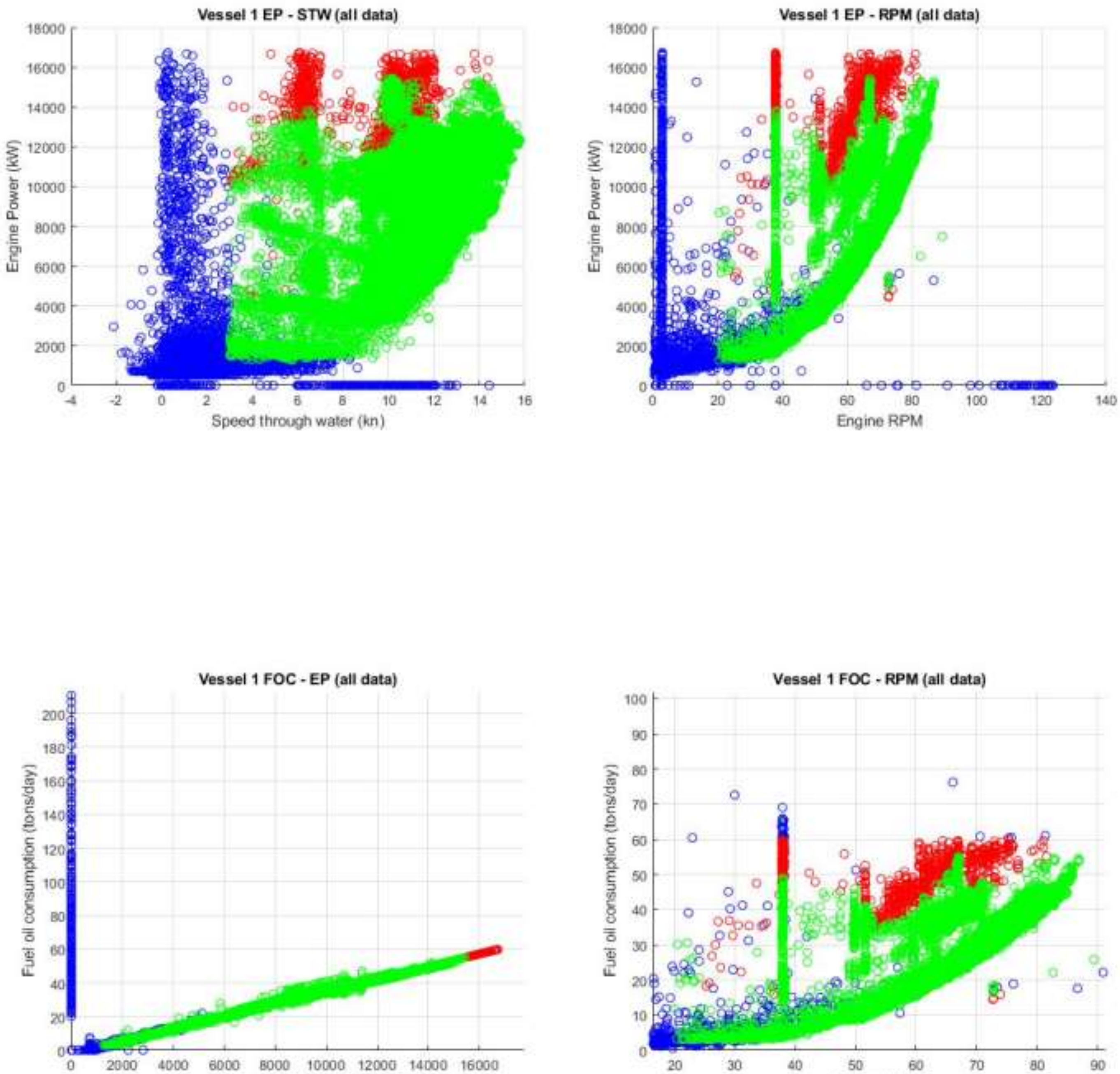

Figure 28: Filter RPM_FOC – Vessel 1

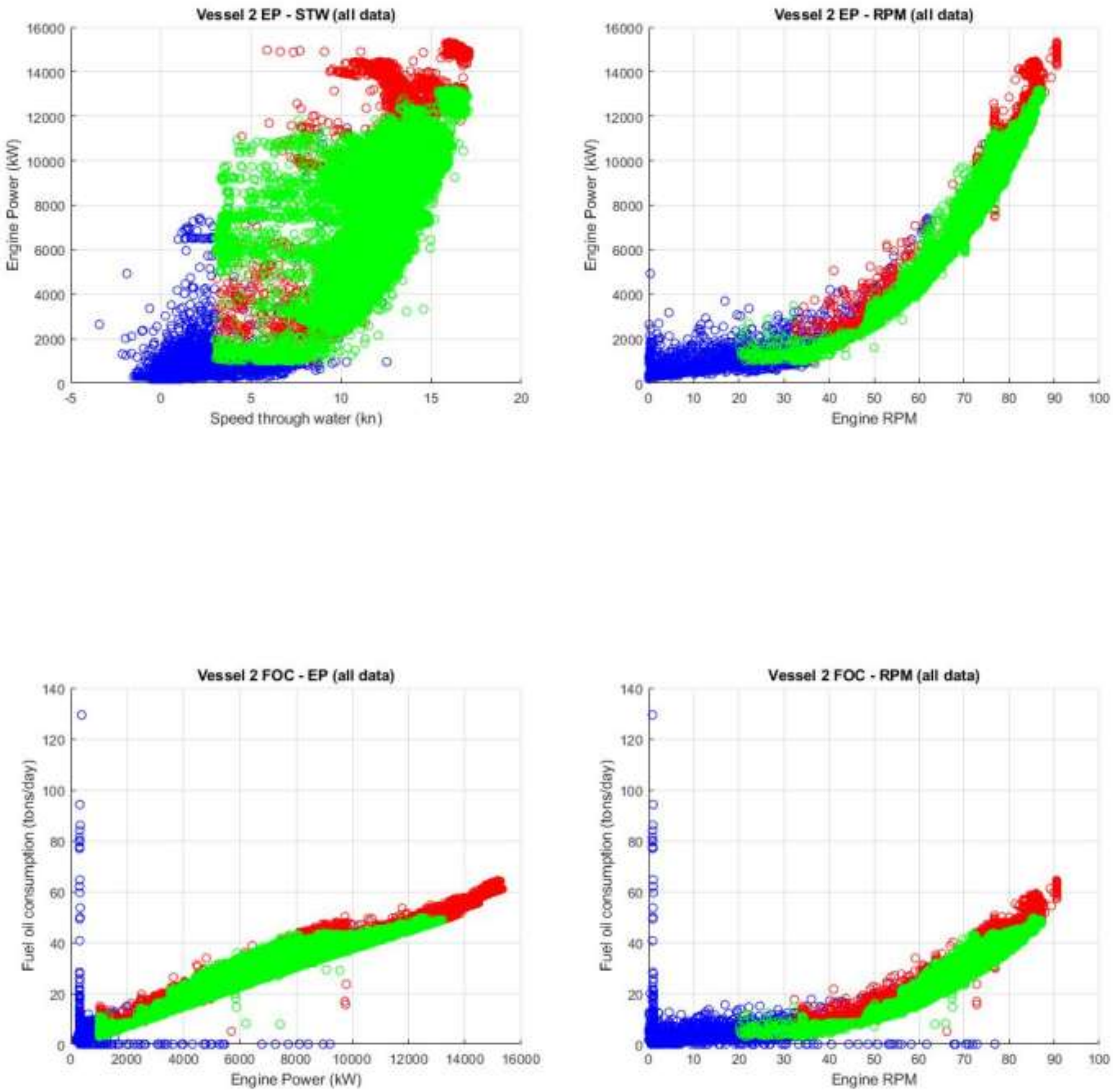

Figure 29: Filter RPM_FOC – Vessel 2.

The effects of the application of the “RPM_FOC” filter on the dataset can be observed with the help of the EP – STW, EP – RPM, FOC – RPM and FOC – EP graphs. The filter has an insignificant effect on the other variables and the relationships that are formed among them, a conclusion that can be easily verified by the graphs’ lack of outlier points (red points).

For Vessel 1, the filter eliminates two regions of the EP – STW graph. The first region ($4 < \mathrm{STW} < 8$ & $\mathrm{EP} > 13{,}000$) is successfully identified as an outlier area, however the second region ($8 < \mathrm{STW} < 12$ & $\mathrm{EP} > 12{,}000$) should be considered as a part of the power – speed curves which are associated with greater hull fouling and/or worse weather conditions and thus, its elimination is not correct. Furthermore, the filter identifies only a small number of outliers in the EP - RPM and FOC - RPM graphs ($\mathrm{RPM} \approx 40$ & $\mathrm{FOC} > 50, \mathrm{EP} > 14{,}000$) for great values of power/consumption while it omits a far greater amount of desirable data points that belong to the 3rd power/consumption – revolutions curve ($50 < \mathrm{RPM} < 70$ & $40 < \mathrm{FOC} < 60, 10{,}000 < \mathrm{EP} < 16{,}000$). Finally, the application of the filter causes the upper right area of the FOC -EP graph to be omitted, an outcome that is considered undesirable since the graph is already sufficiently corrected.

As far as Vessel 2 is concerned, the filter manages to eliminate a significant amount of outlier data points of the EP – STW graph but also discards various data points that belong to higher power – speed curves, which are probably associated with greater hull fouling and/or worse weather conditions. The filter has a negative effect on the already sufficiently corrected power-related graphs since it omits data points associated with greater rpm and power values. In addition to the above, it completely discards the graphs’ areas for $40 < \mathrm{RPM} < 50$ causing an important loss of information concerning the relationship between the power/consumption and the shaft’s revolutions

Overall, the filter manages to identify just a few outlier points for Vessel 1 while omitting a far greater amount of desirable data and thus distorting the dataset. Since the filter impedes the formation of the dataset that better expresses the relationships among the physical quantities rather than facilitating it, it will not be applied in the data correction process.

2.3.2.6 Mean draft – Trim

The TM and TRIM variables are filtered according to the process described in the "Filtering procedure" paragraph. The outlier threshold k and the range v values are shown in Table 12:

Case	Primary: TM	Primary: TRIM
	Secondary: TRIM	Secondary: TM
k	2.5	2.5
v	0.5 tons/day	0.5 rpm

Table 12: Outlier threshold and range values (TM-TRIM).

Both cases are analyzed with the help of graphs for both vessels. For the case in which TM is the primary parameter, the respective filter is called "*TM_TRIM*" while for the one in which TRIM is the primary parameter, the filter is called "*TRIM_TM*". The occurring scatter plots contain data points colored in blue, red or green. The blue points are the ones that are omitted by the threshold filters that are applied during the first part of data correction. The red points are the ones that fulfill the criteria set by the first filtering procedure but are omitted due to the applied single-filter under consideration (TM_TRIM, TRIM_TM). Finally, the green data points are the ones that meet the standards set by the threshold filters and the applied single filter. Presented below are the graphs that are significantly affected by the application of the filter. The effect of the filter on all graphs can be found in the figures included in Appendix A: Data correction – Part II filters.

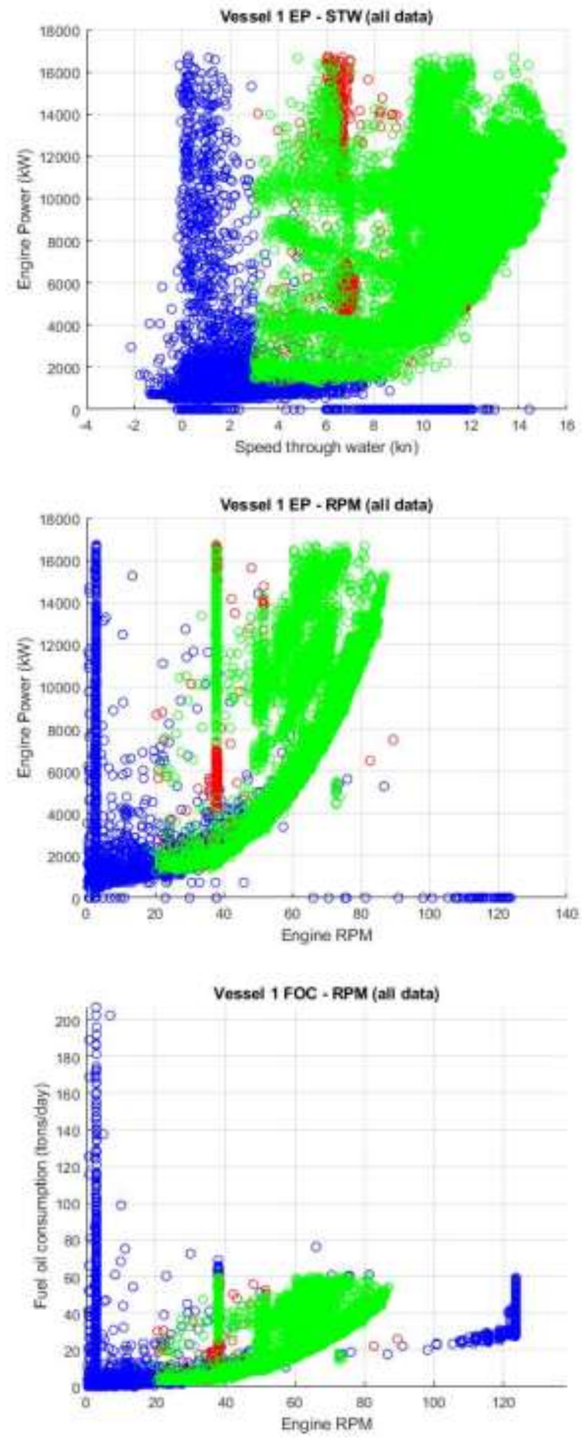

Figure 30: Filter TM_TRIM – Vessel 1

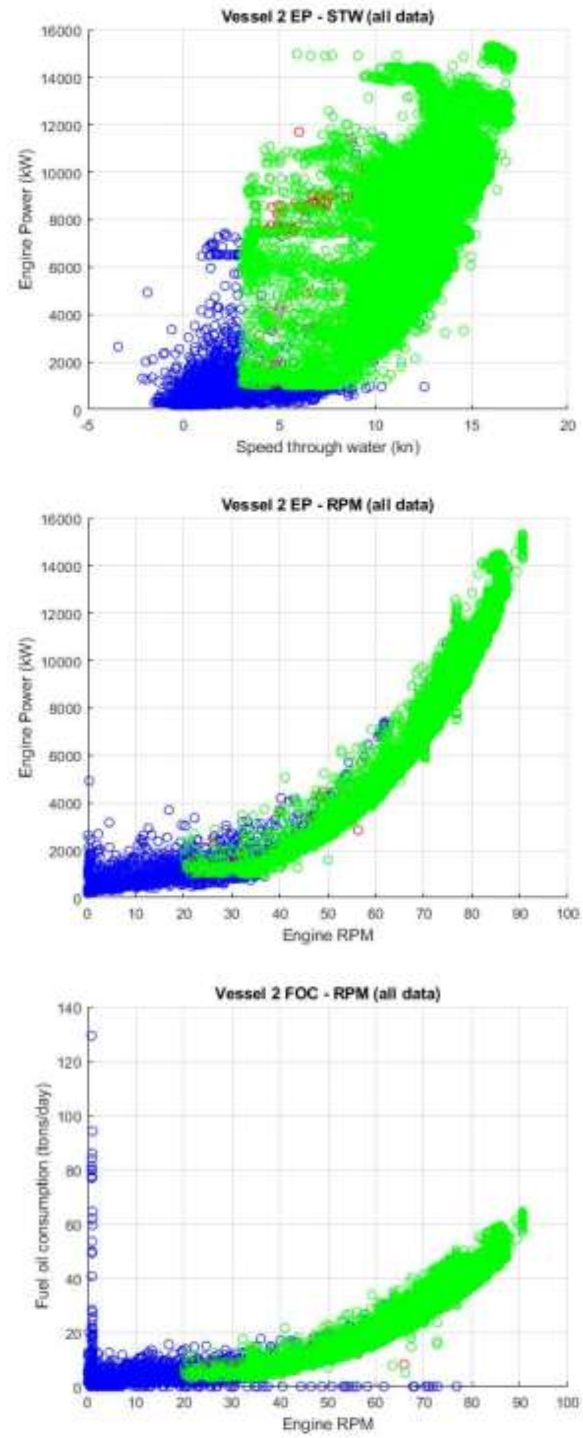

Figure 31: Filter TM_TRIM – Vessel 2.

The effects of the application of the “TM_TRIM” filter on the dataset can be observed with the help of the EP – STW, EP – RPM and FOC – RPM graphs. The filter has an insignificant effect on the other variables and the relationships that are formed among them, a conclusion that can be easily verified by the graphs’ lack of outlier points (red points).

For Vessel 1, the filter successfully eliminates the vertical column of outliers located at the middle area of the EP – STW graph $(6 < \mathrm{STW} < 8)$ without omitting any group of desirable data points. Moreover, it manages to identify the outlier points that form the lower part of the vertical line $(\mathrm{RPM} \approx 40\ \&\ \mathrm{FOC} < 30, \mathrm{EP} < 8{,}000)$ of the EP -RPM and FOC – RPM graphs.

As far as Vessel 2 is concerned, the filter has limited and insignificant effect, failing to further correct the dataset.

Overall, the filter manages to identify a significant amount of outlier data points without omitting any desirable areas. Despite the fact that its effect on the Vessel 2 dataset is limited and that it fails to improve the draft related graphs, it completes the correction of the power/consumption related graphs since it eliminates the lower part of the vertical outlier line that is corrected by the “EP_RPM” filter. Therefore, the implementation of the filter is crucial for the creation of a more accurate dataset.

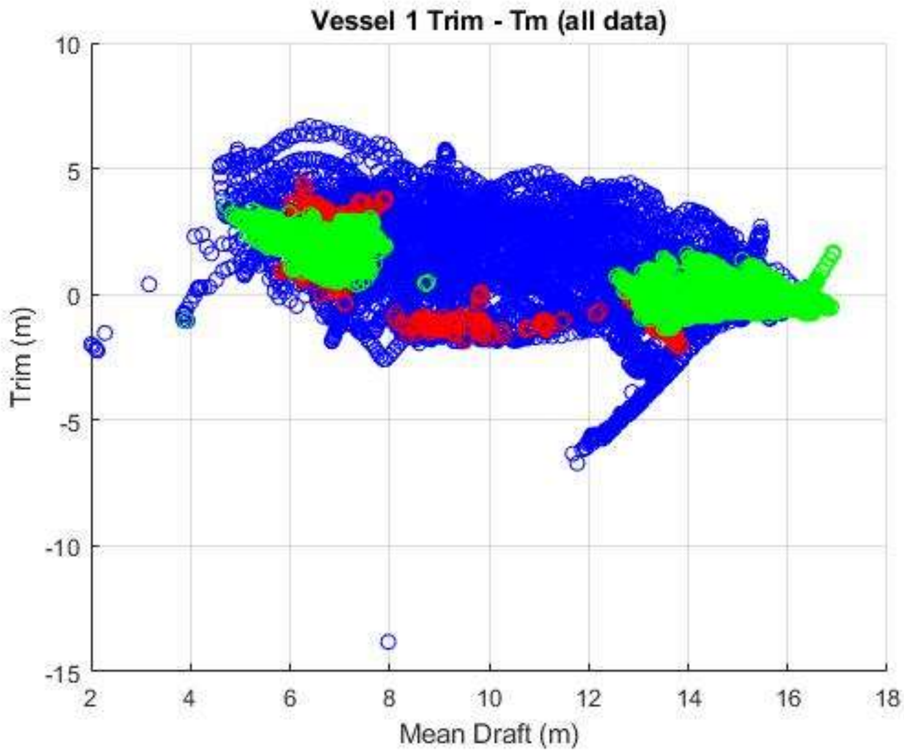

Figure 32: Filter TRIM_TM – Vessel 1.

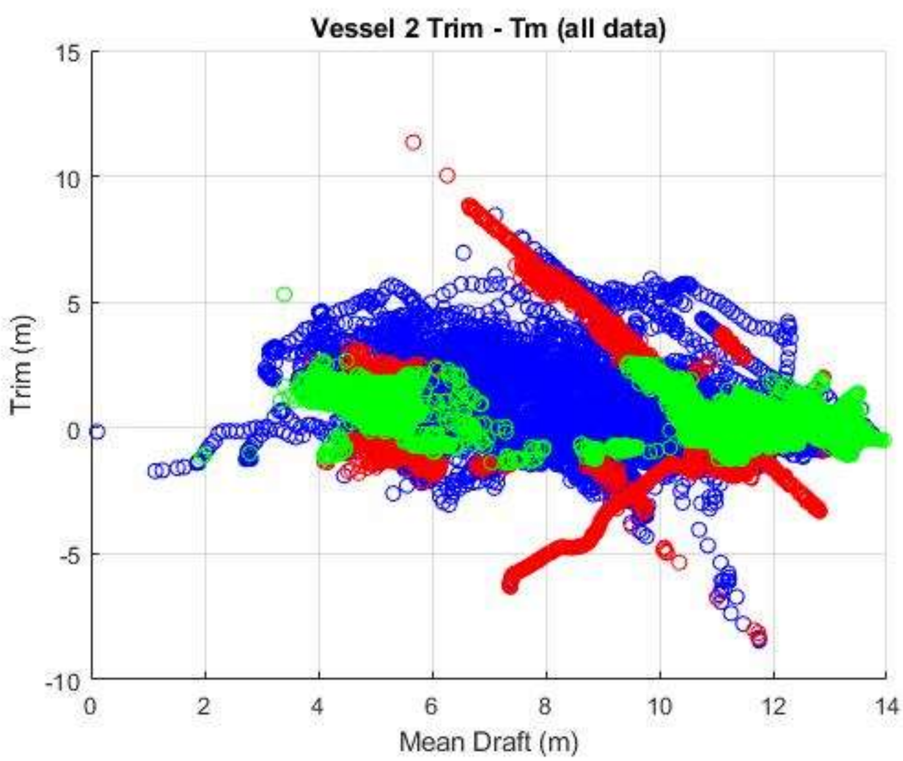

Figure 33: Filter TRIM_TM – Vessel 2.

The effects of the application of the “TRIM_TM” filter on the dataset can be observed with the help of the Trim – Tm graphs. The filter has an insignificant effect on the other variables and the relationships that are formed among them, a conclusion that can be easily verified by the graphs’ lack of outlier points (red points).

For Vessel 1, the filter successfully eliminates the middle area of the Trim – Tm graph $(8 < \mathrm{Tm} < 12)$ that should be considered an outlier region. The application of the filter helps the formation of two “cloud” regions of data points on the graph, which represent the ballast and laden conditions of the vessel.

As far as Vessel 2 is concerned, the filter manages to identify the majority of the outliers and removes the inconsistent diagonal lines that distort the dataset. As a result, two discrete areas of drafts are formed, indicating a clear distinction between the ballast and the laden condition.

Overall, the filter manages to identify a significant amount of outlier data points without omitting any desirable areas. Through its application two bunches of data points are form in the Trim – Tm graphs, each representing the ballast and laden condition of the vessel. The filter is essential in correcting draft/trim values and will be used in the data correction process.

2.3.2.7 Multifilter

The complete and solid correction of the dataset is achieved by the application of a multifilter that effectively combines the selected single filters. The multifilter contains the following sub-filters:

Filter	Primary parameter	Secondary parameter	Outlier threshold k	Range v
SOG_STW	SOG	STW	2	0.5 kn
STW_SOG	STW	SOG	2	0.5 kn
EP_RPM	EP	RPM	2.5	100 kW
TM_TRIM	TM	TRIM	2.5	0.5 m
TRIM_TM	TRIM	TM	2.5	0.5 m

Table 13: Multifilter's single filters.

The application of the multifilter leads to the creation of the following graphs. The occurring scatter plots contain data points colored in blue, red or green. The blue points are the ones that are omitted by the threshold filters that are applied during the first part of data correction. The red points are the ones that fulfill the criteria set by the first filtering procedure but are omitted due to the applied multifilter. Finally, the green data points are the ones that meet the standards set by the threshold filters and the applied multifilter.

The final graphs indicate that the threshold filters applied at the first part of the data correction, along with the multifilter applied at the second part manages to eliminate the vast majority of the outlier data points without omitting desirable data areas that provide valuable information on the performance of the vessels. The filtered dataset better describes the relationships among the physical quantities and thus, can be used as the solid basis of a reliable regression model, as well as of an accurate KPI analysis.

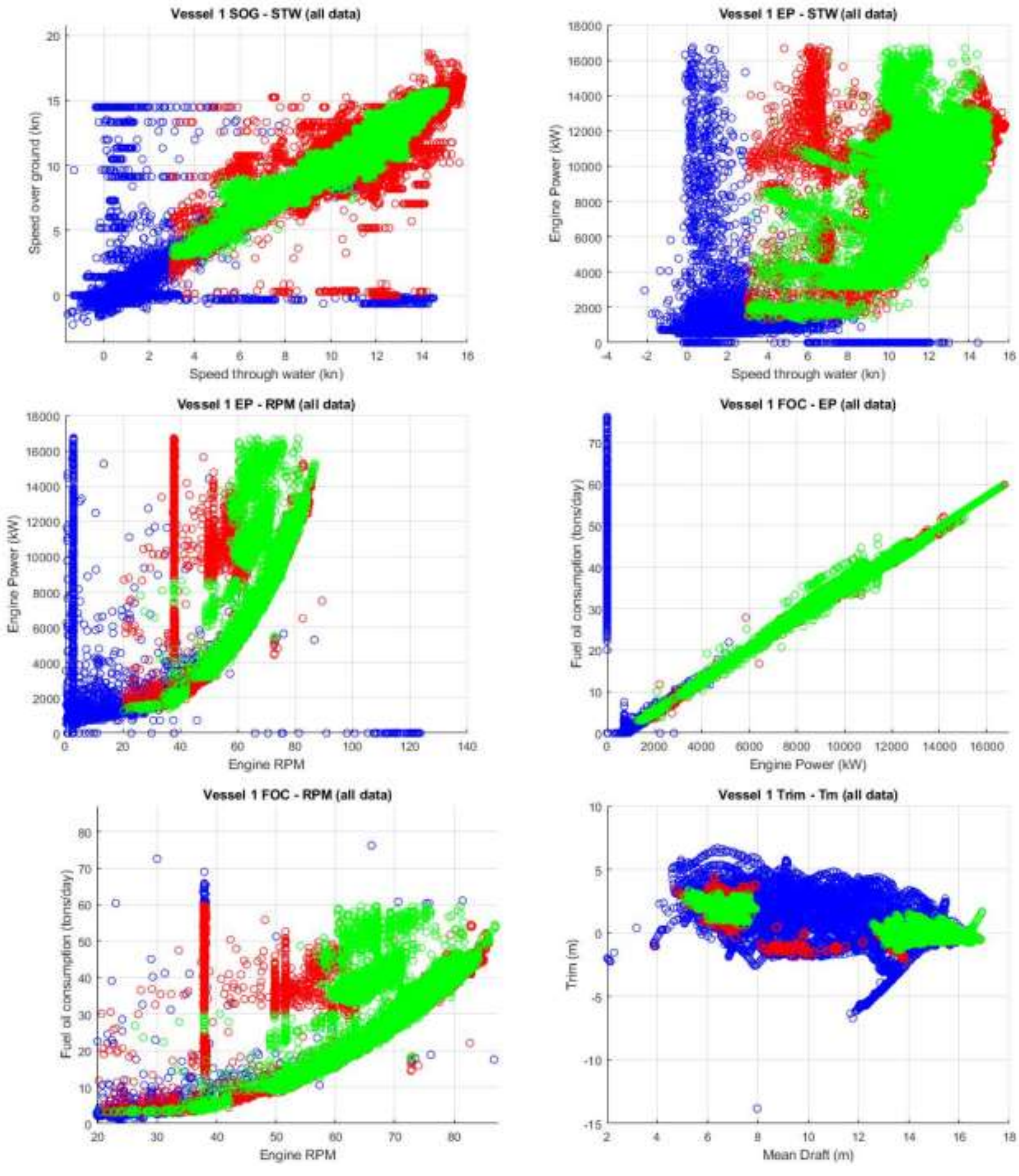

Figure 34: Multifilter Vessel 1.

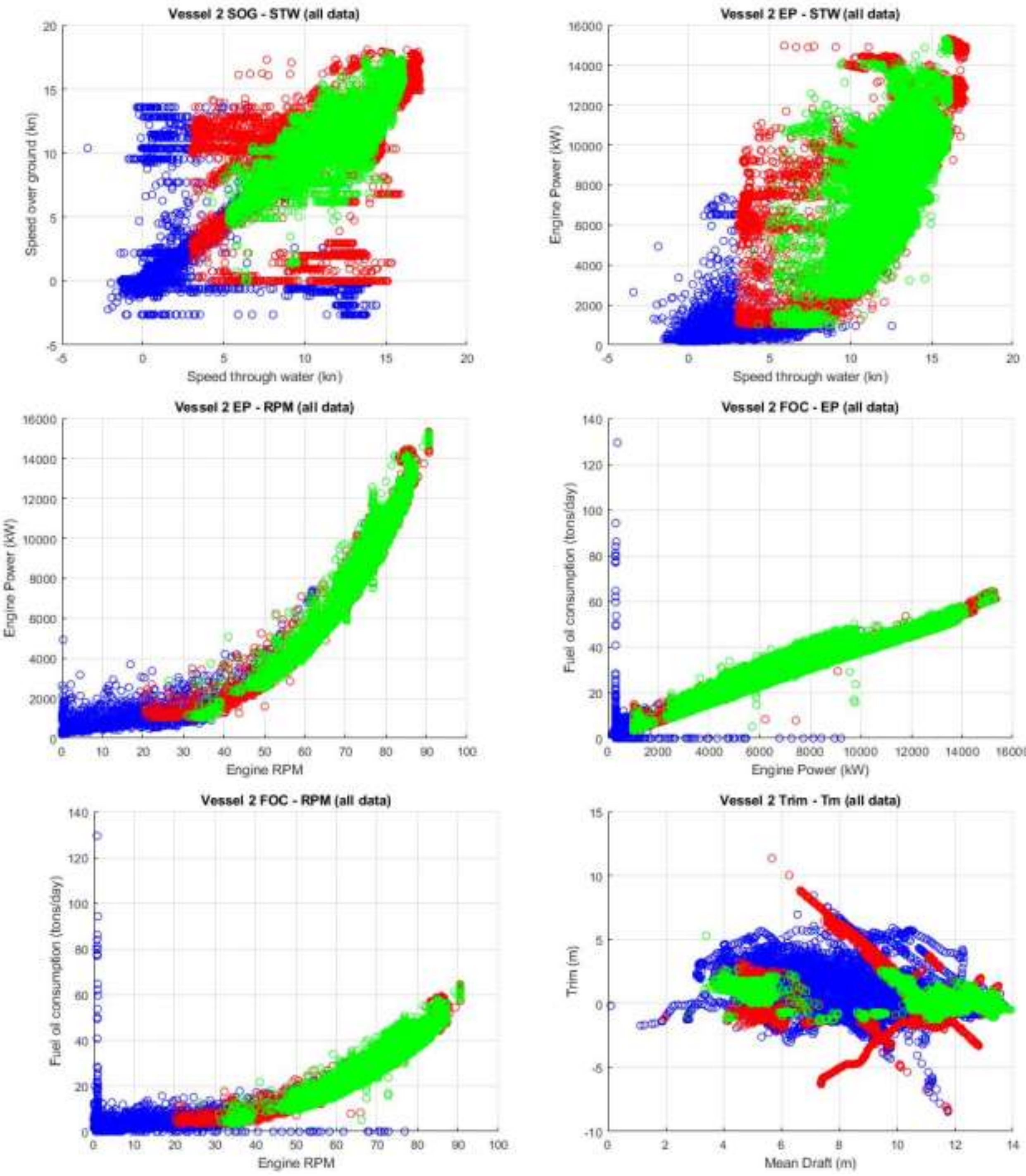

Figure 35: Multifilter Vessel 2.

[This page is intentionally left blanc]

3 Key performance indicators

The aim of the chapter is to calculate some key performance indicators that depict the changes in the performance level of the two vessels and to identify the different operational conditions throughout the examined period of time (i.e. the period prior to dry-dock). Key performance indicators (KPIs) are used as a quantitative method of performance measurement. A KPI analysis shall be able to depict alterations in performance and reach a solid conclusion concerning the impact of the propeller duct on Vessel 1.

The following three KPIs are calculated and analyzed over the monitoring period:

- $\mathrm{KPIa} = \mathrm{P}/\mathrm{n}^3$: It corresponds to the propeller curve coefficient [4]. When the KPI's value decreases, the vessel's performance increases since less engine power is required to maintain constant shaft's revolutions (constant denominator) and greater rpm can be achieved for the same level of engine power (constant numerator).

- $\mathrm{KPIb} = \mathrm{FOC}/\mathrm{P}$: It expresses the specific fuel oil consumption (SFOC). When the KPI's value decreases, the vessel's performance increases since the less amount of fuel is required to maintain the same engine power (constant denominator) and more power can be achieved by consuming the same amount of oil (constant numerator).

- $\mathrm{KPIc} = \mathrm{V}/\mathrm{FOC}$: It expresses the fuel efficiency [5]. When the KPI's value increases, the vessel's performance also increases since for the same amount of consumed fuel higher speed through water is achieved (constant denominator) and for the same speed value less fuel is required (constant numerator). This KPI is calculated separately for the two loading conditions (ballast and laden).

The vessels' performance throughout the observation period is expressed by KPI – time plots that can successfully depict performance-related fluctuations. In order to identify the KPIs' trends over time, the datasets are divided into the following time periods:

$$\text{Vessel 1:}\begin{cases}\text{Period 1A: before propeller polishing}\\ \text{Period 1B: between propeller polishing and dry} - \text{dock}\\ \text{Period 1C: after dry} - \text{dock}\end{cases}$$

$$\text{Vessel 2:}\begin{cases}\text{Period 2A: before dry} - \text{dock}\\ \text{Period 2B: after dry dock}\end{cases}$$

Changes in performance, expressed by the KPIs, can be mainly explained by three events:

- Dry-dock: a repair process which includes the cleaning of the hull. As a result, the ship's resistance is reduced and its propulsion performance is improved.
- Propeller polishing (only for Vessel 1): a repair which greatly improves the propeller's efficiency and, thus, the overall performance of the vessel.
- Duct installation: a fitting procedure that aims at improving the propeller's efficiency and whose impact should be evaluated by the KPI analysis.

Vessel 1 had its propeller polished prior to the dry-dock during which the Mewis duct was installed. It can be understood that the time period between the two actions (Period 1B) should be examined separately from the initial period, during which the vessel monitoring begun, and the final period, during which the vessel operates with a duct. Separating Period 1B from the others is an essential step towards the accurate estimation of the duct's effect on the first vessel's performance since it allows a solid comparison between the two vessels, given that Vessel 2 did not had its propeller polished.

Prior to the KPI analysis, three corrections, different from those of the previous chapter, are applied to the divided dataset in order to improve the KPIs' calculations. The first correction aims at reducing the variance of the draft values by concentrating them around two reference values (ballast and laden drafts). The second one takes into account the effect of the weather on the dataset and sets boundaries on the wind speed and the rudder angle, two previously not filtered parameters. Finally, the engine power and the fuel oil consumption are corrected by the Admiralty Coefficient.

3.1 Draft correction

The drafts of the vessel are expected to form “cloud” regions when plotted, an expectation which is met by the corrected dataset produced in the previous chapter. Each region represents a different loading condition. In the current study, the loading conditions that are analyzed are the “laden” and the “ballast” and as a result the dataset is divided into two groups, one for each condition.

In order to better define these loading conditions, the dataset is further filtered according to the following:

- For each of the two groups (laden and ballast) the mode value of the mean draft is calculated ($T_{m\ mode}$) .
- For each data point the following deviation is calculated:
$$T_{dev} = \frac{|T_m - T_{m\ mode}|}{T_{m\ mode}}$$
- If $T_{dev} > 10\%$ then the data point is omitted.

The result of the above filtered is expressed via the following scatter plots. The blue points are the ones that are within $\pm 10\%$ of the mode values. The black points are omitted.

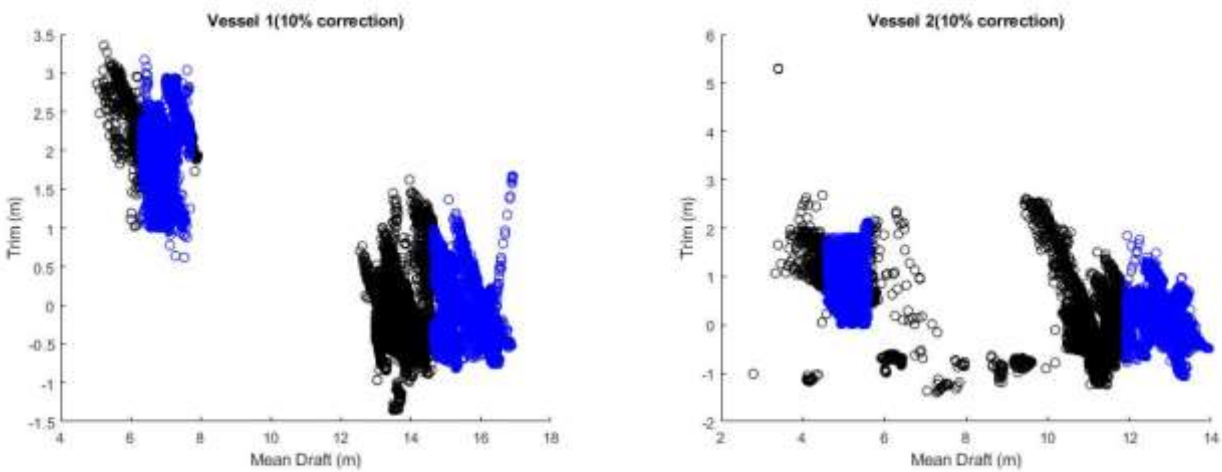

Figure 36: Trim – Mean Draft graph (10% draft correction).

The mean draft values are calculated for both vessels and for both loading conditions

	Ballast	Laden
Vessel 1	6.927	15.561
Vessel 2	5.158	12.859

Table 14: Mean drafts.

3.2 Weather correction

The quality and accuracy of the KPIs can be significantly improved through the application of a weather correction. By neglecting anomalies and bias caused due to extreme weather conditions, the calculated KPIs can better quantify and depict the alterations in the vessels' performance in sea travel.

In order to achieve the above correction, the following criteria are set [6]:

$$\text{Wind Speed (WS)} < 8\ \text{m/s}$$
$$-5 < \text{Rudder Angle (RA)} < 5\ \text{deg}$$

Any data point that fails to comply with the wind speed and rudder angle limitations is not taken into account in the KPI analysis. Extreme wind speeds can cause significant variations of power and propulsion related parameters such as the engine power or the speed through water. In addition, big rudder angles indicate a sudden change of course or an in-port maneuvering which instantaneously distort the dataset.

3.3 Admiralty correction

The KPIs calculation is partly based on the engine power (EP) and fuel oil consumption (FOC) parameters. These parameters are corrected by the Admiralty Coefficient A which is defined:

$$A = \frac{\nabla^{\frac{2}{3}} \cdot V^3}{P} = \frac{\nabla_{des}^{\frac{2}{3}} \cdot V_{des}^3}{P_{des}}$$

For equal ship speed $V = V_{des}$ the propulsion power is:

$$P = P_{des} \cdot \left(\frac{\nabla}{\nabla_{des}}\right)^{\frac{2}{3}}$$

Each power value is corrected by the quantity $\left(\frac{\nabla}{\nabla_{des}}\right)^{\frac{2}{3}}$. However, the vessels' displacements are not included in the initial data provided by LAROS. In order to overcome this setback, the following assumption is made [7]:

$$\left(\frac{\nabla}{\nabla_{des}}\right) \sim \left(\frac{T}{T_{des}}\right)$$

As a result, the engine power and the fuel oil consumption, whose relationship is linear, are corrected by the quantity $\left(\frac{T}{T_{des}}\right)^{\frac{2}{3}}$. The T_{des} is equal to the mean draft, ballast or laden depending on the loading condition.

3.4 KPI Analysis

The three KPIs are calculated and plotted over the examined time period. The KPI – time graphs along with their analysis are presented below. It should be noted that Period 1C and Period 2B (after dry-dock) are divided into two sub-periods: one for the first year after dry-dock and one for the second and a half year. The graphs are accompanied with trendlines that help in identifying the trends of the KPI values in different time periods.

The analysis includes the evaluation of the KPIs' fluctuations over time and the consequent changes in the vessels' performance. An explanation of these alterations, deriving from known events or actions that are expected to affect performance, is provided.

Once the graph analysis is accomplished, a comparison is made between the two vessels, for each KPI, in order to estimate the duct's effect and its magnitude.

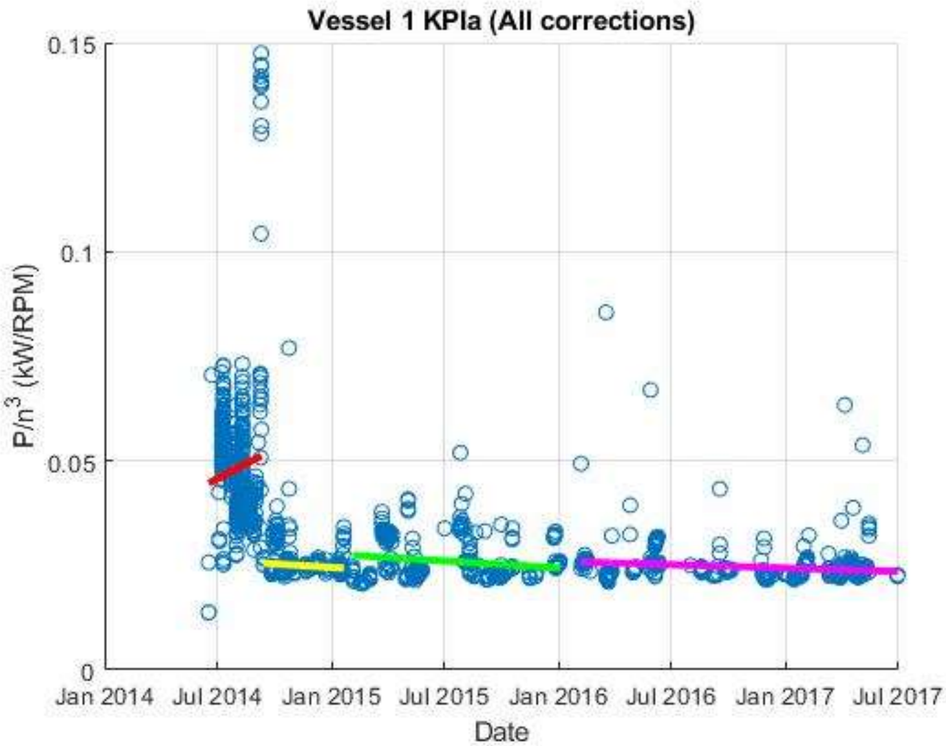

Figure 37: KPIa – time (Vessel 1)

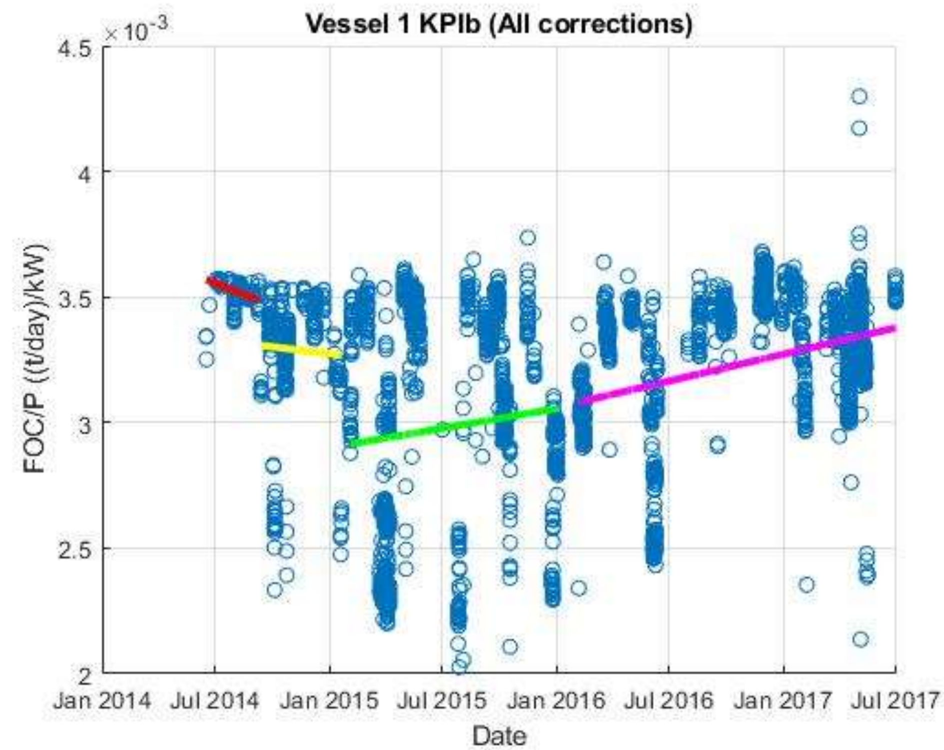

Figure 38: KPIb – time (Vessel 1)

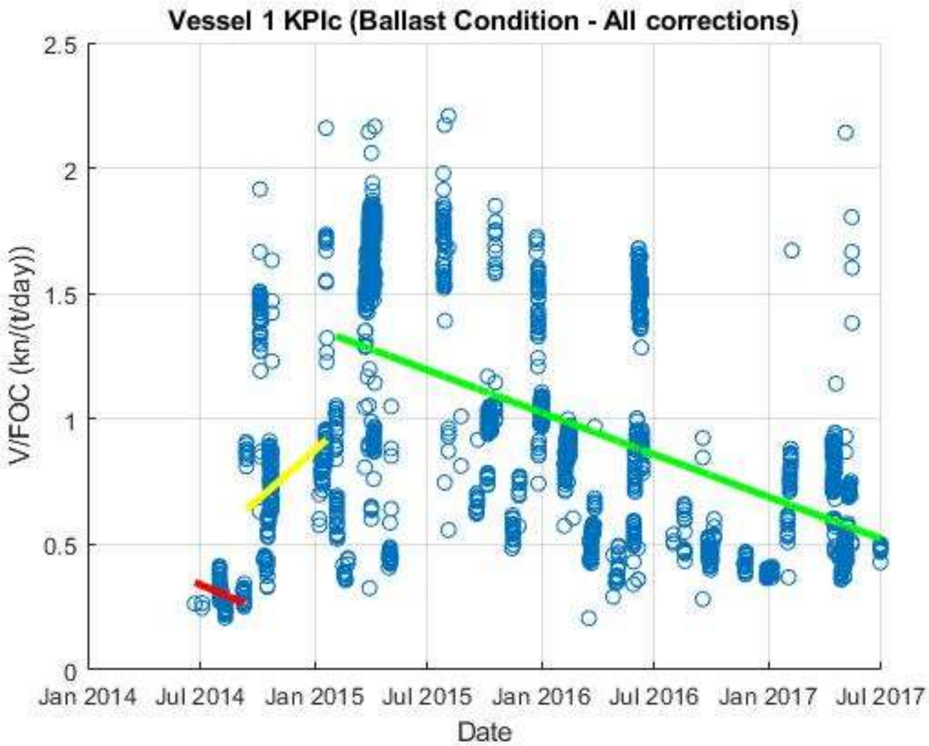

Figure 39: KPIc – time (Vessel 1 – Ballast)

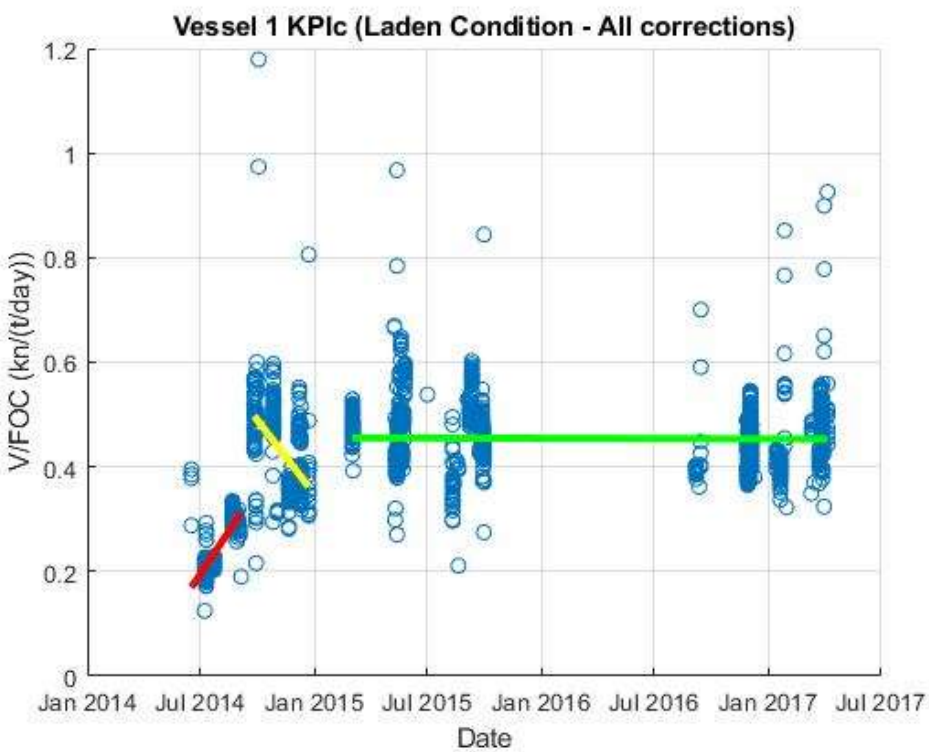

Figure 40: KPIc – time (Vessel 1 – Ballast)

3.4.1 KPIa – Vessel 1

As it can be observed in the graph above, KPIa (P/n^3) presents an upward trend (red line) durng the period 1A, prior to the propeller polishing, starting from 0.045 and increasing just a bit over 0.050. Given that KPIa value and vessel performance are inversely proportianal, it can be concluded that the first period of monitoring is associated with a decreasing performance.

Once the propeller is polished, the KPIa value is reduced by approximately 50% (from 0.050 to 0.025). This reduction depicts the great impact of the propeller polish on the vessel's performance. For the remaining Period 1B, the trendline (yellow line) has a slightly negative slope which indicates a insignificant increase in performance levels.

During Period 1C (1st year afte dry-dock), the KPIa trendline (green line) is almost parallel to the previous one, indicating a similar downward trend that is associated with incerasing performance. However, the trenline is slightly over the one that characterizes the propeller polishing period and only manages to reach KPIa values of under 0.025 at the end of the measuring period (after almost a year) while 1B trendline achieves such low values in just a few months. It can be understood that the effect of the dry-dock during the first year of operation is important but not as strong as the one of the propeller polishing.

During the second year after the duct installation, the KPIa trendline follows a similar pattern with the previous one. While its values are slighlty increased at first, the trendline's negative gradient causes a small reduction in KPIa values.The trendline shows that the KPIa values remain relatively constant and as a result no significant improvement in performance is achieved during the two years following the duct installation.

While the reducton caused by the propeller polishing was about 50%, the further reduction in KPIa values taking place during the 1C period was less than 15%. Despite this fact, the duct's effect should be considered positive since the increased performance levels, which are achieved by the propeller polishing, remain constant for a significant amount of time while also having a small, yet existant, increasing trend (due to the trendlines' downward trend). If the increase of hull fouling is also taken into consideration, it can be estimated that the duct significantly increases performace as it manages to maintain the decreasing trend of KPIa despite the additional obstacle of hull fouling, whose impact grows as time passes.

3.4.2 KPIb – Vessel 1

As it can be observed in the graph above, KPIb (FOC/P) receives high values during the first monitoring period. The trendline (red line) values drop from over 0.0035 to just under 0.0035 showing that the poor performance levels have a small increasing trend.

Once the propeller is polished, KPIb values are reduced by approximately 5%, reaching values of just over 0.0033. Despite the small reduction that is associated with an insignificant imporovement in performance, the trenline of Period 1B (yellow line) indicates a decreasing trend in KPIb values that further increases performance and underlines the positive contribution of the propeller polishing on the vessel's propulsion.

During Period 1C (1^{st} year afte dry-dock), the KPIa trendline (green line) receives values that are significanty smaller than those of the 1B trendline, a fact that reveals an improvement in performance after the dry-dock. At the beginning of the 1^{st} year after dry-dock, a decrease of about 10% is noted in the KPIb trendline values. Despite the fact that the trendline shows an upward trend, which is associated with decreasing performance, the examined KPIb values are significantly lower during Period 1C (1^{st} year) than during Period 1B.

During the second year after the duct installation, the KPIa trendline follows a similar pattern with the previous one, having a significant increasing trend. Trendline values continue to increase causing KPIb values to eventually surpass the limits of the yellow line (Period 1B), in about two years after the dry-dock. The continuing upward trend indicates that KPIb is expected to receive high values, similar to those prior to propeller polishing.

Despite the fact that for KPIb the dry-dock has a greater positive impact than the propeller polishing, it can be assumed that the incease in performace is related to the hull cleaning rather than the duct installation, since performance is steadily reduced as time goes by, an observation that can be explained by an increase in hull fouling. The propeller duct may have slowed the deteriotation of performance levels, a hypothesis that cannot be verified by the current graphs, but it has definitely failed to improve performance in the long-term, being less efficient than hull cleaning.

3.4.3 KPIc Ballast – Vessel 1

As it can be observed in the graph above, KPIc Ballast (V/FOC) receives extremely low values, which are associated with low fuel efficiency and thus, poor performance, during the first monitoring period. In addition to that, the trendline (red line) has a negative slope that causes KPIc Ballast values to further decrease (from 0.35 to 0.26).

Once the propeller is polished, KPIc Ballast values skyrocket from around 0.26 to 0.65 (150% increase), with the yellow trendline receiving that are far greater that those of the red line. This increase in performance becomes greater as the Period 1B trendline presents a steep upward trend that leads to just over 0.9 KPIc Ballast values at the end of the period. The overall 150-200% increase in KPIc Ballast values along with the positive slope of the trendline indicate that the impact of the propeller polishing on performance is enormous.

During Period 1C (1st year afte dry-dock), the KPIc Ballast trendline (green line) receives values that are greater than 1, surpassing the performance levels achieved during the 1B Period. Initially, the trendline’s value is increased by over 50% compared with the 1B trendline (from 0.9 to 1.4), a fact that indicates the positive effect of the dry-dock repairs. As the time passes, the trendline’s values are decreased, however, never dropping below the 1 threshold.

During the second year after the duct installation, the KPIc Ballast trendline continues its downward pattern, taking values from around 0.9 (at the beginning of the period) to around 0.65 (towards the end of the period). Despite the deterioration of performance, it can be observed that, two years after the dry-dock, KPIc Ballast values approach the initial values of Period 1B.

Despite the fact that for KPIc Ballast the dry-dock has a greater positive impact than the propeller polishing, it can be assumed that the incease in performace is related to the hull cleaning rather than the duct installation, since performance is steadily reduced as time goes by, an observation that can be explained by an increase in hull fouling. The propeller duct may have slowed the deteriotation of performance levels, a hypothesis that cannot be verified by the current graphs, but it has definitely failed to improve performance in the long-term, being less efficient than hull cleaning.

3.4.4 KPIc Laden – Vessel 1

As it can be observed in the graph above, KPIc Laden (V/FOC) receives extremely low values, which are associated with low fuel efficiency and thus, poor performance, during the first monitoring period. However, the trendline (red line) presents an upward trend managing to almost double the KPIc Laden value from around 0.15 to just over 0.3.

Once the propeller is polished, KPIc Laden values are increased by about 60% (from 0.3 to 0.5), indicating a significant increase in performance. However, the trendline's (yellow line) downward trend causes the KPIc values to drop to pre-polishing period's levels towards the end of Period 1B. As a result, while the propeller polishing successfully increases performance levels, this increase is not long-term.

During Period 1C (1st year afte dry-dock), the KPIc Laden trendline receives values that are greater than 0.4, surpassing the performance levels achieved during the end of Period 1B. At the beginning of Period 1C, KPIc Laden values are increased by about 30%, a fact that reveals the positive contribution of the dry-dock repairs in the performance of the vessel. The trendline (green line) has an increasing trend, causing the KPIc Ballast values to increase from 0.44 to 0.48 (around 10% increase) in one year. This improvement contradicts the expected deterioration in performance due to hull fouling and thus, underlines the positive effect of the duct installation.

During the second year after the duct installation, the KPIc Laden trendline continues its upward pattern, and, despite being slightly reduced at first, manages to overcome the increaased hull fouling and maintain the achieved level of performance.

The dry-dock trendlines indicate that the KPIc Laden values are successfully maintained between 0.4 and 0.5 with an upward trend that is associated with increased efficiency. Despite the effect of hull fouling, which becomes greater as time goes by, not only are the KPIc Laden values not decreased but they are also steadily increased. This long-term improvement highlights the positive impact of the duct on the vessel's overall performance.

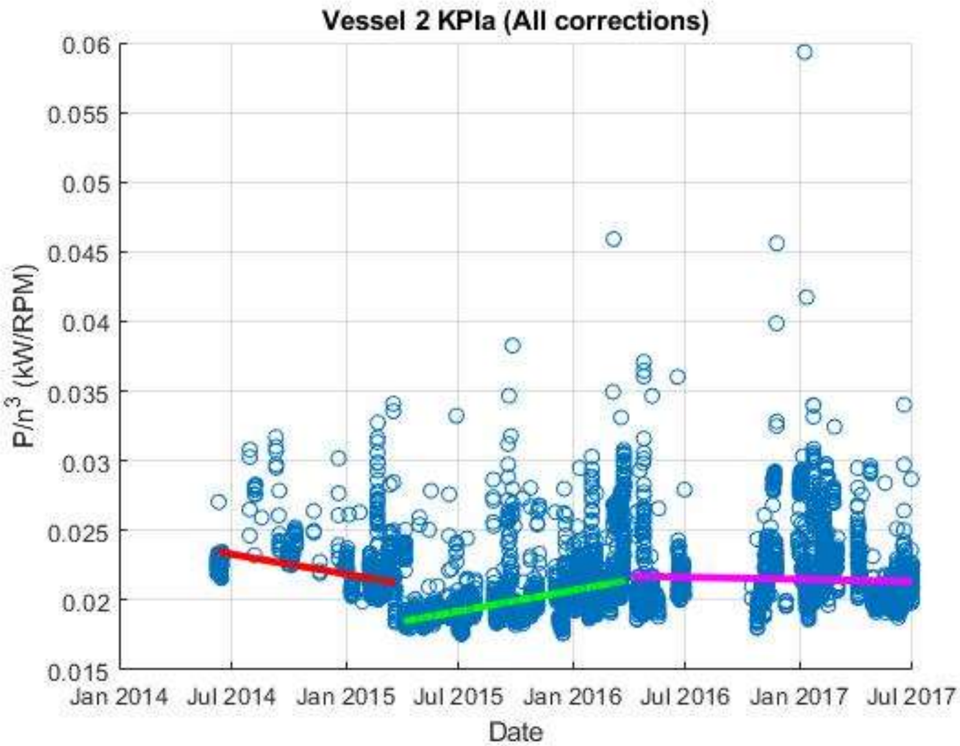

Figure 41: KPIa – time (Vessel 2).

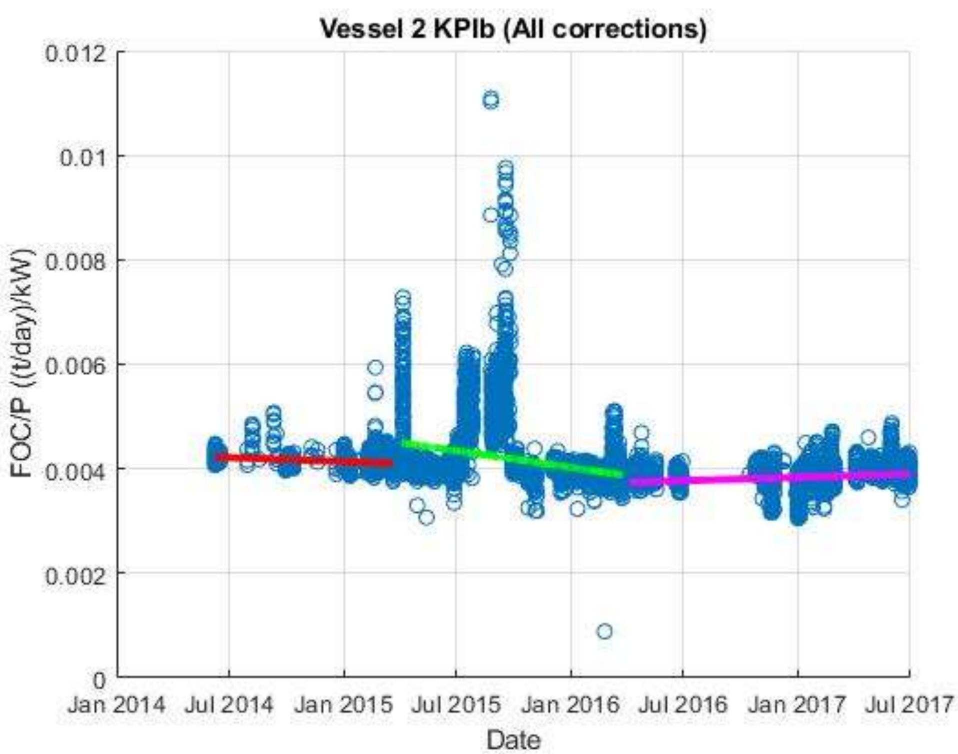

Figure 42: KPIb – time (Vessel 2).

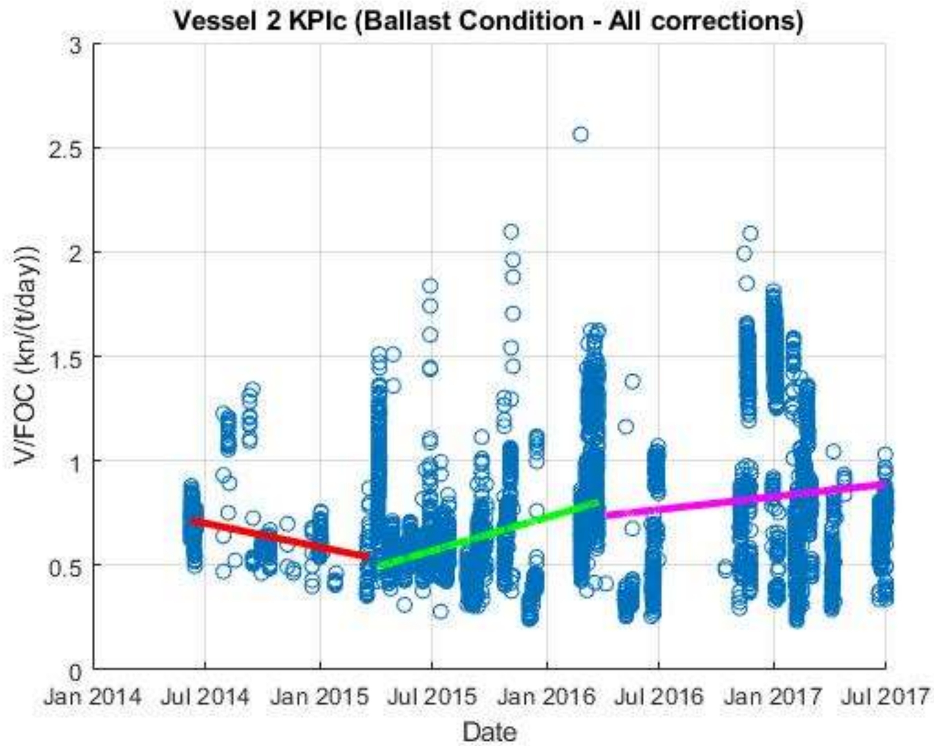

Figure 43: KPIc – time (Vessel 2 – Ballast).

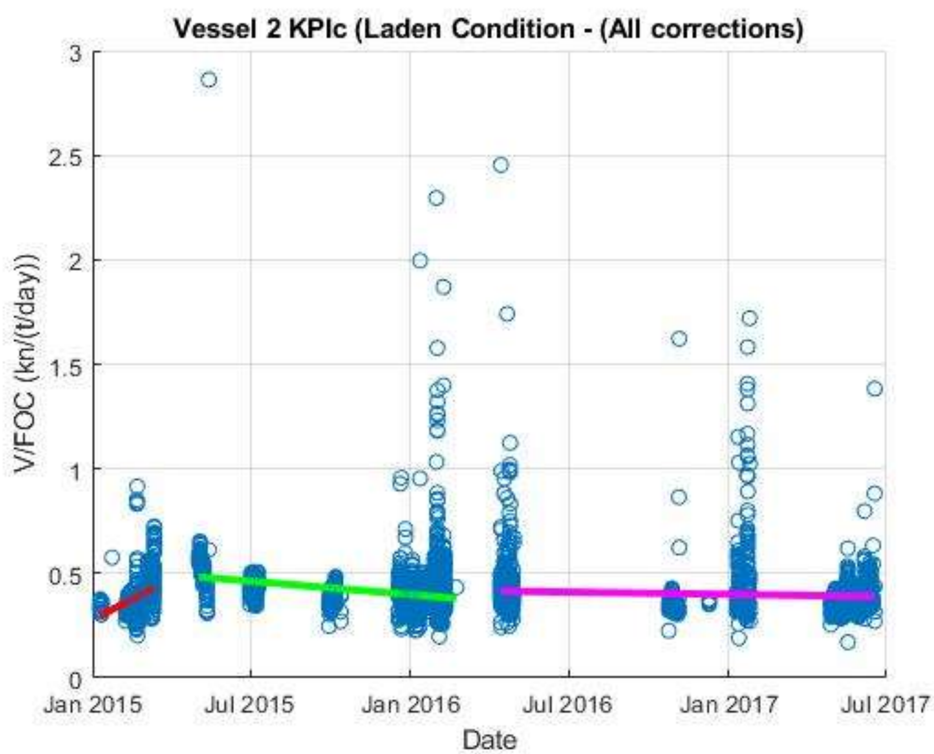

Figure 44: KPIc – Time (Vessel 2 – Laden).

3.4.5 KPIa – Vessel 2

As it can be observed in the graph above, KPIa receives relatively higher values during the pre-dry-dock period than it does during the post-dry-dock period. The trendline (red line) reaches an overall maximum of about 0.0235 at the beginning of Period 2A. However, the gradient of the line is negative, a fact that indicates an improvement in terms of performance as time goes by. Towards the end of Period 2A, KPIa's has a value of about 0.021 (10% decrease).

During Period 2B (1st year afte dry-dock), the KPIa trendline's values (green line) are initially reduced by about 10%, receiving values under 0.020 and around 0.0185. Despite this reduction in KPIa values, which is associated with an increase in performance, the trendline has an upward trend that eventually causes KPIa values to return to pre-dry-dock levels one year after dry-dock (first part of Period 2B). This deterioration in performance can be explained by the hull fouling which gradually increases after the dry-dock repairs. Despite the increase in KPIa values, the threshold value set at the end of Period 2A (end of red line) is just slightly surpassed by Period 2B's fisrts trendline many months after the dry-dock.

During the second year after dry-dock, the KPIa values become steadier, with the trendline (magenta line) becoming almost horizontal with an insignificant negative slope. Despite the expected increase of hull fouling, the performace is no further deteriorated after the first year of the post-dry-dock period. Performance seems to have been stabilized, with KPIa receiving values around 0.021.

Overall, dry-dock initially reduces KPIa values by about 10% and, as the time passes, its effect becomes less significant, probably due to the re-fouling of the hull. However, KPIa is finally stabilized at slightly smaller values, a fact that undelines the small, yet existant, long-term impact of the dry-dock repairs.

3.4.6 KPIb – Vessel 2

As it can be observed in the graph above, KPIb receives relatively higher values during the pre-dry-dock period than it does during the post-dry-dock period. The trendline (red line) is approximately stable and its initial values are around 0.0042. The slightly negative slope of the trendline causes KPIb values to drop to around 0.0041 towards the end of Period 2A, a decrease that is rather insignificant.

During Period 2B (1st year afte dry-dock), the KPIa trendline's values (green line) are initially increased by about 10%, a result that is not anticipated as performance is expected to increase after dry-dock and hull cleaning repairs. A possible explanation for this contradiction is the vertical column of data points that can be spotted at the begging of Period 2B, which is probably an area of undetected outliers that causes a slight distortion in the KPIb's calcalation. This assumption is stregthened when the trendline is examined, as its significant negative gradient quickly reduces the KPIb values and eventually causes them to drop below 0.0040, revealing the positive impact of the dry-dock repairs.

During the second year after dry-dock, the trendline (magenta line) receives values under 0.0040, an evidence of the dry-dock's long term impact. The trendline's upward term can be explained by the gradual hull fouling, whose impact becomes greater as time passes.

Overall, similarly to the previous KPI values, the KPIb values are initially reduced by the dry-dock repairs, an effect that becomes less significant in the long-term, causing performance to return close to its pre-dry-dock levels in about two years.

3.4.7 KPIc Ballast – Vessel 2

As it can be observed in the graph above, KPIc Ballast receives relatively lower values during the pre-dry-dock period than it does during the post-dry-dock period. In addition to that, the trendline (red line) has a negative slope causing an overall reduction of 25% during Period 2A (from 0.72 to 0.54), an evidence of the deterioration of performance before the dry-dock.

During Period 2B (1st year afte dry-dock), the KPIc Ballast trendline's values (green line) begin to increase as the line's gradient is positive. The improvement in performance levels is gradual and significant, as an overall 50% increase is achieved towards the end of the first post-dry-dock year (from 0.54 to 0.8). The fuel efficiency in the ballast condition maanges to reach higher levels, a fact that indicates the dry-dock's significant impact on the particular KPI.

During the second year after dry-dock, the trendline (magenta line) continues its upward trend but with a smaller gradiend. Despite the expected deterioration in performance due to the increased hull fouling, not only KPIc Ballast values are not decreased, but they also manage to achieve a further increase of more than 10% (from 0.8 to 0.9).

Overall, the long-term effect of the dry-dock is extremely positive for the particular KPI as the trendlines' values are almost doubled in the two year period following the dry-docking.

3.4.8 KPIc Laden – Vessel 2

As it can be observed in the graph above, KPIc Laden receives relatively lower values during the pre-dry-dock period than it does during the post-dry-dock period. However, the trendline (red line) has an upward trend that increases KPIc Laden values from 0.3 to about 0.43 (40% increase), thus achieving a significant and unexpected increase in performance prior to the dry-dock

During Period 2B (1st year afte dry-dock), the KPIc Laden trendline's values (green line) are initially increased by about 10%, a result that is anticipated as performance is expected to increase after dry-dock and hull cleaning repairs. Despite that, the increase is followed by a downward trend that cause the KPIc Laden values to eventually drop at 0.38 towards the end of the first post-dry-dock year, an indication of the weakening of the dry-dock's effect on performance.

During the second year after dry-dock, the trendline (magenta line) is almost horizontal and stabilizes KPIc Laden values at around 0.40. Despite the expected increase of hull fouling, the performace is no further deteriorated after the first year of the post-dry-dock period.

Overall, while the dry-dock manages to achieve a small increase in KPIc Laden values in the short-term, its impact seems to weaken in the long-term, causing KPIc Laden values to drop to pre-dry-dock levels.

3.4.9 Comparison

The first graph is the scatter plot of KPIa – time for both vessels. The moving mean of KPIa is plotted in the second graph. Blue and green are the colors representing the data of Vessel 1 while magenta and red are the ones indicating Vessel 2's data points.

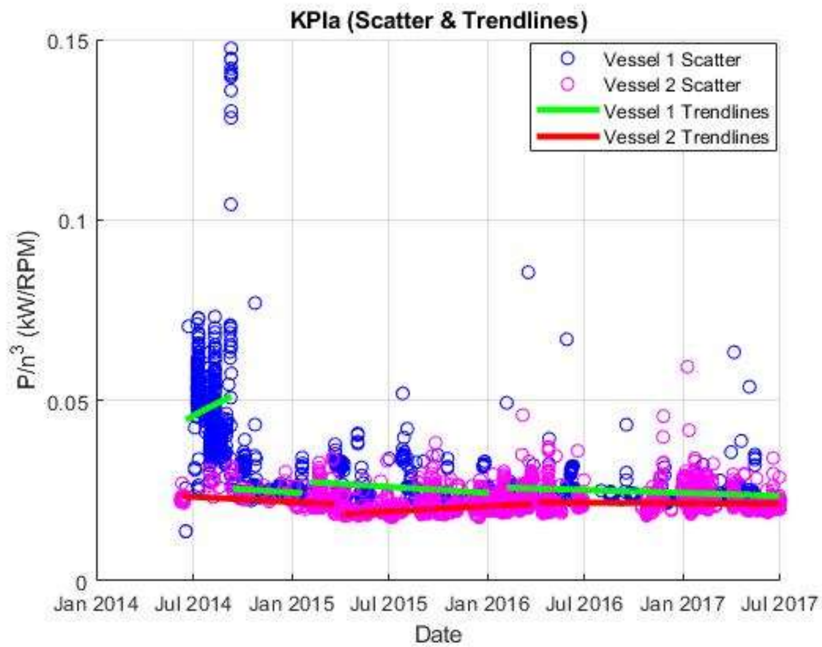

Figure 45: KPIa – time (Both Vessels).

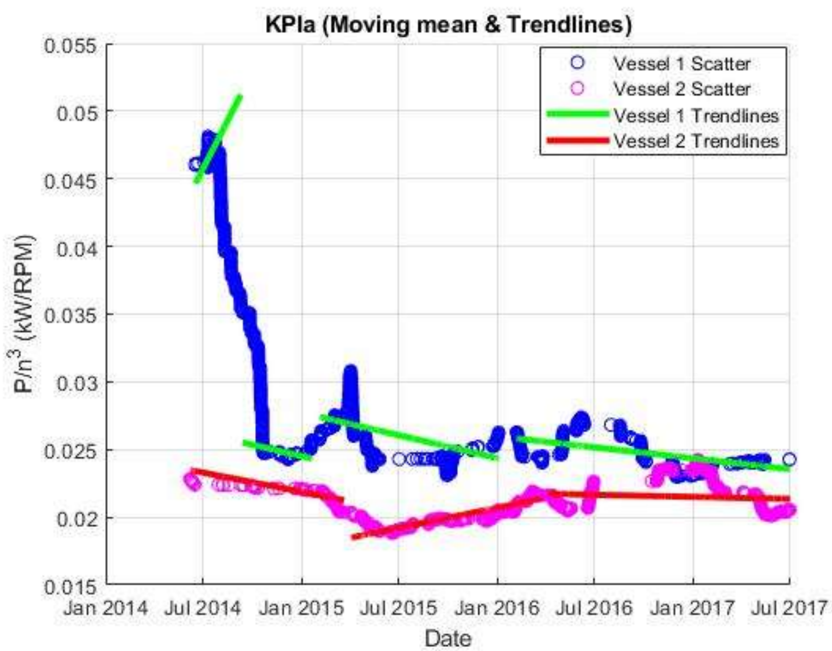

Figure 46: KPIa (moving mean) – time (Both Vessels).

As it can be observed in the graphs above, that initial difference between the two vessels' KPIas is significant. In the pre-dry-dock period (Periods 1A and Period 2A respectively) Vessel 1 receives KPIa values of around 0.045 while Vessel 2 receives values that are almost half in size (about 0.023). In addition to that, the trendline of Vessel 1 has an upward trend while that of Vessel 2 a downward one, a fact that creates even greater difference in the vessels' KPIas. Towards the end of Period 1A, the KPIa values of Vessel 1 are more than double those of Vessel 2. The gap between the two KPIas depicts the significant difference in the performance levels of the two similar vessels and highlights the poor efficiency of Vessel 1.

Once Vessel 1 has its propeller polished, its KPIa collapses to nearly half its previous values (from 0.045 to 0.026) managing to cover the majority of difference with Vessel 2's KPIa. The magnitude of the drop as well as the time it took to happen are accurately depicted at the moving mean graph in the form of an almost vertical line. The polishing of the propeller improves Vessel 1's performance in such way that an expected common level of performance is approached. Apart from narrowing the difference, the propeller polishing seems to create ground for further improvement as Period 1B's trendline is almost parallel to that of Period 2A, indicating that the two KPIas decrease at similar rates. As a result, the performance gap between the two vessels is temporarily stabilized.

The two KPIas initially react differently to the dry-dock repairs. Vessel 1's KPIa is increased from 0.026 to around 0.0275 (less than 10% increase) while Vessel 2's is significantly reduced (about 20%). However, this widening of the gap between the two KPIas has a short-term effect, as the trendline of Period 1C is downward while that of Period 2B upward. The contrast between the two trends reveals that while the performance of Vessel 2 is gradually deteriorating, a result that can be expected due to the increasing hull fouling, Vessel 1's performance is actually improved despite the fouling. This contradictory pattern can be explained by the duct installation which manages to decrease KPIa for Vessel 1 in the long-term, when the effect of the hull cleaning repair is weakened.

During the second year after the dry-dock, Vessel 2's trendline seems to have stabilized at a value of 0.0215 while Vessel 1's continues to decrease, but at a lower rate. The reduction of Vessel 1's reduction rate is anticipated as the fouling occurring two years after the dry-dock is definitely more severe. However, due to the increased performance achieved by the duct, the KPIa of Vessel 1 continues its slight decrease. As a result, the vessel's performance gap reaches an overall minimum at the end of the measuring period (0.0235 vs 0.0215).

The impact of the duct is revealed as time passes and the effect of the propeller polishing and hull cleaning are weakened. Despite the fact that propeller polishing manages to breach the initially huge gap, it is due to the duct that not only is the main ground maintained but also a further narrowing of the difference is achieved in the long-term.

The first graph is the scatter plot of KPIb – time for both vessels. The moving mean of KPIb is plotted in the second graph. Blue and green are the colors representing the data of Vessel 1 while magenta and red are the ones indicating Vessel 2's data points.

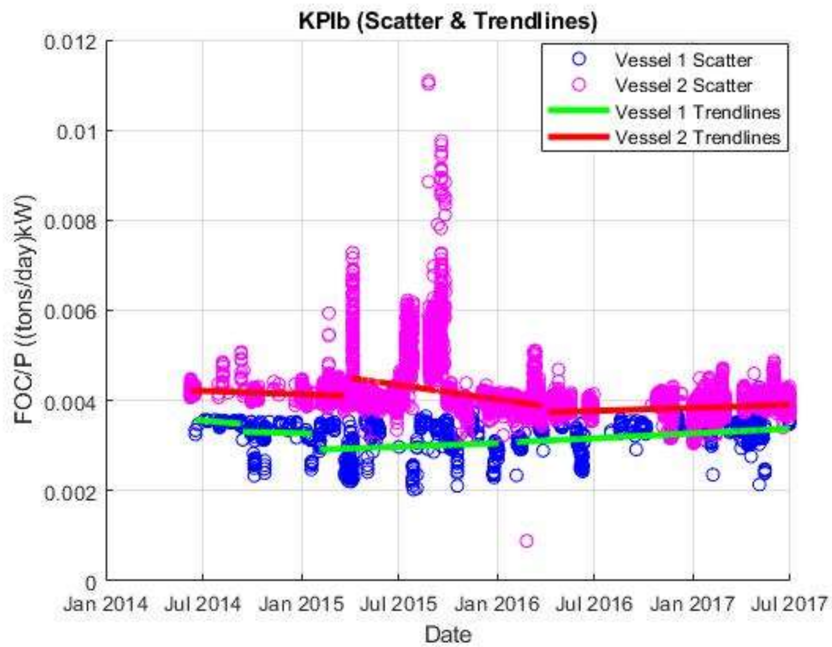

Figure 47: KPIb – time (Both Vessels).

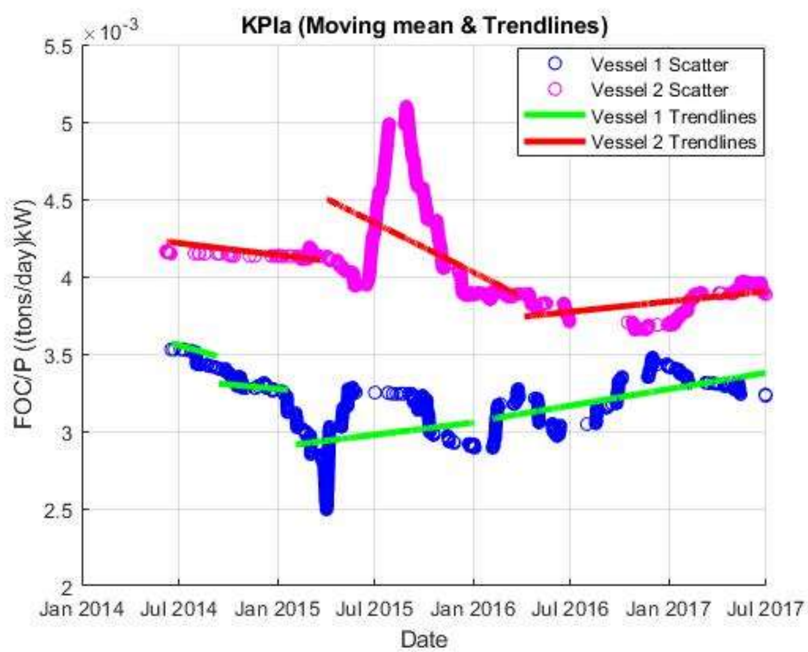

Figure 48: KPIb (moving mean) – time (Both Vessels).

As it can be observed in the above graphs, the specific fuel oil consumption of Vessel 1 is less than that of Vessel 2 throughout the examined period of time. Initially, during the beginning of Periods 1A and 2A, Vessel 1's KPIb receives values around 0.0036 while Vessel 2's around 0.0042. In addition to that, while both trendlines have a negative slope, the Period 1A's slope is greater and as a consequence KPIb reduces at a faster pace for Vessel 1 than it does for Vessel 2, widening the initial performance gap (about 15% difference at the end of Period 1A).

Once Vessel 1 has its propeller polished, Vessel 1's KPIb values drop to around 0.0033 (about 10% reduction) while the respective trendline becomes almost parallel to that of Period 2A, causing the two KPIbs to decrease at a similar rate. Despite the positive impact of the propeller polishing on Vessel 1's KPIb which is depicted by the slight drop of the values, its effect is not long-standing as the reduction rate is lowered (slope of the trendline).

The two KPIbs initially react differently to the dry-dock repairs. Vessel 1's KPIa is reduced from 0.0033 to 0.0029 (12% decrease) while Vessel 2's is significantly increased from 0.0041 to 0.0045 (about 10%). However, this widening of the gap between the two KPIas has a short-term effect, as the trendline of Period 1C is slightly upward while that of Period 2B steeply downward. By the end of Period 1C, however, the gap remains significant and greater than the initial one (0.0031 vs 0.0040) as the vessels' initial reactions to the dry-dock have not been counterbalanced by the trends. The effect of the dry-dock seems to last longer for Vessel 2 than it does for Vessel 1, whose performance deteriorates towards the end of the first post-dry-dock year.

During the second year after the dry-dock, Vessel 1's trendline is almost identical to the previous one, indicating that the performance patterns are not altered as time passes. As a result, KPIb continues to rise for Vessel 1, an action that is anticipated due to the increase of hull fouling, and eventually reaches pre-dry-dock values (around 0.0034). As far as Vessel 2 is concerned, its KPIb also follows an upward trend during the second post-dry-dock year. However, Period 2B's trendline has a smaller gradient, in absolute terms, than Period 1C's and as a result the initial difference between KPIbs is gradually reduced (3.1 vs 3.75 → 3.4 vs 3.9).

Overall, and despite the various fluctuations, the KPIb difference between the two vessels is not significantly reduced throughout the examined period. Moreover, Vessel 2's performance seems to improve slightly over time, while Vessel 1's improves but only for the short-term. The effect of the duct is not depicted in the particular KPI as the deterioration of Vessel 1's performance, due to the hull fouling and the weakening of the dry-dock effect, is not counterbalanced in the long run.

The first graph is the scatter plot of KPIc (Ballast) – time for both vessels. The moving mean of KPIc Ballast is plotted in the second graph. Blue and green are the colors representing the data of Vessel 1 while magenta and red are the ones indicating Vessel 2's data points.

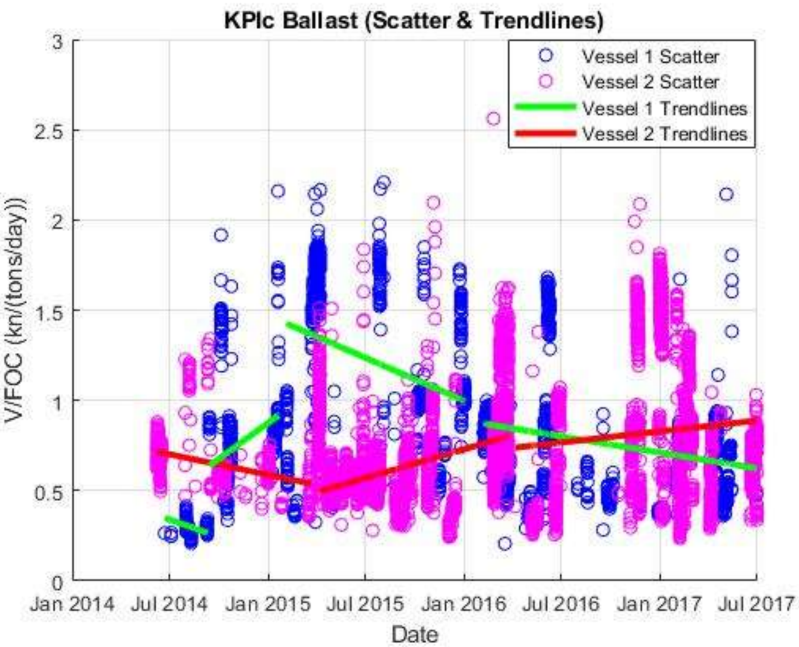

Figure 49: KPIc – time (Ballast – Both Vessels)

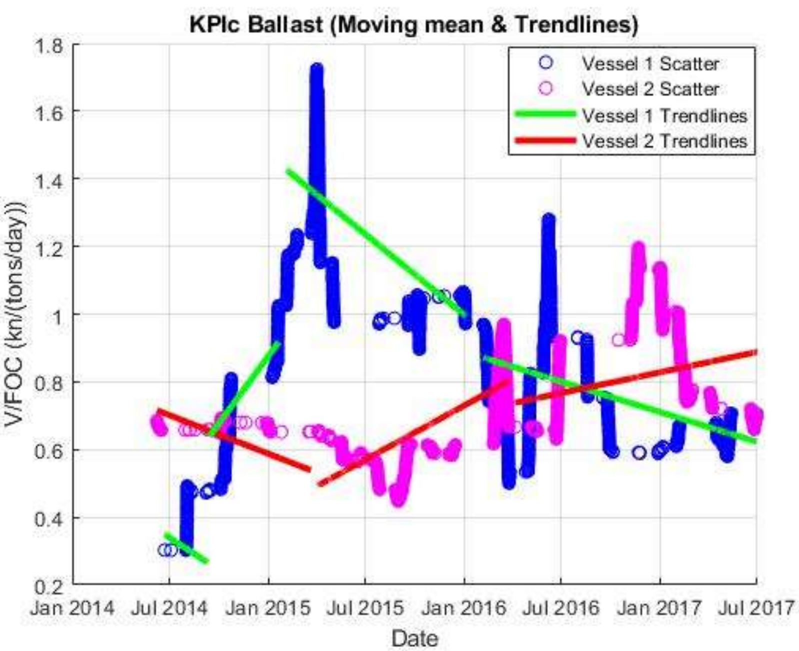

Figure 50: KPIc (moving mean) – time (Ballast – Both Vessels)

As it can be observed in the above graphs, the Vessel 2's fuel efficiency is initially higher than Vessel 1's, reaching more than double KPIc Ballast values (0.72 vs 0.35). The trendlines of Periods 1A and 2A are both downward, with that latter having a smaller slope which indicates that the deterioration of KPIc Ballast, and thus of performance, is slower for Vessel 2. As a consequence, towards the end of period 1A, the difference between the two KPIc Ballast is slightly increased (0.65 vs 0.27).

Once Vessel 1 has its propeller polished a significant alteration in performance is noticed. Vessel 1's KPIc Ballast values are instantly increased by about 150% (from 0.26 to 0.64) causing the Period 1B's trendline to surpass the Period 2A's one very quickly. In addition to that, the Vessel 1's trendline is steeply upward in contrast with the Period 2A's trendline which is downward. As a result, the performance gap between the two vessels is widened as time goes by, with Vessel 1's KPIc Ballast reaching a value of 0.92 while the respective value of Vessel 2 is less than 0.58. This significant alteration in Vessel 1's performance underlines the positive effect of the propeller polishing, which manages to increase fuel efficiency by a rate of about 150% in a small period of time.

The two KPIc Ballast initially react differently to the dry-dock repairs. Vessel 1's KPIc Ballast is significantly increased from 0.92 to 1.43 (50% decrease) while Vessel 2's decreases from 0.54 to 0.49 (about 10%). However, this widening of the gap between the two KPIas has a short-term effect, as the trendline of Period 1C is downward while that of Period 2B upward. By the end of Period 1C, however, the gap remains significant (1.00 vs 0.73) as the vessels' initial reactions to the dry-dock have not been counterbalanced by the trends. The effect of the dry-dock seems to last longer for Vessel 2 than it does for Vessel 1, whose performance deteriorates towards the end of the first post-dry-dock year.

During the second year after the dry-dock, Vessel 1's trendline continues its downward pattern, indicating that performance is reduced as the time passes, a phenomenon that is possibly explained by the constantly increasing hull fouling. On the other hand, Vessel 2's trendline, despite suffering an initial drop, continues its upward trend but at a lower slope, causing the KPIc Ballast values to increase at a lower rate. Eventually, Vessel's 2 trendline surpasses Vessel 1's and the performance gap between the two vessels continues to grow given their trends. Towards the end of the measuring period, the difference between the two KPIc Ballast is about 0.3 (0.62 vs 0.89) with Vessel 1's values returning to a similar level as the one achieved at the beginning of Period 1B (propeller polishing).

Overall, despite Vessel 1's initial increased performance due to the propeller polishing and the dry-dock, Vessel 2 manages to reach higher KPIc Ballast values in the long-term. The effect of the duct is not depicted in the particular KPI as the deterioration of Vessel 1's performance, due to the hull fouling and the weakening of the dry-dock effect, is not counterbalanced in the long run.

The first graph is the scatter plot of KPIc (Laden) – time for both vessels. The moving mean of KPIc Laden is plotted in the second graph. Blue and green are the colors representing the data of Vessel 1 while magenta and red are the ones indicating Vessel 2's data points.

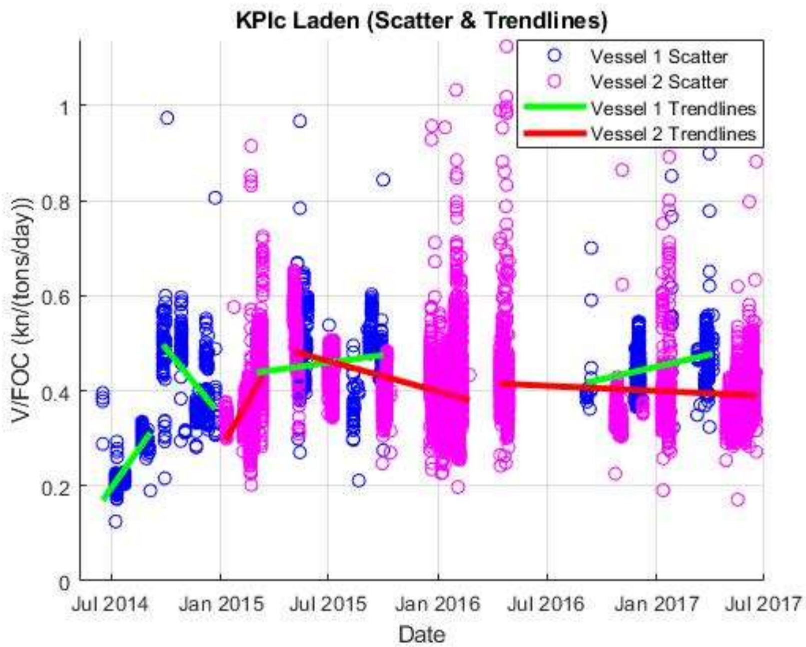

Figure 51: KPIc – time (Laden – Both Vessels).

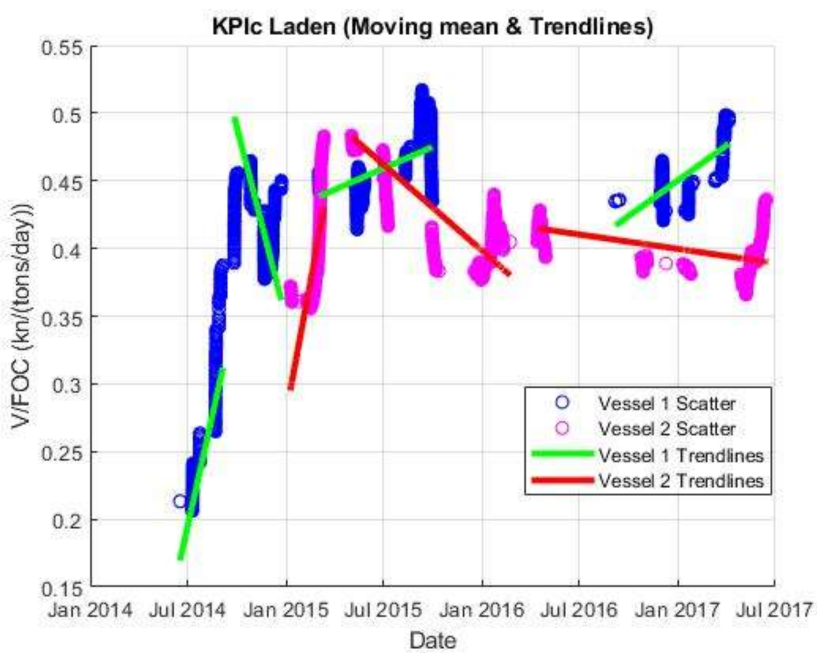

Figure 52: KPIc (moving mean) – time (Laden – Both Vessels).

As it can observed in the graphs above, Vessel 1's KPIc Laden values are initially significantly low (around 0.17) while Vessel's 2 are higher (around 0.29), with Period 2A beginning after the end of Period 1B (propeller polishing). The initial low values are counterbalanced by the upward trends of the Period 1A's and Period 2A's trendline, which cause the KPIc Laden values to reach 0.31 and 0.43 respectively (80% increase vs 40% increase). The initial performance gap between the two is narrowed due to Vessel 1's higher increase rate (greater slope).

Once Vessel 1 has its propeller polished, its KPIc Laden is increased to 0.5 (about 60% increase), managing to surpass Vessel 2's values by significantly improving fuel efficiency. However, the effect of the propeller polishing is gradually weakened and Period 1B's trendline is downward. As a result, at the end of the period, Vessel 1's KPIc Laden values are decreased by 30% (from 0.5 to 0.36), approaching the pre-polishing performance level. It can be understood that while the propeller polishing manages to instantly increase fuel efficiency, and thus performance, its effect is quickly reduced.

Initially, the two vessels reactions to the dry-dock repairs are similar. Vessel's 1 KPIc Laden is increased by about 20% (from 0.36 to 0.44) while Vessel 2's also increases but a slower rate (10% increase from 0.43 to 0.48). Due to Period 1B's downward trend and Period 2A's upward, Period 2B's trendline manages to surpass Period 1C's for a small period of time. However, Vessel 1's trendline is slightly upward, achieving KPIc Laden values of around 0.475 (almost 10% increase) by the end of the first post-dry-dock year, while Vessel 2's trendline is downward and the respective KPIc Laden is reduced by about 20% in the first post dry-dock year (from 0.48 to 0.38).

At the second post-dry-dock year, Vessel 2's KPIc Laden initially increases to 0.41 and continues its decline, but at a lower rate, reaching values around 0.39 at the end of the measuring period. On the other hand, Vessel 1's trendline is steeply upward and manages to counterbalance an initial 15% reduction of KPIc Laden values (from 0.475 to 0.415) reaching values around 0.48, greater than those achieved during the first post-dry-dock year.

Overall, Vessel 1 manages to reach KPIc Laden values that approach the overall maximum achieved during the propeller polishing, towards the end of the measuring period, when the effect of the propeller polishing and the dry-dock is severely weakened if not complete eliminated. At the same time, Vessel 2's KPIc Laden follows a more anticipated pattern by initially increasing after dry-dock and eventually declining due to the weakening of the dry-dock's impact. The difference in the performance pattern of the two vessels can be explained by the propeller duct which successfully manages not only to preserve the KPIc Ballast values achieved after dry-dock but also to increase them, counterbalancing the negative effect of hull fouling and achieving greater fuel efficiency in the long run.

[This page is intentionally left blanc]

4 Regression analysis

Regression analysis is a procedure for estimating the relationship between a dependent variable (the response) and one or more independent variables (the predictors) [8]. The aim of this chapter is to produce a preliminary model that can predict the fuel oil consumption (response) of the two vessels in the post dry-dock era, which is divided into two parts, one for the first post dry-dock year (DD1) and one for the second (DD2).

As observed by the FOC – EP graphs, the relationship between the two variables is linear and, thus, a linear regression model predicting the consumption given the shaft power is expected to produce solid results, as shown in the PhD thesis of L. G. Aldous [9]. However, this study aims to create a preliminary regression model that makes predictions for the fuel oil consumption through the utilization of other sea travel related variables such as the speed through water, the mean draft, the trim, the wind speed and the rudder angle. For the speed variable (STW), its square value is also examined along with the rest of the variables as it appears to better approach the observed FOC – STW relationship.

The regression dataset is based on the dataset produced in the Data analysis chapter and the extra filters and corrections applied at the Key performance indicators chapter are ignored. However, an additional filter concerning the speed through water is applied, omitting speed values less than 8 knots. This elimination of slow speeds, which account for a very limited portion of the dataset, causes an improvement of the regression models and leads to better predictions of the fuel consumption without defying the natural aspect of the problem since such vessels rarely travel in speeds under 8 knots.

Initially, the chapter introduces some basic principles and statistical quantities of regression analysis. Afterwards, the correlation of the variables is calculated and a regression model is selected by a “best subsets” analysis. The main characteristics of the model are presented and discussed before a case study is performed to allow for comparisons between the two time periods and the two vessels, under different operational scenarios.

4.1 Multiple linear regression

A population model for a multiple linear regression model that relates a y variable to p x variables can be written as:

$$y_i = \beta_0 + \beta_1 \cdot x_{i\,1} + \beta_2 \cdot x_{i\,2} + \cdots + \beta_p \cdot x_{i\,p} + \varepsilon_i$$

where:

- y_i : the i-th observation of the dependent variable.
- x_{ij} : the i-th observation of the j-th independent variable.
- β_0 : the regression intercept term.
- β_j : the slope coefficient of the j-th independent variable.
- ε_i : the error term of the i-th observation (normal distribution).

It can be understood that the model relies on the assumption that there is a linear relationship between the independent variable and the predictors. Each β coefficient represents the change in the mean response, $E(y)$, per unit increase in the associated predictor variable when all the other predictors are held constant. The intercept term, β_0, represents the mean response, $E(y)$, when all the predictors are zero.

The MLR model that makes predictions for the y variable can be written as:

$$\hat{y}_i = b_0 + b_1 \cdot x_{i\,1} + b_2 \cdot x_{i\,2} + \cdots + b_p \cdot x_{i\,p}$$

where:

- $\hat{y}_i$: the predicted/fitted value of the i-th observation of the dependent variable y.
- x_{ij} : the i-th observation of the j-th independent variable.
- b_j : the sample estimates of the β_j coefficients and are calculated as follows:

  Let the following 2-predictor MLR model:

  $$y_i = \beta_0 + \beta_1 \cdot x_{i\,1} + \beta_2 \cdot x_{i\,2} + \varepsilon_i$$

  that can be written in matrix form:

  $$Y = X \cdot B + E \rightarrow \begin{bmatrix} y_1 \\ y_2 \\ \vdots \end{bmatrix} = \begin{bmatrix} 1 & x_{i\,1} & x_{i\,2} \\ 1 & x_{i+1\,1} & x_{i+1\,2} \\ \vdots & \vdots & \vdots \end{bmatrix} \cdot \begin{bmatrix} \beta_0 \\ \beta_1 \\ \beta_2 \end{bmatrix} + \begin{bmatrix} \varepsilon_1 \\ \varepsilon_2 \\ \vdots \end{bmatrix}$$

  then: $B = (X^T \cdot X)^{-1} \cdot X^T \cdot Y$, where X is the design matrix and Y the observed dependent variable.

A residual (error) term is calculated for each observation:

$$e_i = y_i - \hat{y}_i$$

4.2 Coefficient of determination

The coefficient of determination, commonly known as R^2, is a very significant characteristic of regression models. It explains how much of the variation in the response can be explained by the variation in the independent variables. Let y be the dependent variable and f the fitted value predicted by the regression model. Then, R^2 can be calculated by the following formula:

$$R^2 = 1 - \frac{SS_{RES}}{SS_{TOT}}$$

where:

- $SS_{TOT} = \sum (y_i - \bar{y})^2$: the total sum of squares of the dependent variable. $\bar{y}$ is the mean value of y.
- $SS_{RES} = \sum (y_i - f_i)^2$: the residual sum of squares.

R^2 receives values in the [0, 1] interval that express the fitting of the regression model:

- $R^2 = 0$: The model always predicts $\bar{y}$. The outcome cannot be predicted by any of the independent variables.
- $R^2 = 1$: The model always predicts the observed y_i value and has no residuals. The outcome can be predicted without error from the independent variables.

R^2 increases as more predictors are added to the model. However, it should be noted that adding predictors to a model can actually lead to worse predictions despite the increase of the coefficient of determination. By adding many variables to a model, it becomes overly customized to fit the peculiarities and the random noise of the sample rather than reflecting the entire population. This phenomenon is known as overfitting and is a common problem in regression models.

Sometimes an adjusted R^2 is used in regression analysis to account for the spurious increase of the coefficient of determination when extra predictors are added to the model. For a model with n data points and p independent variables the adjusted R^2 is calculated by the following formula:

$$R^2_{ADJ} = 1 - (1 - R^2) \cdot \frac{n - 1}{n - p - 1}$$

Finally, the predicted R^2 is calculated as:

$$R^2_{PRED} = 1 - \frac{PRESS}{SS_{TOT}}$$

where the predictive residual error sum of squares, or PRESS, is calculated as the sum of the squares of all the resulting prediction errors that occur by removing each observation in turn and refitting the model with the remaining observations.

4.3 Multicollinearity - Variance inflation factors

In a multiple linear regression model, one must not only account for the relationships between each predictor and the response but also for the relationships among the predictors. In an ideal regression model, all the independent variables are correlated with the dependent one but not with each other. However, that ideal model cannot be achieved as the predictors correlate with each other, either highly or lowly. Multicollinearity occurs when a predictor of the model can be linearly predicted from the other independent variables with a substantial degree of accuracy. The presence of collinearity causes the coefficients of the model to change erratically in response to small changes in the data. While the phenomenon does not reduce the reliability of the model and its predicting strength within the sample dataset, it may produce a regression model that gives invalid results about individual predictors and cannot distinguish which variables are redundant with respect to others.

The severity of multicollinearity can be quantified by the Variance Inflation Factors (VIFs). The numerical value of VIF is the percentage to which the variance (i.e. standard error squared) is inflated for each coefficient due to multicollinearity. For example, a $\mathrm{VIF} = 1.8$ suggests that the variance of the particular coefficient is 80% greater than it would be if there was no multicollinearity.

A Variance Inflation Factor is calculated for each independent variable of the model according to the following procedure:

- Assume the following regression model:

$$y = \beta_0 + \beta_1 \cdot x_1 + \beta_2 \cdot x_2 + \cdots + \beta_p \cdot x_p + \varepsilon$$

- For each independent variable x_j, a regression model is calculated with x_j as the response and the rest of the variables as the predictors. For example, for the x_1 variable the following model is produced:

$$x_1 = a_0 + a_2 \cdot x_2 + a_3 \cdot x_3 + \cdots a_p \cdot x_p$$

- The coefficient of determination R_j^2 is calculated for the above model. The variance inflation factor of the x_j variable is given by the following formula:

$$\mathrm{VIF}_j = \frac{1}{1 - R_j^2}$$

As a result, it can be understood that high values of VIF are indicators of multicollinearity since they occur for high values of R_j^2, which suggest that the respective predictor can be accurately linearly predicted by the rest of the independent variables. On the other hand, VIF's minimum value is 1 and indicates that the examined variable is not correlated with the others.

The VIF's threshold value for the presence of collinearity is a subject of debate. As a rule of thumb, VIF's threshold is taken at 10 but some conservative approaches reduce it to 5 or even 2.5.

4.4 Standard deviation

The regression analysis includes the calculation of the standard deviation S of the distance between the data values (y) and the fitted values (f) (standard error). S is measured in the units of the response.

$$S = \sqrt{\frac{\sum_{1}^{N}(x_i - \bar{x})^2}{n - 1}}$$

where $x = y - f$ and n is the number of observations in the sample.

4.5 Standard error of coefficient

In a regression model the standard error of the coefficient (SE) is calculated for each predictor variable x according to the following formula:

$$SE = \frac{S}{\sqrt{\sum_i (x_i - \bar{x})^2}}$$

where S is the standard error of the model.

The standard error of the coefficient is always positive and it measures how precisely the model estimates the coefficient's unknown value. The smaller the standard error the more precise the estimate.

4.6 T-value

The T-statistic is the ratio of the departure of the estimated value of a parameter from its hypothesized value to its standard error. In regression models, the T-value is used to measure, for each variable (including the constant), the ratio between the coefficient b and its standard error (SE). The T-value is calculated by the following formula:

$$T - \text{value} = \frac{b}{SE}$$

4.7 Mallow's C_p

The regression analysis often incudes a preliminary procedure called best subsets, which aims to identify the subset or subsets that best meet some fitting criteria, such as a large R^2 value or a small Mean Squared Error ($MSE = S^2$). During this process, a statistical quantity named Mallow's C_p is calculated in order to assess the size of the bias introduced into the responses by the presence of a model that lacks important predictors, an underspecified model.

Mallow's C_p is calculated for each one of the examined regression models (all the possible combinations among the predictors) by the following formula:

$$C_p = k + 1 + \frac{(MSE_j - MSE_{all})}{MSE_{all}} \cdot (n - k - 1)$$

where:

- k : the number of the variables of the examined model.
- n : the number of observations (data points).
- MSE_j : the mean squared error of the examined model.
- MSE_{all} : the mean squared error of the unique model that combines all the predictors.

Ideally, Mallow's C_p would be calculated with the help of the population's variance, σ^2, but that is not possible. Instead the mean squared error of the model containing all the candidate predictors (MSE_{all}) is used as an estimate of σ^2. For this to be done, it is assumed that the full model containing all the variables has no bias, an assumption that may not be valid but cannot be tested without additional information. The usage of MSE_{all} also guarantees that the full model has a $C_p = k + 1$.

Models with a small value of Mallow's C_p have a small estimated total variation in predicted responses. When C_p is near or below $k + 1$ the bias is low or none but when it is much greater than $k + 1$ the bias is significant. Since the full model's C_p is always equal to $k + 1$, Mallow's C_p should not be used to assess its bias.

In general, when conducting a best subset analysis, the model or models with C_p values near $k + 1$ are more preferable for selection. If no such model exists, it can be an indicator that some important predictors may be missing.

4.8 F-value

Let y express the dependent variable and f present the fitted value which is predicted by the regression model. The F-value of the model is calculated as:

$$\mathrm{F-value} = \frac{SS_{REG}/DF_{REG}}{SS_{RES}/DF_{RES}} = \frac{R^2}{1-R^2} \cdot \frac{n-p-1}{p}$$

where:

- $SS_{REG} = \sum(f_i - \bar{y})^2$: the regression sum of squares.
- $DF_{REG} = p$: the degrees of freedom of the regression model and p is the number of the model's predictors.
- $SS_{RES} = \sum(y_i - f_i)^2$: the residual sum of squares.
- $DF_{RES} = n - 1 - p$: the degrees of freedom of the residuals (error) and n is the number of observations.

The F-value is also calculated for each independent variable as:

$$\mathrm{F-value} = \frac{SS_{ADJ\ REG}}{SS_{RES}/DF_{RES}} = \frac{SS_{ADJ\ REG}}{S^2}$$

where:

- $SS_{ADJ\ REG}$: the adjusted regression sum of squares of the independent variable.
- $SS_{RES} = \sum(y_i - f_i)^2$: the residual sum of squares.
- $DF_{RES} = n - 1 - p$: the degrees of freedom of the residuals (error) and n is the number of observations.

The adjusted regression sum of squares of each independent variable occurs as follows:

- The respective variable is removed from the model and a new model is formed with the rest variables as the predictors.
- For the new model, the new regression sum of squares is calculated.
- The difference between the regression sums of squares of the two models is the adjusted regression sum of squares of the removed predictor.

It can be understood that the $SS_{ADJ\ REG}$ quantifies the amount of variation in the response data that is explained by the respective term of the model.

4.9 P-value

The P-value is a probability that measures the evidence against the null hypothesis. Lower probabilities provide stronger evidence against the null hypothesis.

To determine whether each main effect and the interaction effect is statistically significant, the P-value of each term is compared to a significance level α that is usually set at 0.05. The alpha value indicates the percentage of the risk of concluding that an effect exists when it does not. If the P-value is greater than the selected significance level then the effect is not statistically significant, whereas if its equal or less then the effect of the term is statistically significant.

The P-value of the model as well as of each predictor is calculated with the help of T-value as follows:

$$\mathrm{P-value} = 2 \cdot \left(1 - \mathrm{T}(\mathrm{x}|\mathrm{v})\right) = 2 \cdot (1 - \int_{-\infty}^{\mathrm{x}} \frac{\Gamma(\frac{\nu+1}{2})}{\Gamma(\frac{\nu}{2})} \cdot \frac{1}{\sqrt{\nu \cdot \pi}} \cdot \frac{1}{\left(1+\frac{t^2}{\nu}\right)^{\frac{\nu+1}{2}}} \mathrm{dt}$$

where:

- $\mathrm{x} = \mathrm{T} - \mathrm{value}$: the absolute t value of the model or the independent variable.
- $\nu\ = \mathrm{n} - 1 - \mathrm{p}$: the degrees of freedom of the error, for a model with n data points and p predictors.
- T : T-distribution’s cumulative distribution function.
- $\Gamma(\mathrm{x}) = (\mathrm{x} - 1)!$: the gamma-function.

Alternatively, The P-value of the model as well as of each predictor is calculated with the help of F-value as follows:

$$\mathrm{P-value} = 1 - \mathrm{F}(\mathrm{x}|\mathrm{v}_1, \mathrm{v}_2) = 1 - \int_{0}^{\mathrm{x}} \frac{\Gamma(\frac{\mathrm{v}_1+\mathrm{v}_2}{2})}{\Gamma(\frac{\mathrm{v}_1}{2}) \cdot \Gamma(\frac{\mathrm{v}_2}{2})} \cdot (\frac{\mathrm{v}_1}{\mathrm{v}_2})^{\frac{\mathrm{v}_1}{2}} \cdot \frac{t^{\frac{\mathrm{v}_1}{2}-1}}{\left[1+\left(\frac{\mathrm{v}_1}{\mathrm{v}_2}\right) \cdot t\right]^{\frac{\mathrm{v}_1+\mathrm{v}_2}{2}}} \mathrm{dt}$$

where:

- $\mathrm{x} = \mathrm{F} - \mathrm{value}$: the absolute f value of the model or the independent variable.
- v_1 : the degrees of freedom of the model (equal to the sum of independent variables) or of the independent variable (equals 1).
- $\mathrm{v}_2 = \mathrm{n} - 1 - \mathrm{p}$: the degrees of freedom of the error, for a model with n data points and p predictors.
- F : F-distribution’s cumulative distribution function.
- $\Gamma(\mathrm{x}) = (\mathrm{x} - 1)!$: the gamma-function.

4.10 Correlation

The correlation among the variables of the regression (possible predictors and response) is quantified by the Pearson Correlation Coefficients which are presented below.

	STW	STW^2	TM	WS	RA	TRIM	FOC
STW	1						
STW^2	0.997	1					
TM	0.179	0.138	1				
WS	0.121	0.114	0.099	1			
RA	−0.022	−0.013	−0.198	−0.051	1		
TRIM	−0.166	−0.122	−0.938	−0.060	0.159	1	
FOC	0.842	0.837	0.391	0.454	−0.056	−0.322	1

Table 15: Pearson correlation coefficients (Regression – Vessel 1 – DD1).

	STW	STW^2	TM	WS	RA	TRIM	FOC
STW	1						
STW^2	0.997	1					
TM	0.198	0.167	1				
WS	0.033	0.016	0.379	1			
RA	0.055	0.062	−0.264	−0.141	1		
TRIM	−0.217	−0.187	−0.855	−0.372	0.189	1	
FOC	0.725	0.714	0.529	0.494	−0.119	−0.459	1

Table 16: Pearson correlation coefficient (Regression – Vessel 1 – DD2).

	STW	STW^2	TM	WS	RA	TRIM	FOC
STW	1						
STW^2	0.997	1					
TM	0.147	0.130	1				
WS	−0.006	−0.010	−0.318	1			
RA	0.113	0.122	−0.218	0.113	1		
TRIM	−0.142	−0.135	−0.643	0.105	0.151	1	
FOC	0.668	0.665	0.130	−0.237	−0.110	−0.279	1

Table 17: Pearson correlation coefficient (Regression – Vessel 2 – DD1).

	STW	STW^2	TM	WS	RA	TRIM	FOC
STW	1						
STW^2	0.997	1					
TM	0.444	0.412	1				
WS	−0.205	−0.208	−0.124	1			
RA	−0.016	−0.008	−0.264	−0.040	1		
TRIM	−0.440	−0.433	−0.592	0.077	0.227	1	
FOC	0.766	0.760	0.613	−0.224	−0.174	−0.434	1

Table 18: Pearson correlation coefficient (Regression – Vessel 2 – DD2).

4.11 Best subsets

A best subsets analysis is conducted in order to determine the most suitable regression model for the examined dataset and variables. The results of this analysis are presented in the tables below. More specifically, for each possible number of variables the best two models are picked and their respective R^2, Mallow's C_p, and S are shown.

Number of variables	R^2	C_p	S	STW	STW^2	TM	TRIM	WS	RA
1	70.89	30647	4.525	✓	×	×	×	×	×
1	70.06	31944	4.589	×	✓	×	×	×	×
2	83.49	10823	3.408	✓	×	×	×	✓	×
2	83.09	11460	3.449	×	✓	×	×	✓	×
3	89.28	1726	2.747	×	✓	✓	×	✓	×
3	88.20	3424	2.882	✓	×	✓	×	✓	×
4	89.95	663	2.659	✓	✓	✓	×	✓	×
4	89.89	758	2.667	×	✓	✓	✓	✓	×
5	90.30	114	2.612	✓	✓	✓	✓	✓	×
5	90.00	592	2.653	✓	✓	✓	×	✓	✓
6	90.37	7	2.603	✓	✓	✓	✓	✓	✓

Table 19: Best subsets (Vessel 1 – DD1).

Number of variables	R^2	C_p	S	STW	STW^2	TM	TRIM	WS	RA
1	52.50	37391	5.757	✓	×	×	×	×	×
1	50.94	39417	5.850	×	✓	×	×	×	×
2	74.61	8676	4.208	✓	×	×	×	✓	×
2	74.27	9121	4.237	×	✓	×	×	✓	×
3	80.52	1003	3.686	×	✓	✓	×	✓	×
3	79.99	1690	3.736	✓	×	✓	×	✓	×
4	81.14	208	3.628	×	✓	✓	✓	✓	×
4	80.68	807	3.672	✓	×	✓	✓	✓	×
5	81.23	91	3.619	×	✓	✓	✓	✓	✓
5	81.21	119	3.621	✓	✓	✓	✓	✓	×
6	81.30	7	3.613	✓	✓	✓	✓	✓	✓

Table 20: Best subsets (Vessel 1 – DD2).

Number of variables	R^2	C_p	S	STW	STW^2	TM	TRIM	WS	RA
1	44.65	13411	6.794	✓	✗	✗	✗	✗	✗
1	44.23	13674	6.820	✗	✓	✗	✗	✗	✗
2	63.30	1835	5.533	✗	✓	✓	✗	✗	✗
2	62.78	2156	5.572	✓	✗	✓	✗	✗	✗
3	64.56	1054	5.437	✗	✓	✓	✓	✗	✗
3	64.22	1264	5.463	✗	✓	✓	✗	✓	✗
4	65.45	504	5.369	✗	✓	✓	✓	✗	✓
4	65.22	643	5.386	✗	✓	✓	✓	✓	✗
5	66.16	64	5.313	✗	✓	✓	✓	✓	✓
5	65.62	400	5.355	✓	✓	✓	✓	✗	✓
6	66.25	7	5.306	✓	✓	✓	✓	✓	✓

Table 21: Best subsets (Vessel 2 – DD1).

Number of variables	R^2	C_p	S	STW	STW^2	TM	TRIM	WS	RA
1	58.75	7330	6.456	✓	✗	✗	✗	✗	✗
1	57.78	7946	6.531	✗	✓	✗	✗	✗	✗
2	68.61	1020	5.632	✗	✓	✓	✗	✗	✗
2	68.00	1410	5.687	✓	✗	✓	✗	✗	✗
3	69.20	641	5.579	✗	✓	✓	✗	✗	✓
3	68.90	835	5.606	✗	✓	✓	✗	✓	✗
4	69.65	356	5.538	✗	✓	✓	✓	✗	✓
4	69.54	424	5.548	✗	✓	✓	✗	✓	✓
5	69.96	156	5.510	✗	✓	✓	✓	✓	✓
5	69.92	185	5.514	✓	✓	✓	✓	✗	✓
6	70.20	7	5.488	✓	✓	✓	✓	✓	✓

Table 22: Best subsets (Vessel 2 – DD2).

It can be observed that Vessel 1's regression models have greater R^2 values than Vessel 2's which cannot surpass the 70% threshold that is easily achieved by almost all Vessel 1's models. As a result, Vessel's 1 dataset provides better FOC predictions than Vessel 2's.

Speed is the most important independent variable of the FOC regression models as it solely explains a lot of the variation of the predicted fuel oil consumption, something depicted by the big R^2 values of the single-variable models. While STW appears to have a slight advantage in terms of R^2 in the single-variable models, $\mathrm{STW}^2$is preferred when 3 or more variables are included in a model. Both variables are highly correlated with FOC as well as with each other. As a consequence, only one of them is included in the final model in order to avoid multicollinearity problems. Due to its better predictions in multi-variable models as well as to its better approach of the true FOC – STW relationship, $\mathrm{STW}^2$is preferred over STW.

With the exception of the case Vessel 2 – DD1, the fuel oil consumption is more correlated with the mean draft than it is with the trim. This relative advantage of TM is shown in the above models as when only one of two variables can be picked, TM is always preferred over TRIM. Taking the above into account along with the fact that in all cases mean draft and trim are highly correlated, the chosen regression model shall contain the TM variable but not the TRIM one. If both predictors were picked, their respective VIFs would be high indicating the presence of multicollinearity which would affect the model and should be avoided.

The addition of the wind speed variable (WS) significantly increases R^2 and reduces the $\mathrm{C_p}$ and S values for Vessel 1's models. As a result, WS is the second more significant variable and is chosen right after the speed variables. However, its impact is less significant on Vessel 2's models, for which the TM variable is more crucial. Overall, WS introduces the impact of the weather to the models and manages to improve their prediction without causing multicollinearity since it is not significantly correlated with any of the other predictors. As a result, it is chosen as a predictor of the regression.

The addition/subtraction of the rudder angle variable (RA) to/from a model has very little impact on the calculated statistical quantities, a fact that clearly indicates its statistical insignificance to the regression analysis. This conclusion perfectly agrees with the low correlation of RA with FOC which is quantified by the Pearson Correlation Coefficients of the previous paragraph.

The 3-variable model that is chosen ($\mathrm{STW}^2 - \mathrm{TM} - \mathrm{WS}$) provides satisfactory R^2 values, compared with the maximum possible ones that are achieved by the 6-variable model without including many predictors, a choice that may cause overfitting or lead to an unnecessarily complicated model. The model used by *A. A Safaei et al. (2019)* [10], utilizes the speed through water, the displacement and the wave height to predict the fuel oil consumption of 4 VLCCs, achieving high R^2 values. Similarly, the current model combines 3 physical quantities that characterize sea travel; the vessel's speed, its loading condition (expressed by the mean draft rather than the displacement) and the weather conditions (expressed by the wind speed rather than the wave height).The chosen predictors are lowly correlated and, thus, the risk of multicollinearity is avoided.

4.12 Regression models

The following models are chosen for the four examined case (vessels & years). TM is the mean draft in meters, WS the wind speed in m/s and STW the speed through water in knots. The fuel oil consumption (FOC) is calculated in tons/day.

Vessel 1 – DD1

$$\mathrm{FOC} = -16.19712 + 0.51255 \cdot \mathrm{TM} + 0.30107 \cdot \mathrm{WS} + 0.21118 \cdot \mathrm{STW}^2$$

Term	Coefficient	SE coefficient	T-value	P-value	VIF
Constant	−16.19712	0.11943	−135.618	0.000	-
TM	0.51255	0.00548	93.498	0.000	1.027
WS	0.30107	0.00237	127.264	0.000	1.020
STW^2	0.21118	0.00075	282.671	0.000	1.030

Table 23: Regression model's coefficients (Vessel 1 – DD1).

S	R^2	R^2 adjusted	R^2 predicted	Mallow's C_p
2.747	89.276%	89.274%	89.269%	1726

Table 24: Regression model summary (Vessel 1 – DD1).

Source	Degrees of Freedom	$SS_{ADJ\ REG}$	$MS_{ADJ\ REG}$	F-value	P-value
Regression	3	951289	317096	42032.551	0.000
TM	1	65950	65950	8741.958	0.000
WS	1	122186	122186	16196.248	0.000
STW^2	1	602793	602793	79902.901	0.000
Error	15147	114270	8	–	–
Total	15150	–	–	–	–

Table 25: Regression model – analysis of variance (Vessel 1 – DD1).

Vessel 1 – DD2

$$\mathrm{FOC} = -13.05877 + 0.61781 \cdot \mathrm{TM} + 0.32492 \cdot \mathrm{WS} + 0.19678 \cdot \mathrm{STW}^2$$

Term	Coefficient	SE coefficient	T-value	P-value	VIF
Constant	−13.05877	0.13953	−93.594	0.000	–
TM	0.61781	0.00700	88.315	0.000	1.205
WS	0.32492	0.00262	123.908	0.000	1.171
STW^2	0.19678	0.00086	230.138	0.000	1.032

Table 26: Regression model's coefficients (Vessel 1 – DD2).

S	R^2	R^2 adjusted	R^2 predicted	Mallow's C_p
3.686	80.524%	80.521%	80.516%	1003

Table 27: Regression model summary (Vessel 1 – DD2).

Source	Degrees of Freedom	$SS_{ADJ\ REG}$	$MS_{ADJ\ REG}$	F-value	P-value
Regression	3	1364482	454827	33474.157	0.000
TM	1	105976	105976	7799.582	0.000
WS	1	208611	208611	15353.216	0.000
STW^2	1	719634	719634	52963.291	0.000
Error	24289	330025	14	–	–
Total	24292	1694507	–	–	–

Table 28: Regression model – analysis of variance (Vessel 1 – DD2).

Vessel 2 – DD1

$$FOC = -8.65822 + 1.01502 \cdot TM - 0.26713 \cdot WS + 0.17884 \cdot STW^2$$

Term	Coefficient	SE coefficient	T-value	P-value	VIF
Constant	−8.65822	0.20848	−41.530	0.000	−
TM	1.01502	0.01095	92.712	0.000	1.133
WS	−0.26713	0.01149	−23.249	0.000	1.114
STW^2	0.17884	0.00122	146.559	0.000	1.018

Table 29: Regression model's coefficients (Vessel 2 – DD1).

S	R^2	R^2 adjusted	R^2 predicted	Mallow's C_p
5.463	64.218%	64.213%	64.204%	1254

Table 30: Regression model summary (Vessel 2 – DD1).

Source	Degrees of Freedom	$SS_{ADJ\ REG}$	$MS_{ADJ\ REG}$	F-value	P-value
Regression	3	1122540	374180	12537.751	0.000
TM	1	256529	256529	8595.578	0.000
WS	1	16131	16131	540.511	0.000
STW^2	1	641039	641039	21479.492	0.000
Error	20958	625476	30	−	−
Total	20961	1748016	−	−	−

Table 31: Regression model – analysis of variance (Vessel 2 – DD1).

Vessel 2 – DD2

$$\mathrm{FOC} = -7.22912 + 1.13224 \cdot \mathrm{TM} - 0.14341 \cdot \mathrm{WS} + 0.17122 \cdot \mathrm{STW}^2$$

Term	Coefficient	SE coefficient	T-value	P-value	VIF
Constant	−7.22912	0.20693	−34.935	0.000	–
TM	1.13224	0.01401	80.830	0.000	1.207
WS	−0.14341	0.01073	−13.361	0.000	1.047
STW^2	0.17122	0.00128	133.546	0.000	1.242

Table 32: Regression model's coefficients (Vessel 2 – DD2).

S	R^2	R^2 adjusted	R^2 predicted	Mallow's C_p
5.606	68.898%	68.893%	68.882%	835

Table 33: Regression model summary (Vessel 2 – DD2).

Source	Degrees of Freedom	$SS_{ADJ\ REG}$	$MS_{ADJ\ REG}$	F-value	P-value
Regression	3	1328415	442805	14088.709	0.000
TM	1	205347	205347	6533.527	0.000
WS	1	5611	5611	178.521	0.000
STW^2	1	560539	560539	17834.651	0.000
Error	19080	599680	31	–	–
Total	19083	1928095	–	–	–

Table 34: Regression model – analysis of variance (Vessel 2 – DD2).

The constant term is in all cases negative and its absolute value is reduced by almost 50% from Vessel 1's models to Vessel 2's. On the other hand, while a unit change of Vessel 2's mean draft causes about one-unit change of the fuel consumption, Vessel 1's TM has about half the impact of FOC. Finally, despite a slight gradual reduction of STW^2 coefficients from the first case (Vessel 1 – DD1) to the last (Vessel 2 – DD2), all values are close to each other, ranging from approximately 0.17 to 0.21.

Despite the variations described above, the most notable difference between the two vessels' model is the coefficients concerning wind speed. Vessel 1's models have positive WS coefficients (around 0.3) while Vessel 2's negative ones. This change of sign reflects both a physical phenomenon and a statistical one. It can be implied that throughout the measuring period, Vessel 2 experienced more journeys/travel hours of favorable winds that aided the vessel's navigation while Vessel 1 had fewer hours of fair winds. As a result, the increase of wind speed is a favorable phenomenon for Vessel 2's navigation as it reduces the amount of fuel needed to reach a certain speed, whereas such increase has a opposite effect on Vessel 1, forcing it to increase the fuel consumption in order to overcome the added wind resistance. Despite the possible validity of the above assumption, for its proper assessment an additional physical quantity is needed: the wind speed's (relative) direction. If the direction of the wind speed is to be provided then a more proper evaluation of the above assumption can be conducted by introducing another predictor to the regression models and assessing its effect on the response variable. However, the data for the wind direction are not available for the examined vessels so such an assessment cannot be made. Instead, despite the sign contradiction, the discussed 3-variable model is used for both vessels in this preliminary regression analysis. Due to the larger amount of fitting of Vessel 1's models (higher R^2 values), it can be assumed that in a more complete and solid model, the WS coefficient would be positive.

With the exception of the above inconsistency, the chosen model has an adequate performance. The variables P – values are extremely small (less than 10^{-16}), a fact that indicates their statistical significance, mainly due to the vast amount of data points. In addition, the calculated Variance Inflation Factors of the selected predictors are very low (just above 1), suggesting that there are no multicollinearity problems in the models as the independent variables are not significantly correlated, a conclusion also confirmed by the Pearson correlation coefficients (Correlation).

The fitting of the chosen model is depicted by $\mathrm{FOC}_{\mathrm{predicted}}$ vs $\mathrm{FOC}_{\mathrm{observed}}$ graphs for each examined case. To provide a better visualization of the model's fitting, the ideal fitting line $y = x$ is shown in red.

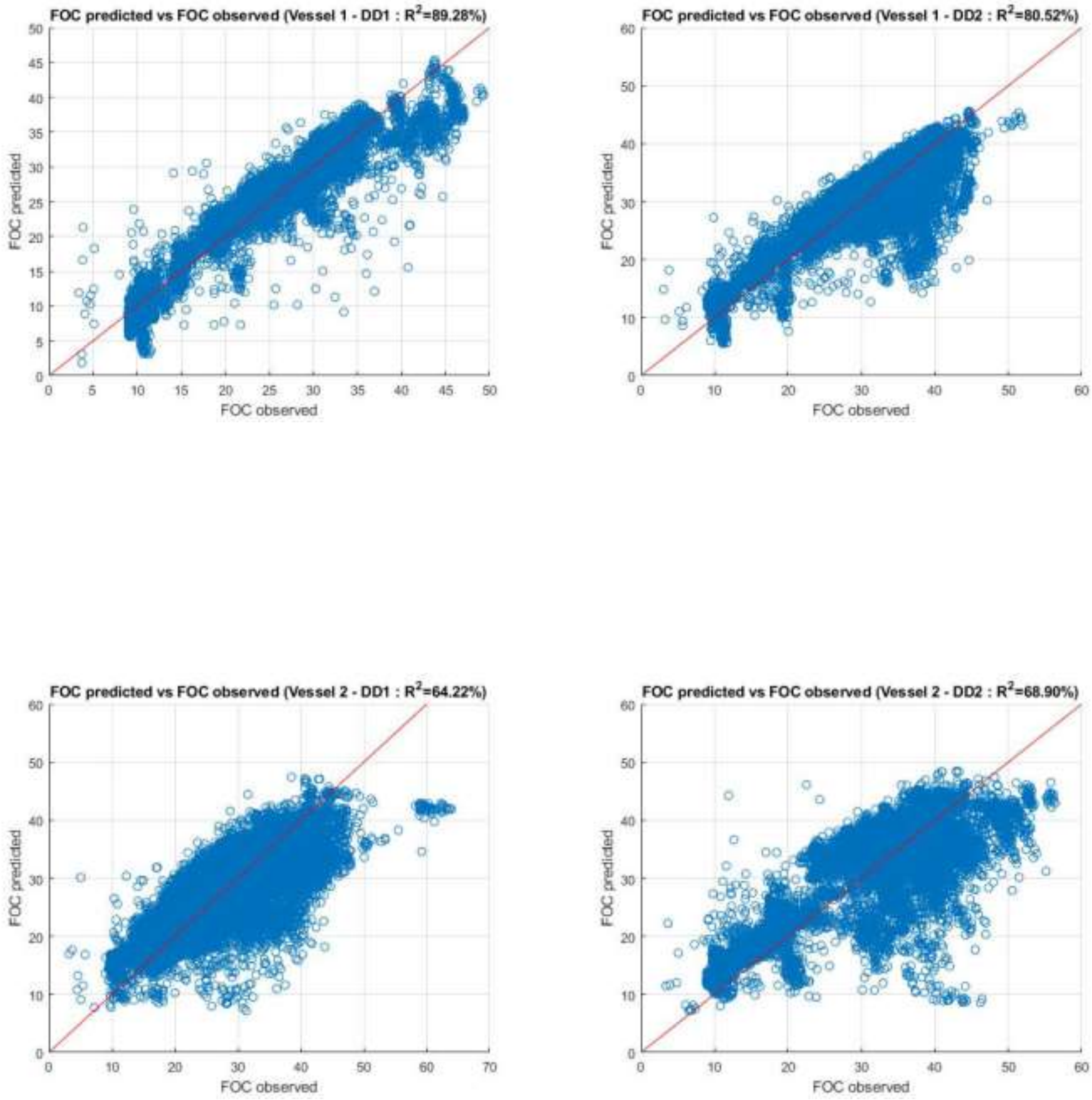

Figure 53: FOCpredicted vs FOCobserved (regression fitting).

4.13 Case study

For the selected 3-variable regression model, a case study is performed in order to evaluate and compare the FOC predictions between the two examined periods (DD1 & DD2) as well as between the two vessels (Vessel 1 & Vessel 2). Four different cases are examined with each case concerning a different wind speed and loading condition (expressed by the mean draft).

The 4 examined cases are:

- <u>Case 1</u>: $\mathrm{WS} = 0\ \mathrm{m/s}$ & $\mathrm{T_m} = \mathrm{T_{ballast}}$
- <u>Case 2</u>: $\mathrm{WS} = 0\ \mathrm{m/s}$ & $\mathrm{T_m} = \mathrm{T_{laden}}$
- <u>Case 3</u>: $\mathrm{WS} = 10\ \mathrm{m/s}$ & $\mathrm{T_m} = \mathrm{T_{ballast}}$
- <u>Case 4</u>: $\mathrm{WS} = 10\ \mathrm{m/s}$ & $\mathrm{T_m} = \mathrm{T_{laden}}$

where the mean draft for the ballast and the laden condition are the values calculated in the Draft correction paragraph.

The first part of the case study (Part A: DD1 vs DD2) is concerned with the comparison of fuel oil consumption values between the two examined periods (DD1 & DD2) for both vessels. Predictions are provided by the selected regression model whose predictors' values differ from case to case (WS & TM). Six different characteristic speed through water values are examined: $\mathrm{STW} = 10 - 15$ kn.

The second part of the case study (Part B: Vessel 1 vs Vessel 2) is concerned the comparison of fuel oil consumption values between the two vessels (Vessel 1 & Vessel 2) for each examined period. In contrast with the previous part, Part B does not focus on a specific speed through water value. Instead, the $\mathrm{FOC} - \mathrm{STW}^2$ curve of each vessel is produced by the respective regression model for Case 1 and Case 2. The vessels' curves are plotted in a common figure and compared over time (DD1 & DD2) for a range of STW values.

Only Cases 1 and 2 are examined at Part B due to the contradiction between the WS coefficients' sign (positive for Vessel 1 and negative for Vessel 2). It can be understood that a comparison involving the wind speed between the two vessels cannot be supported.

4.13.1 Part A: DD1 vs DD2

Vessel 1's fuel oil consumptions for each case and examined speed through water value are summarized in Table 35.

STW	CASE 1		CASE 2		CASE 3		CASE 4	
	DD1	DD2	DD1	DD2	DD1	DD2	DD1	DD2
10 knots	8.47	10.90	12.90	16.23	11.48	14.15	15.91	19.48
	29%		**26%**		**23%**		**22%**	
11 knots	12.91	15.03	17.33	20.37	15.92	18.28	20.34	23.61
	16%		**18%**		**15%**		**16%**	
12 knots	17.76	19.56	22.19	24.89	20.77	22.81	25.20	28.14
	10%		**12%**		**10%**		**12%**	
13 knots	23.04	24.48	27.47	29.81	26.05	27.73	30.48	33.06
	6%		**9%**		**6%**		**8%**	
14 knots	28.74	29.79	33.17	35.12	31.76	33.04	36.18	38.37
	4%		**6%**		**4%**		**6%**	
15 knots	34.87	35.50	39.29	40.83	37.88	38.75	42.30	44.08
	2%		**4%**		**2%**		**4%**	

Table 35: FOC predicted values Vessel 1 (Regression – Case study: Part A).

As it can be observed in the above tables that Vessel 1 generally consumes less fuel oil when travelling at lower speeds, a prediction that is in accordance with the real-time operation expectations. Furthermore, in each case, the predicted FOC is greater for DD2 than for DD1. However, the increase becomes significantly smaller as the speed rises, leading to insignificant differences (2-6%) for $\mathrm{STW} = 14 - 15\ \mathrm{kn}$. Through the comparison of the percentages for the pairs Case 1 – Case3 and Case 2 – Case 4 it can be understood that while wind speed generally increases FOC (positive coefficient) it has no significant effect on the relative DD1 - DD2 differences, which mainly depend on STW and TM. Another observation is that greater drafts (laden condition) cause about a "+2%" increase in the aforementioned gap for all speed except the lowest one. Overall, while the duct's long-term effect is not depicted by the predicted FOC values, the stabilization of the values between DD1 and DD2, expressed by the percentage difference, for the high speeds indicates an increased performance that may be related to the Mewis duct. However, this is but an assumption that may or may not be verified by the high level of uncertainty that lies within the 2-6% difference.

Vessel 2's fuel oil consumptions for each case and examined speed through water value are summarized in Table 36.

STW	CASE 1		CASE 2		CASE 3		CASE 4	
	DD1	DD2	DD1	DD2	DD1	DD2	DD1	DD2
10 knots	14.46	15.73	22.28	24.45	11.79	14.30	19.61	23.02
	9%		**10**%		**21**%		**17**%	
11 knots	18.22	19.33	26.03	28.05	15.55	17.89	23.36	26.61
	6%		**8**%		**15**%		**14**%	
12 knots	22.33	23.27	30.15	31.99	19.66	21.83	27.48	30.55
	4%		**6**%		**11**%		**11**%	
13 knots	26.80	27.55	34.62	36.27	24.13	26.11	31.95	34.83
	3%		**5**%		**8**%		**9**%	
14 knots	31.63	32.17	39.45	40.89	28.96	30.74	36.78	39.46
	2%		**4**%		**6**%		**7**%	
15 knots	36.82	37.14	44.63	45.85	34.15	35.70	41.96	44.42
	1%		**3**%		**5**%		**6**%	

Table 36: FOC predicted values Vessel 2 (Regression – Case study: Part A).

As it can be observed in the above tables that Vessel 2 generally consumes less fuel oil when travelling at lower speeds, a prediction that is in accordance with the real-time operation expectations. Furthermore, in each case, the predicted FOC is greater for DD2 than for DD1. However, this increase becomes smaller as the speed rises, leading to $1-7\%$ differences for $\text{STW} = 14 - 15$ kn. While the increase of draft leads to greater FOC values, wind speed has an opposite effect that is expressed by the negative coefficient of the WS variable. Wind speed seems to significantly increase the relative difference of FOC between DD1 and DD2 while TM has a more limited effect.

Overall, the assumption made for Vessel 1 seems to be invalid if the patterns of Vessel 2 are taken into consideration. While the consumption is higher in the DD2 period, the relative difference is gradually reduced as speed is increased for both vessels. This similarity does not allow for the relative reduction to be attributed to the Mewis duct.

4.13.2 Part B: Vessel 1 vs Vessel 2

Case 1

Vessel 1 is predicted to consume less fuel oil than Vessel 2 for both periods DD1 and DD2. The difference in FOC between the vessels is greater for lower speeds (about 6 tons/day for DD1 and 5 tons/day for DD2) and reduces as speed increases. The difference is minimized (about 1.5 ton/day) at 15 knots. Both vessels' FOC values increase during DD2, however, Vessel 2's increase is smaller, causing the difference between the fuel consumption of the vessels to drop during the second post dry-dock year.

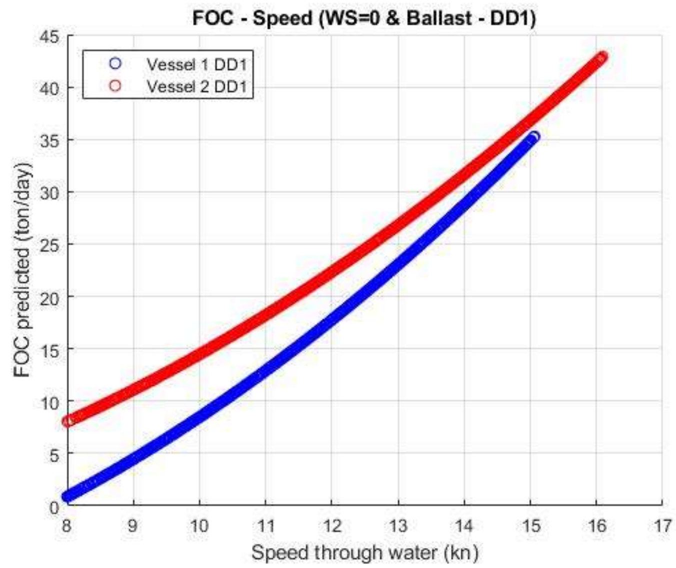

Figure 54: FOC – STW^2 (Case 1 – DD1).

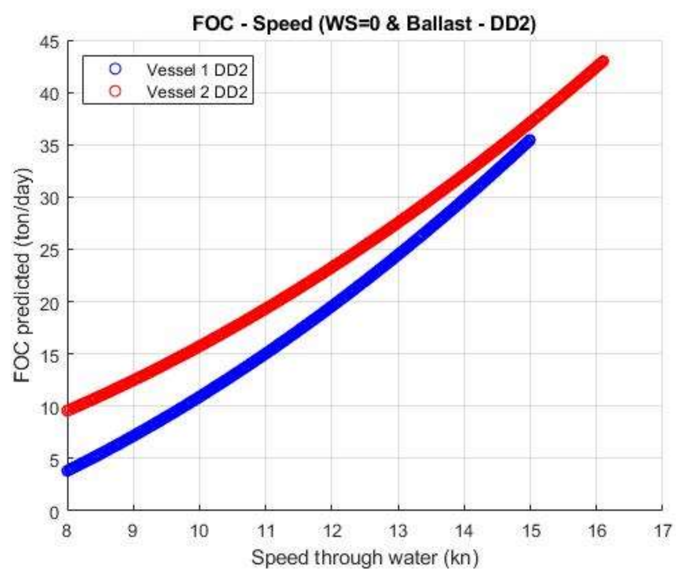

Figure 55: FOC – STW^2 (Case 1 – DD2).

Case 2

Vessel 1 is predicted to consume less fuel oil than Vessel 2 for both periods DD1 and DD2. Compared with Case 1's (Ballast condition), Case 2's fuel consumptions are generally greater, a fact that is expected due to the added cargo weight. In the laden condition, the difference in consumption between the two vessels is greater than the one in the ballast condition, underlining Vessel 1's added performance advantage in increased drafts which can be attributed to the Mewis duct. Once again, the gap between the vessels' FOC is reduced with the increase of speed.

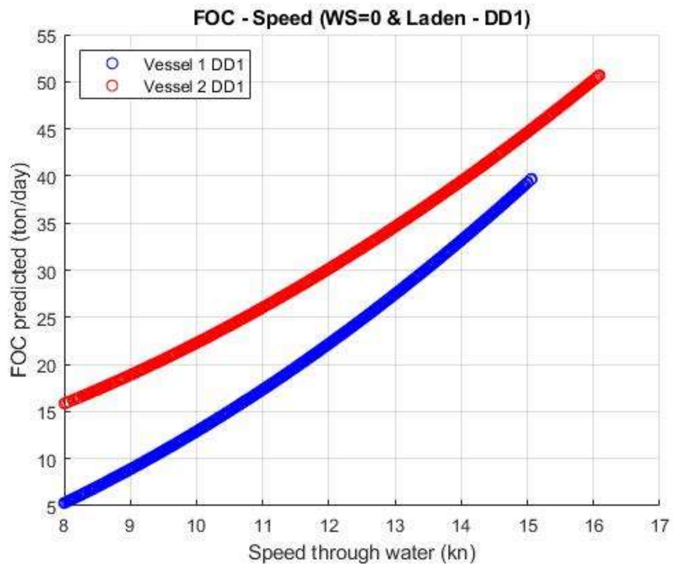

Figure 56: FOC – STW^2 (Case 2 – DD1).

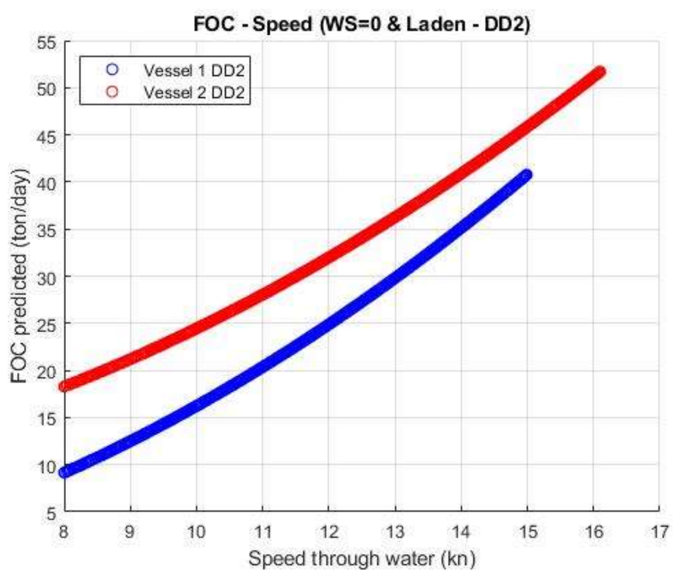

Figure 57: FOC – STW^2 (Case 2 – DD2).

[This page is intentionally left blanc]

5 Conclusions

The diploma thesis attempts to evaluate the propulsive efficiency of an energy-saving device, the Mewis propeller duct, through the utilization of a practical performance monitoring framework. For this purpose, two sister vessels are monitored for a three-year period, during which one had a Mewis duct installed. The task is to assess the duct's effect by performing comparison between the pre-duct and the post-duct era as well as between the two sister vessels for the same period. The study approaches the problem via two routes; a Key Performance Indicator (KPI) analysis and a regression model.

The first step of performance monitoring is the measurement of propulsion-related physical quantities by onboard measuring devices. A database is created as the output of this procedure. The examined dataset of the current thesis contains more than 200,000 data points gathered during a three-year period. It can be understood that one major prerequisite for proper conclusions to be drawn, is a vast database that quantifies the vessel's behavioral patterns through time and allows for the evaluation of the long-term impact of performance-altering events, such as a hull cleaning repair or a duct installation. The occurring database contains various points that do not correspond with the physical relationships that bind the measured quantities or that simply do not have a physical meaning. These points occur either due to the devices' miscalculations or while the vessel is in non-operational state, such as waiting to enter a port or being loaded. Since the propulsive efficiency is under consideration, such points that do not represent sea-travel data need to be omitted; that is achieved through a data correction process whose aim is to detect the outliers and eliminate them without discarding desirable data that provide valuable information. This procedure, while belonging to the initial steps of performance monitoring evaluation methods, should be considered of vital importance as it is responsible for "cleaning" the dataset from points that cause distortion between the measurements and the true physical relationships among the quantities. Therefore, a corrected dataset is the solid basis of the evaluation method performed, which, in the particular case, is the KPI analysis and the regression analysis.

The Key performance indicators chapter attempts to quantify, for both vessels, the performance's fluctuations via three KPIs. The first KPI ($\mathrm{KPI_a} = \mathrm{P/n^3}$) shows that while Vessel 2 performance is higher at first, Vessel 1 manages to narrow the gap once its propeller is polished. Despite the expectation for this improvement to be short-term, Vessel 1's performance, expressed by KPIa, has a constantly upward trend, even towards the end of the examined period when the effect of dry-dock repairs is significantly weakened. On the other hand, Vessel 2 notices an increase in performance after dry-dock, which has a one-year lasting upward trend, while its performance seems to have been stabilized for the rest of the examined period. The difference in the long-term trends of KPIa underline the effect of the Mewis duct on Vessel 1; when the effects of the propeller polishing and the other dry-dock repairs, such as the hull cleaning, are weakened by time, Vessel 1 shows an improving performance trend that is attributed to the only event with long-term impacts, the Mewis duct fitting. Despite the revealing results occurring from the study of KPIa, KPIb ($\mathrm{P/FOC}$) and KPIc ($\mathrm{V/FOC}$) (for the ballast condition) do not depict the effect of the Mewis duct, which is, however, highlighted when KPIc is examined in the laden condition. Vessel 1's KPIc laden is initially lower that Vessel 2's, a fact that is translated in initially higher performance levels for the latter. Despite that Vessel 1's performance is boosted by the propeller polishing, the boost seems to be short-term as the performance's trendline is declining. Both vessels notice an increase in their respective KPIc laden values right after dry-dock. This increase is accompanied with gradual improvement of performance over time for Vessel 1, while Vessel 2 shows a constantly deteriorating performance. Once again, when the vessels' performance is examined in the long run, it can be noticed that Vessel 1's steadily rises while Vessel 2's declines. These contradicting patterns are explained when the duct's impact is brought into the equation; as the time passes and the hull is slowly fouled again, Vessel 1 achieves greater results than Vessel 2 in the laden loading condition. As a result, it can be deduced that in greater drafts, which occur for loaded ships, the effect of the Mewis duct is enhanced.

The Regression analysis chapter aims to approach the problem under a different scope. The post dry-dock era is divided into two sub-periods (DD1 & DD2) for which regression models are produced as an attempt to predict the fuel oil consumption given some sea-travel related values, specifically the speed through water, the wind speed, the rudder angle, the ship's mean draft and trim. Out of the available predictors, only three (STW, WS, TM) are chosen for the final models which achieve satisfactory fitting without being overcomplicated or affected by multicollinearity. Vessel 1's models provide more solid predictions, in terms of R^2 and standard error, than Vessel 2's, for which the wind speed's coefficients are negative signifying that FOC increases as WS increases. This contradiction between the two vessels models may be attributed to Vessel 2 experiencing fairer winds than Vessel 1 that aided its propulsion instead of increasing wind resistance. This, however, remains an assumption that cannot be verified unless the relative direction of the wind speed is provided. If the lower R^2 values of Vessel 2 models are also taken into account, it can be understood that the regression would provide significantly better predictions if the relative wind speed direction is introduced along with other weather-related data, such as the wave height. Despite the presented limitations of the discussed preliminary regression models, some important conclusions can be drawn concerning the examined predictors. The rudder angle is very loosely correlated with FOC and as a consequence its contribution to the model is insignificant. On the other hand, speed through water, and especially its square value, can alone explain a lot of the variation in the predictions (R^2) and its participation in the model is vital. As far as the mean draft and trim are concerned, it is important that one of them is used in the model as predictions are improved. Their high correlation with each other advises against their simultaneous use which introduces multicollinearity to the models. Finally, the wind speed is also considered a valuable predictor that, if combined with the relative wind direction and other weather-related variables, can lead to solid FOC predictions and highly fitted models. Part A of the case study does not reveal the effect of the duct. Part B provides more encouraging results. For both the ballast and the laden no-wind cases, Vessel 1 is predicted to consume less than Vessel 2 for the entire period. This performance advantage is increased for the laden condition, a fact that is in terms with the enhanced duct effect in the greater drafts revealed by KPIc laden.

Bibliography

[1] International Maritime Organization, "IMO Train the Trainer (TTT) course on Energy Efficient Ship Operation : Module 4 - Ship Board Energy Management," International Maritime Organization, London, 2016.

[2] T. W. F. Hasselaar, "An investigation into the development of an advanced ship performance monitoring and analysis system," Newcastle University , Newcastle upon Tyne, 2010.

[3] P. Karagiannidis, "Data-driven Ship Propulsion modeling with applications in the Performance Anaysis and Fuel Consumption prediction," National Technical University of Athens, Athens, 2019.

[4] N. Themelis, C. Spandonidis & C. Giordamlis, "Evaluating the Efficiency of an Energy-Saving Device by Performance Monitoring," in *Hull Performance & Insight Conference (HullPIC)*, Gubbio, 2019.

[5] J. P. Petersen, D. J. Jacobsen & O. Winther, "Statistical modelling for ship propulsion efficiency," *Journal of Marine Science and Technology*, vol. 17, no. 1, pp. 30 - 39, 2012.

[6] ISO, "ISO 19030: Ships and marine technology - Measurement of changes in hull and propeller perfomance. Part 2: Default method," ISO, Geneva, 2016.

[7] MAN Diesel & Turbo, "Basic Principles of Ship Propulsion," [Online]. Available: https://spain.mandieselturbo.com/docs/librariesprovider10/sistemas-propulsivos-marinos/basic-principles-of-ship-propulsion.pdf?sfvrsn=2.

[8] P. J. Rousseeuw, Robust Regression and Outlier Detection, Antwerp: John Wiley & Sons, 1987.

[9] L. G. Aldous, "Ship Operational Efficiency : Performance Models and Uncertainty Analysis," University College London, London, 2015.

[10] A. A. Safaei, H. Ghassemi & M. Ghiasi, "VLCC's fuel consumption prediction modeling based on noon report and automatic identification system," *Cogent Engineeering*, vol. 6, no. 1, 2019.

[This page is intentionally left blanc]

Appendix A: Data correction – Part II filters

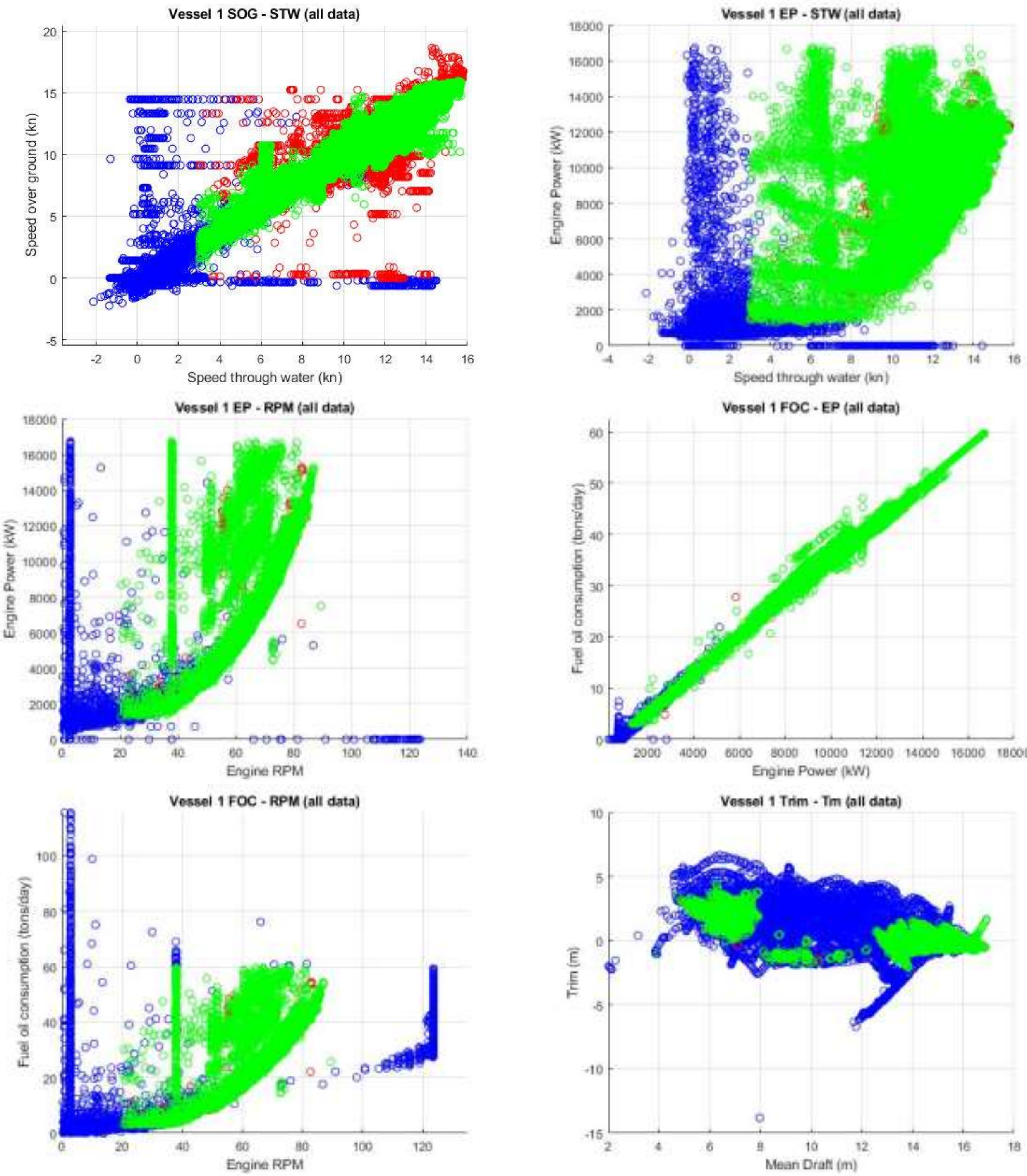

Figure 58: Filter STW_SOG – Vessel 1.

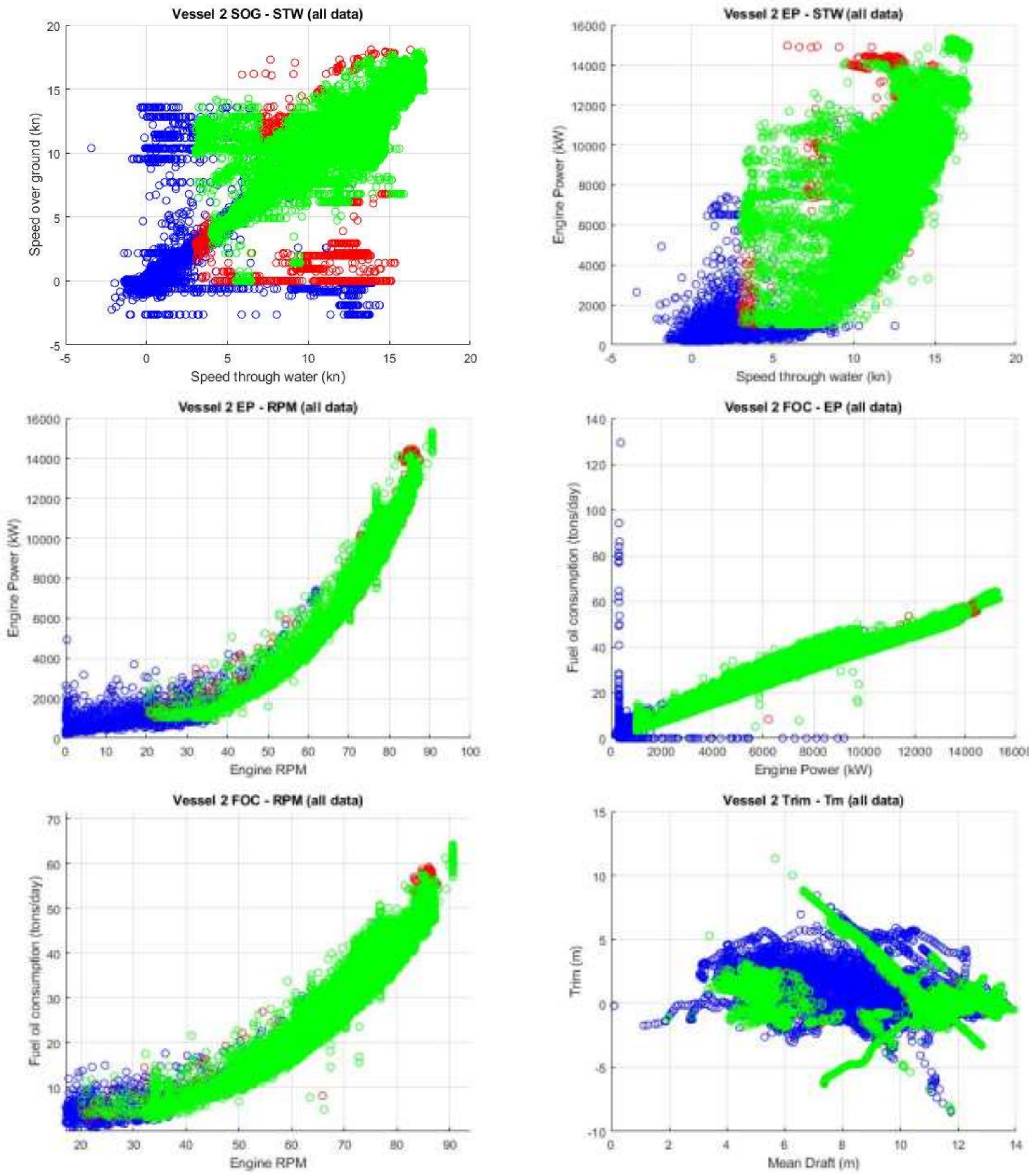

Figure 59: Filter STW_SOG – Vessel 2.

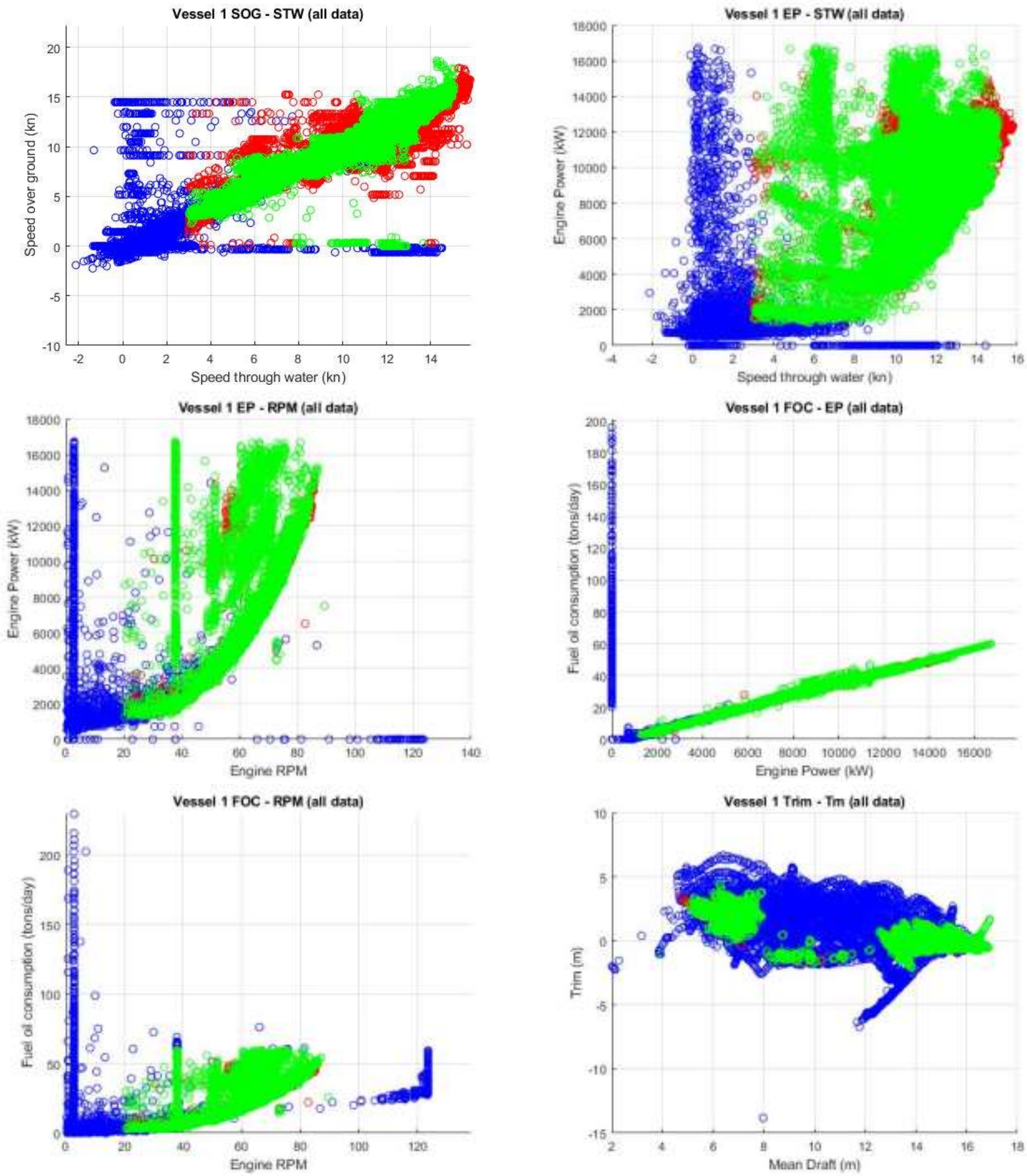

Figure 60: Filter SOG_STW – Vessel 1.

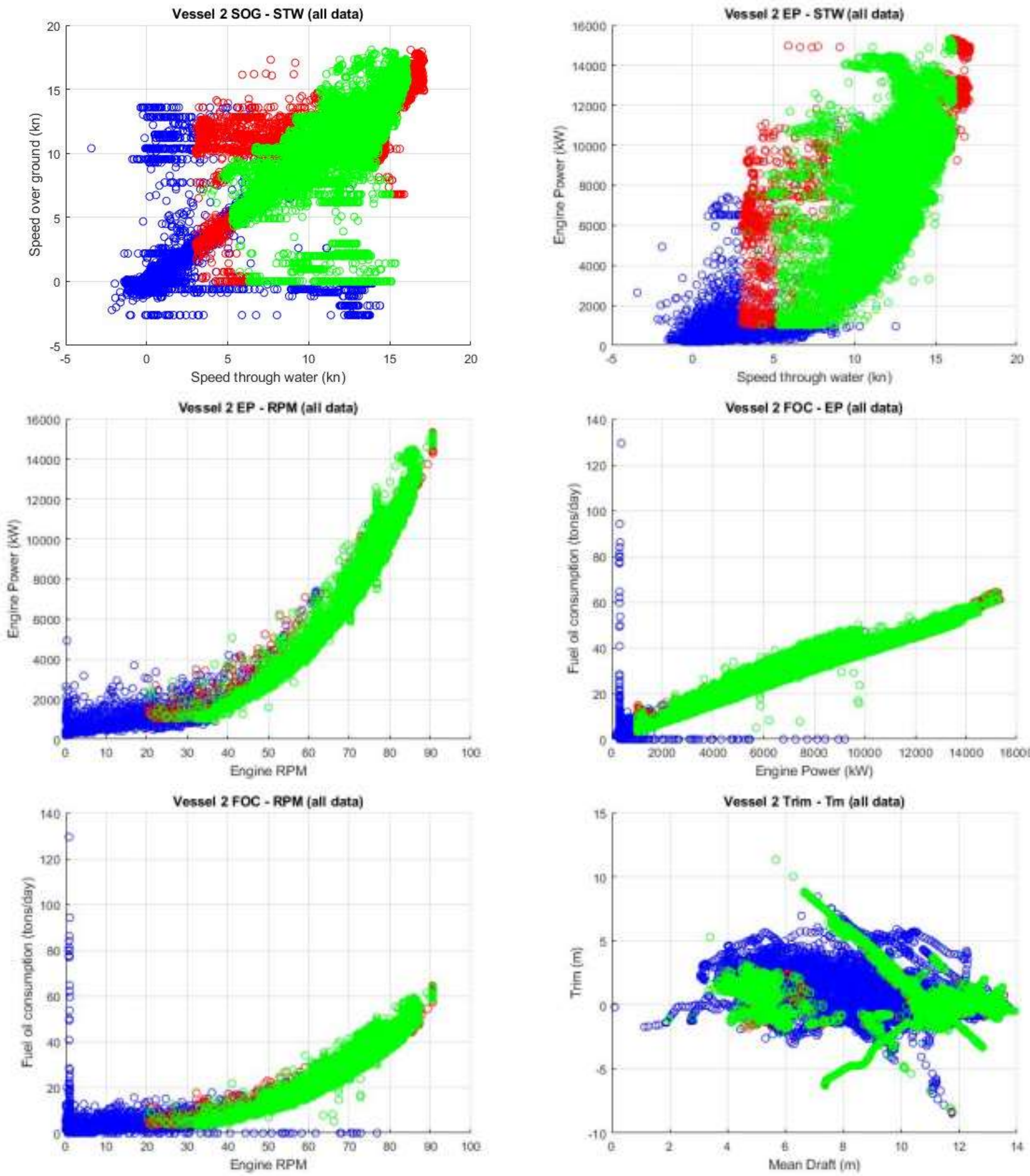

Figure 61: Filter SOG_STW – Vessel 2.

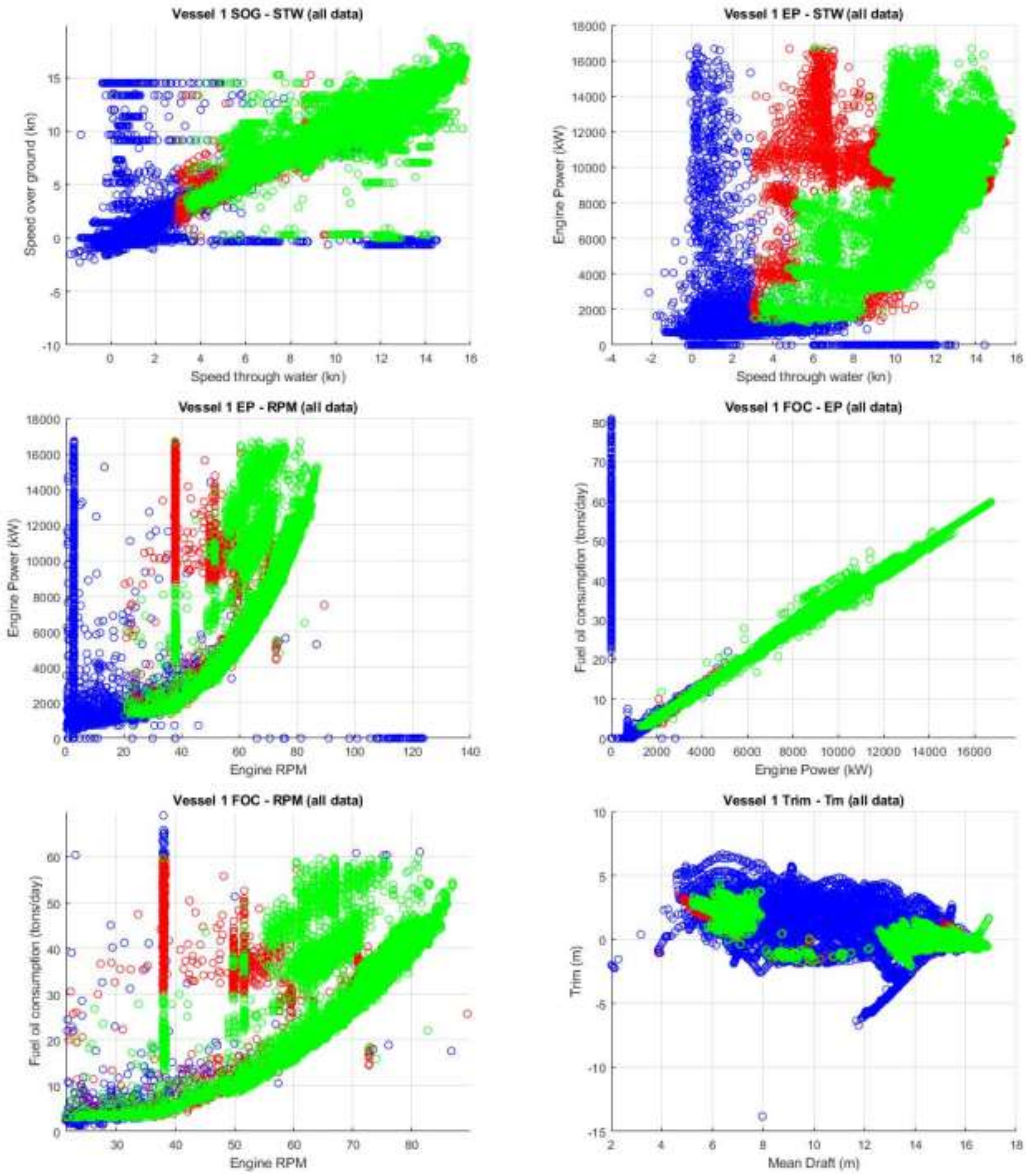

Figure 62: Filter EP_STW – Vessel 1.

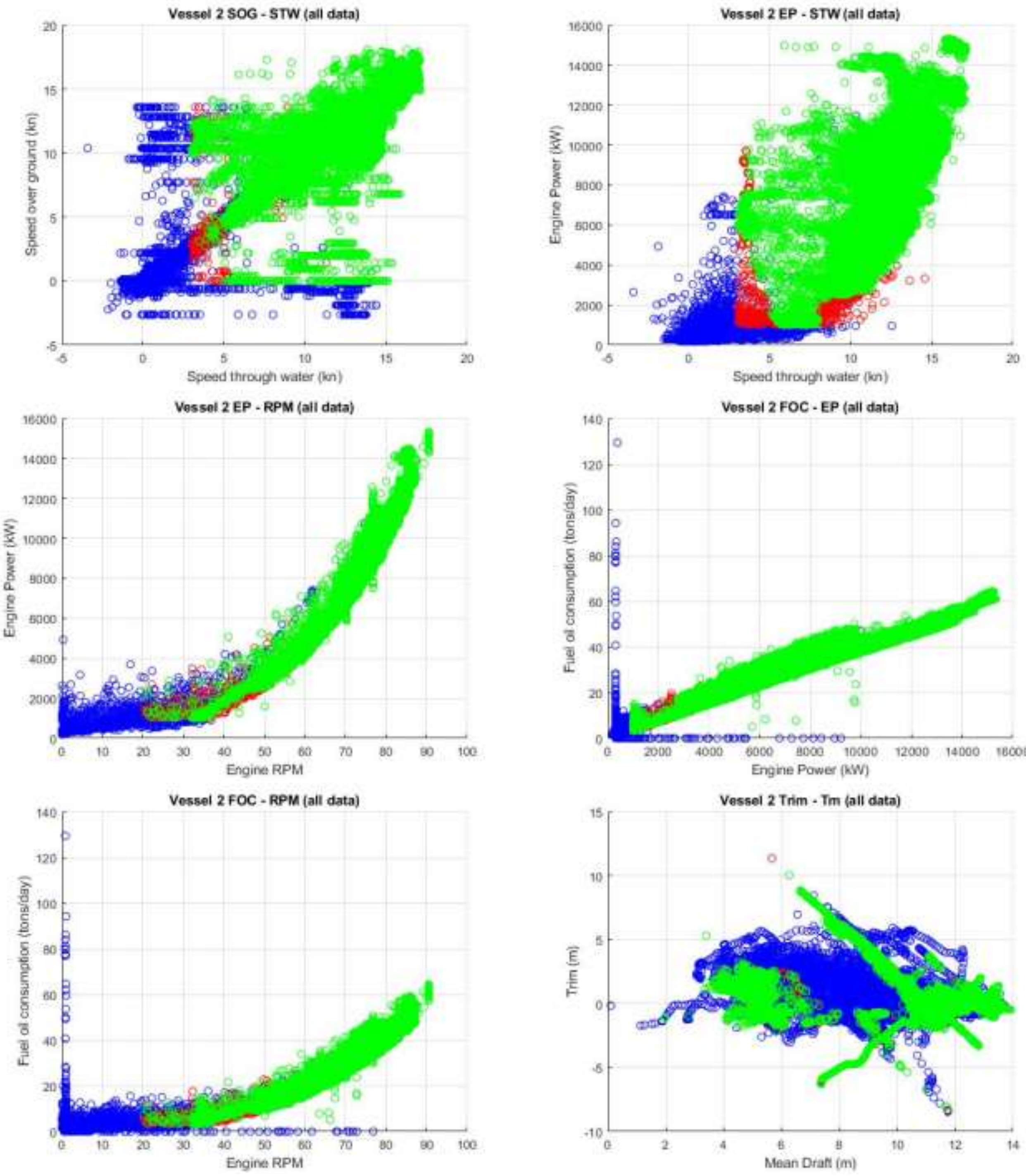

Figure 63: Filter EP_STW – Vessel 2.

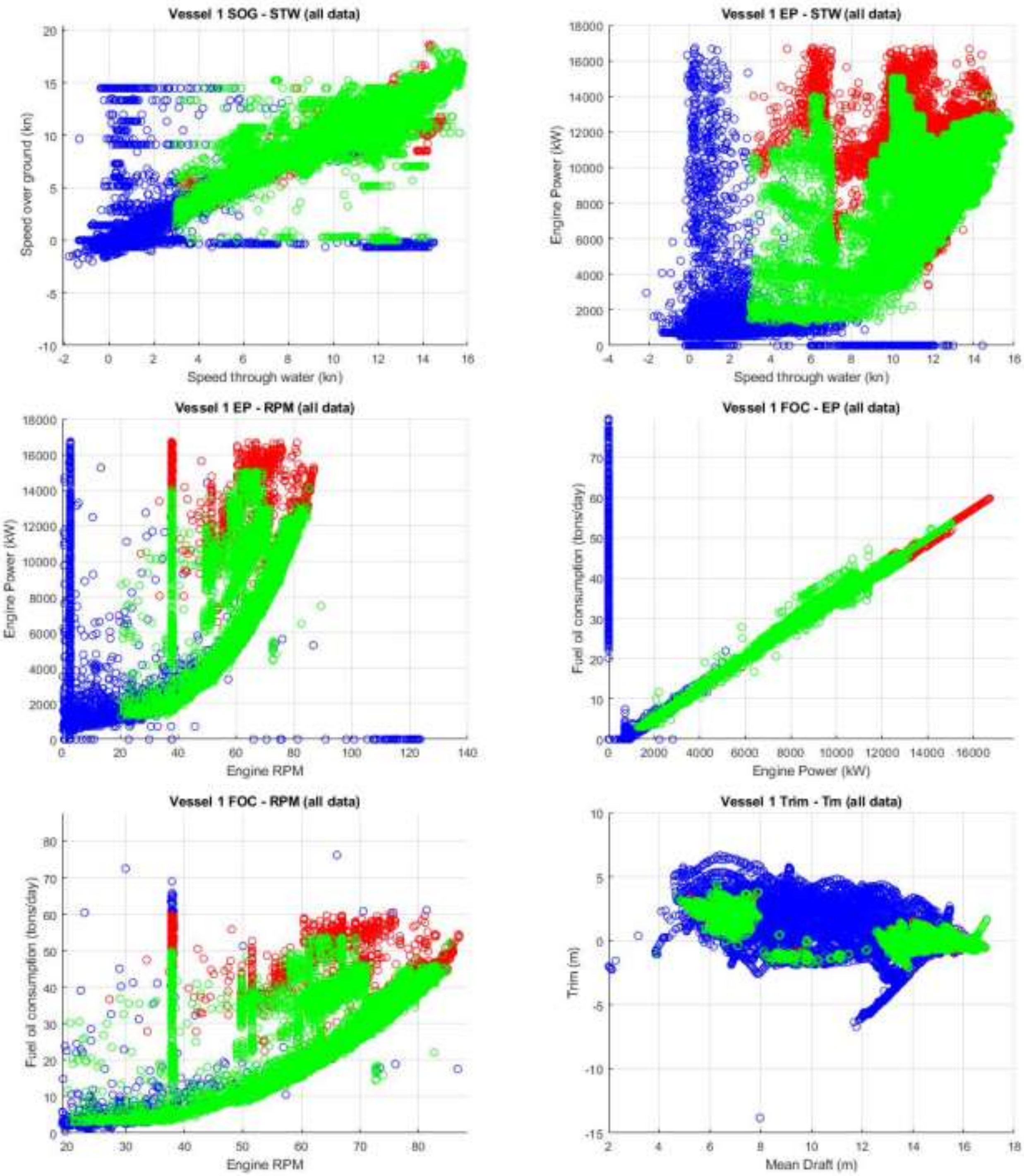

Figure 64: Filter STW_EP – Vessel 1.

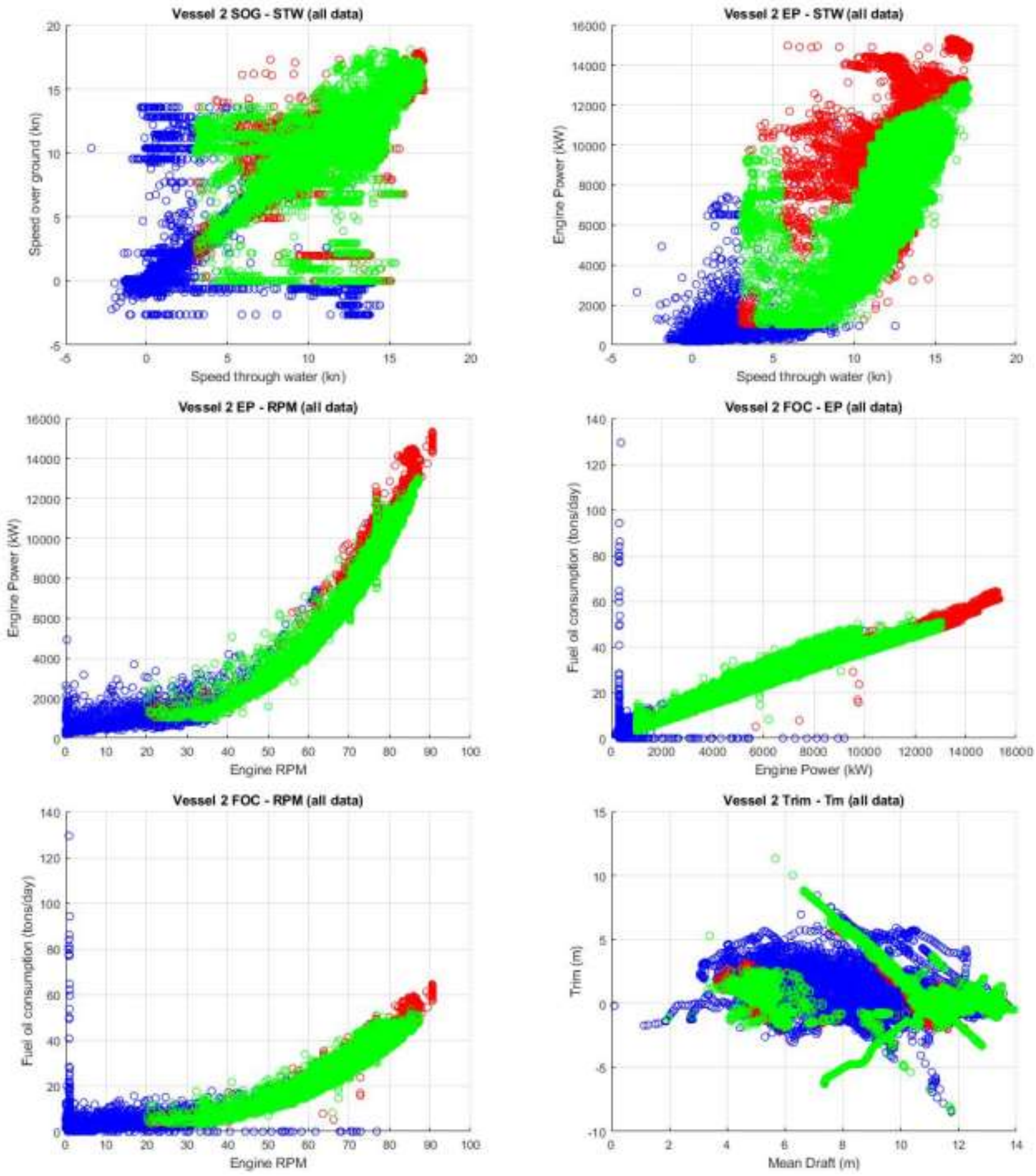

Figure 65: Filter STW_EP – Vessel 2.

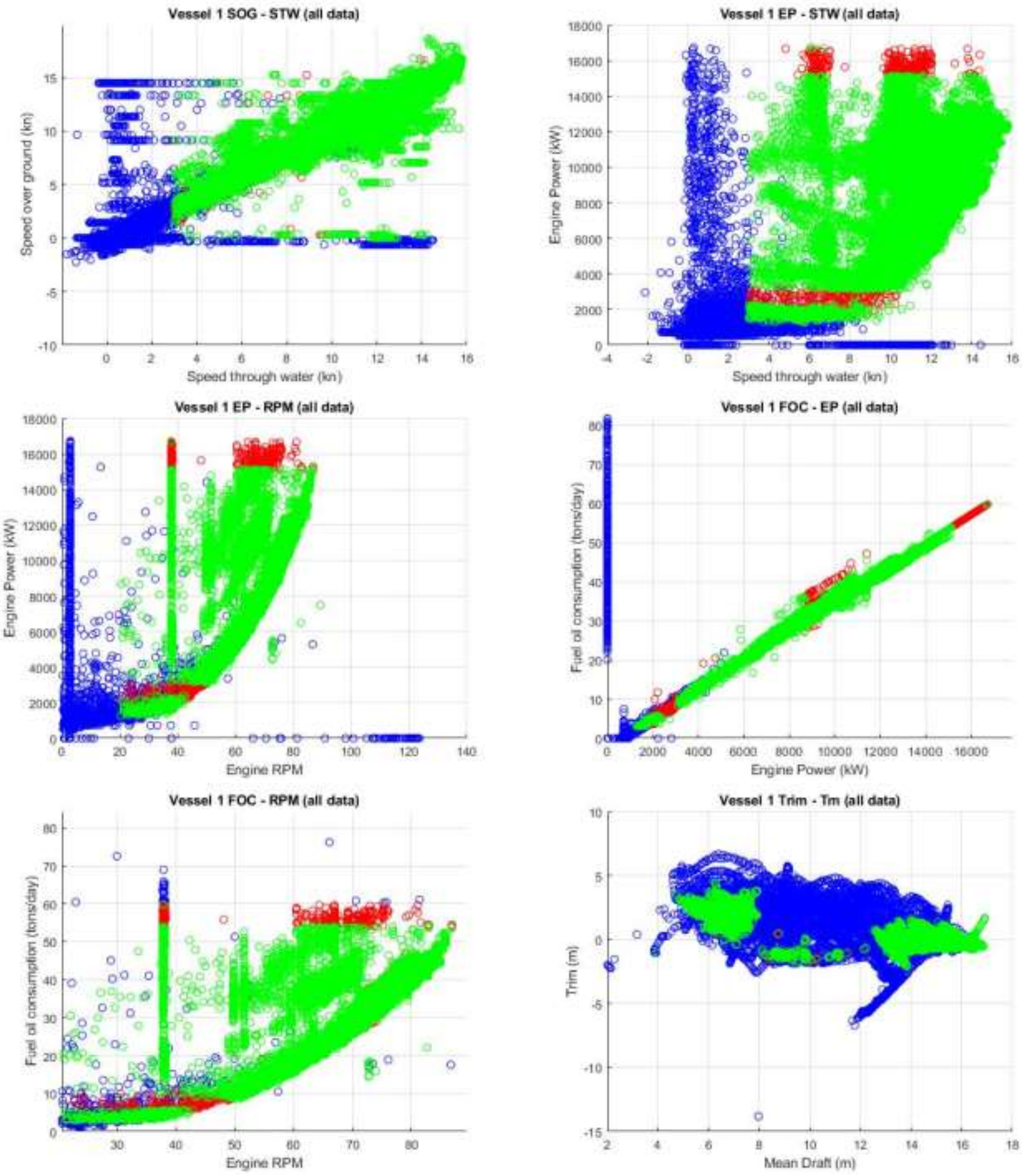

Figure 66: Filter EP_FOC – Vessel 1.

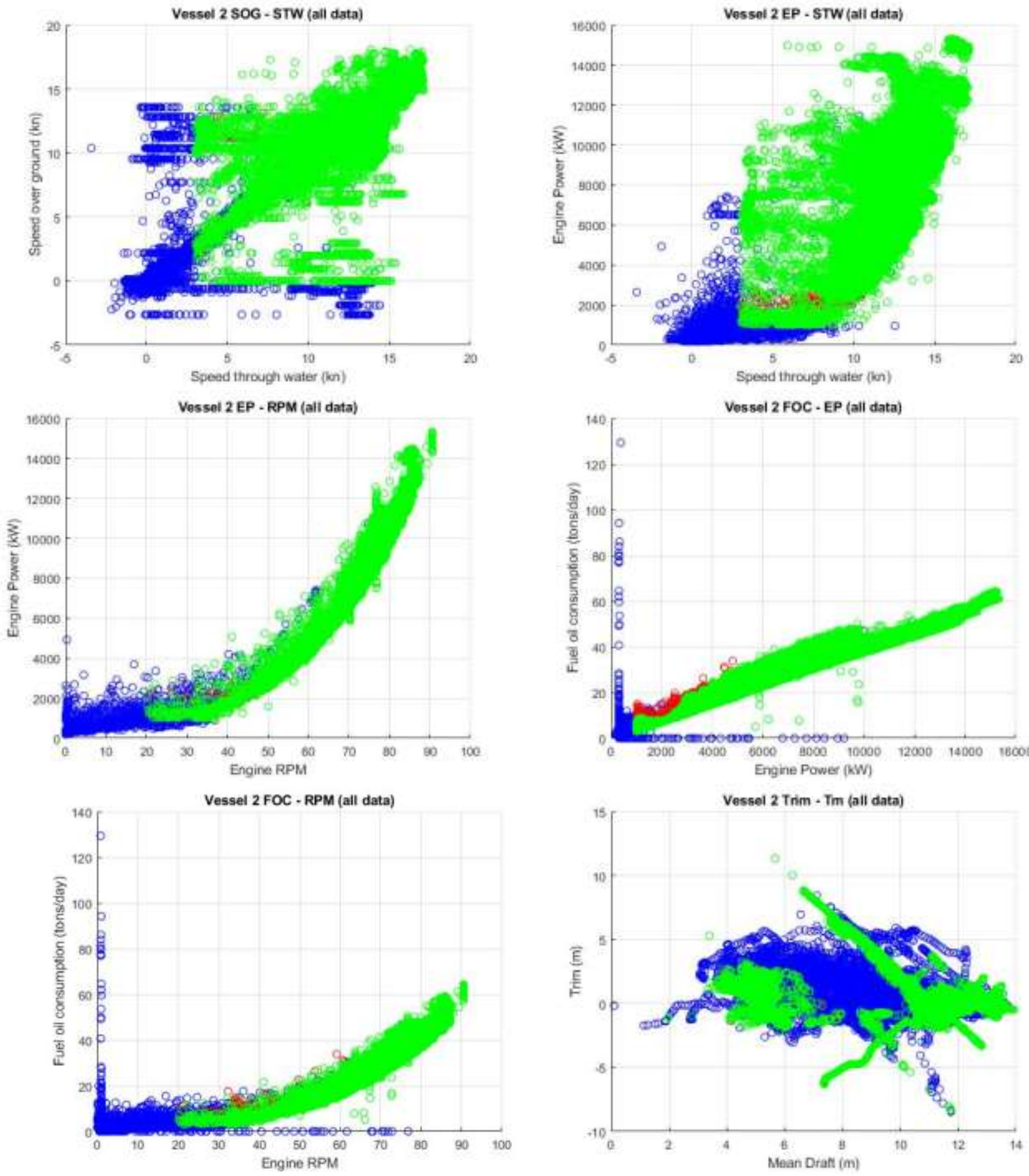

Figure 67: Filter EP_FOC – Vessel 2.

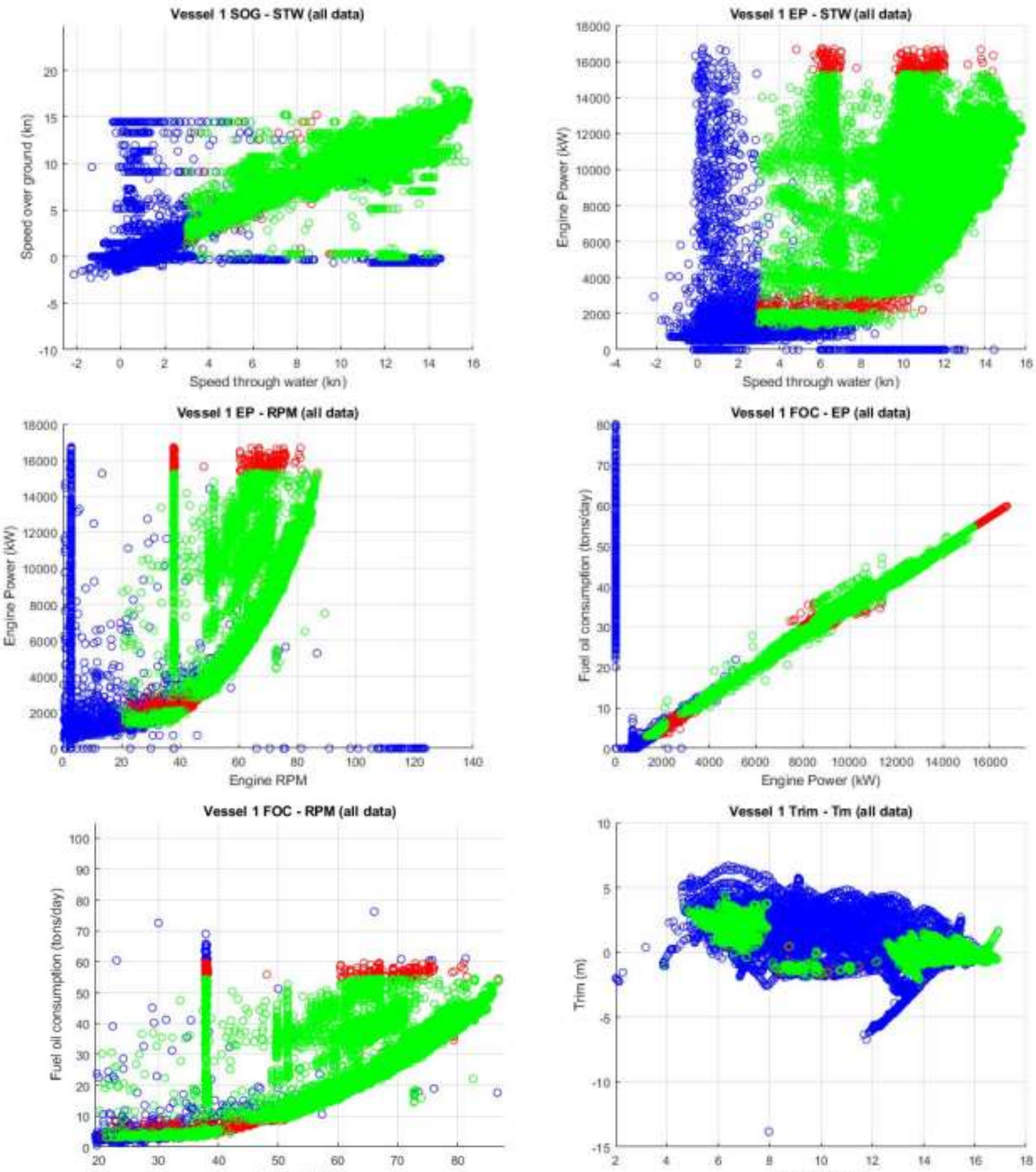

Figure 68: Filter FOC_EP – Vessel 1.

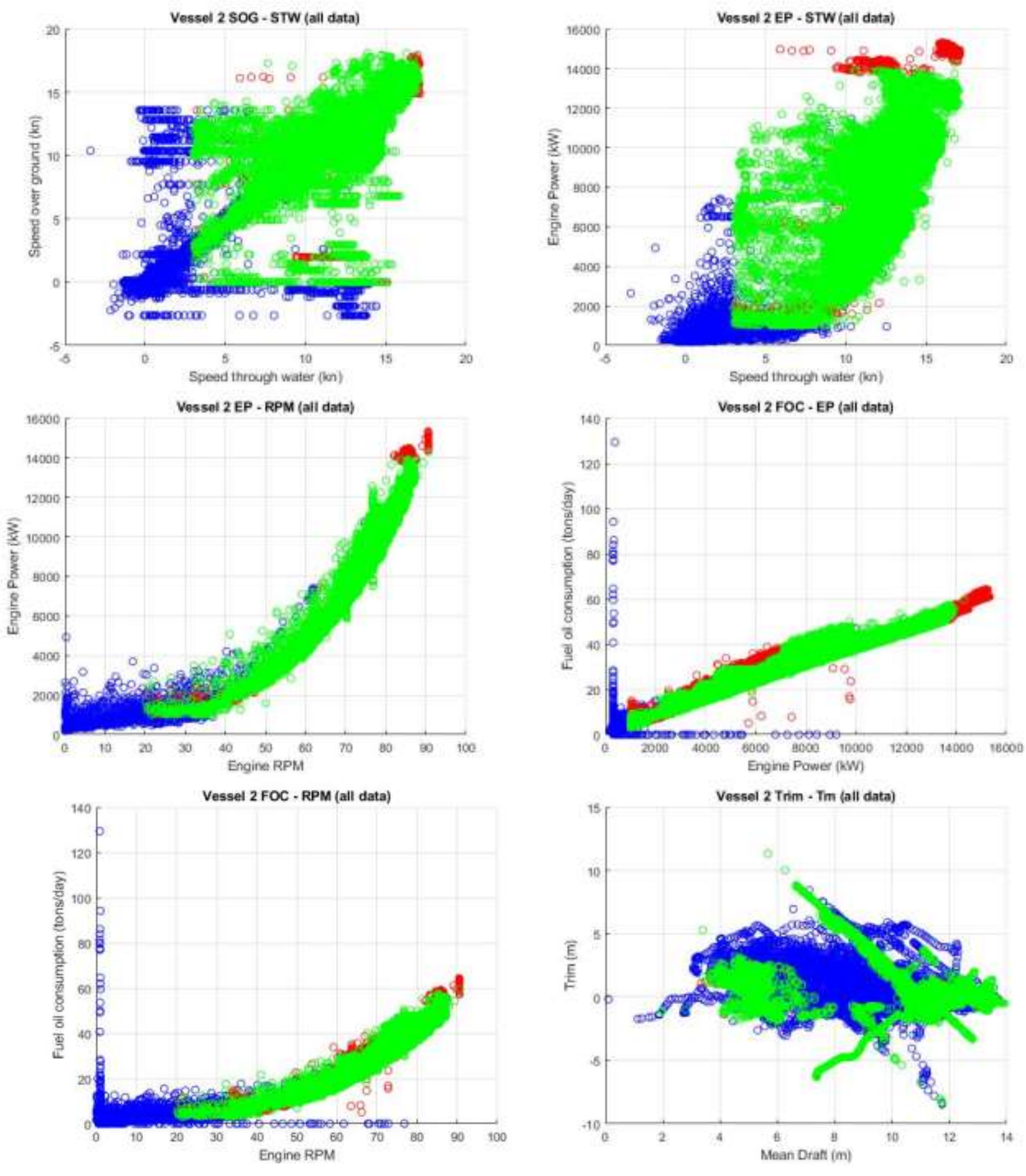

Figure 69: Filter FOC_EP – Vessel 2.

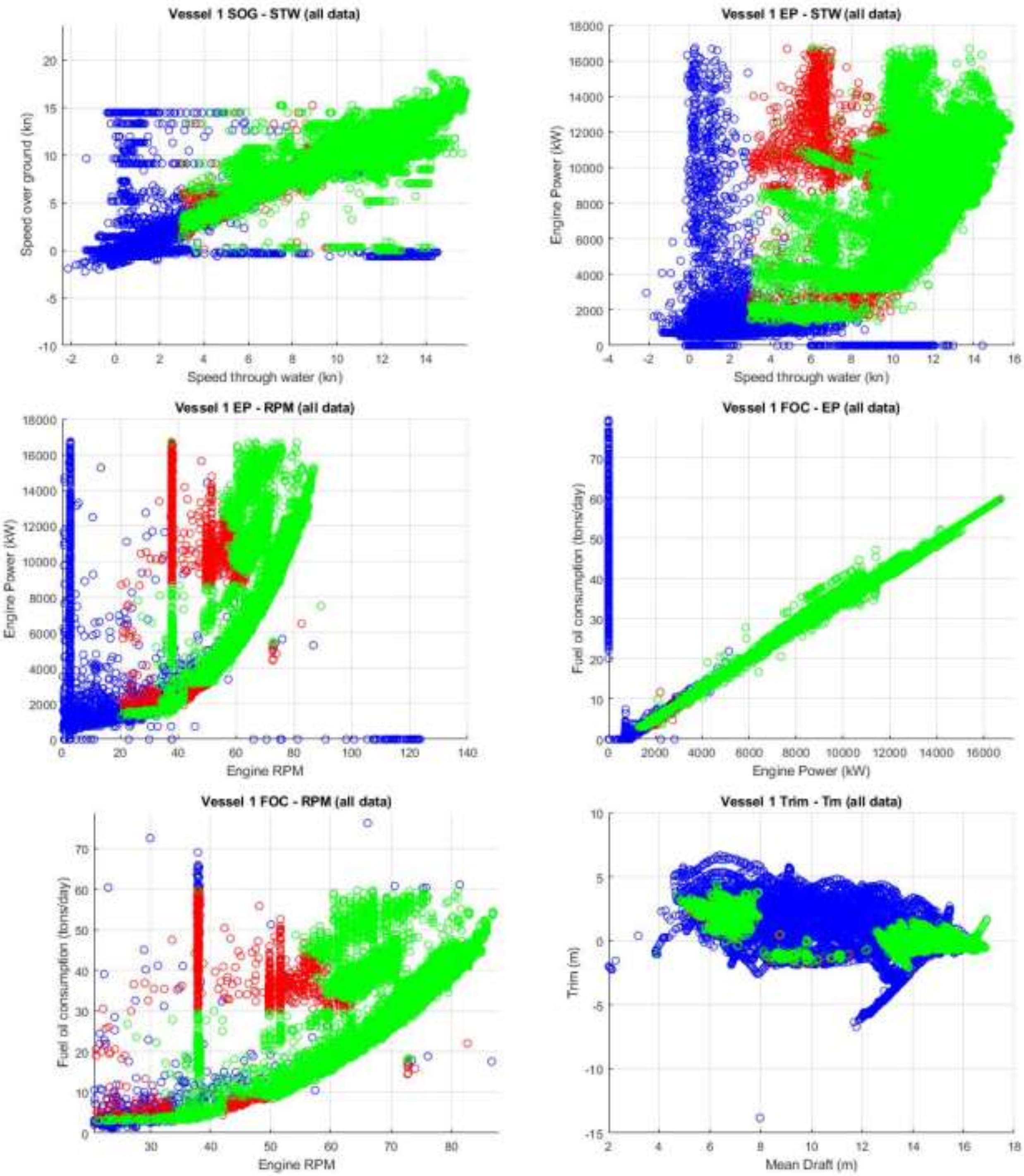

Figure 70: Filter EP_RPM – Vessel 1.

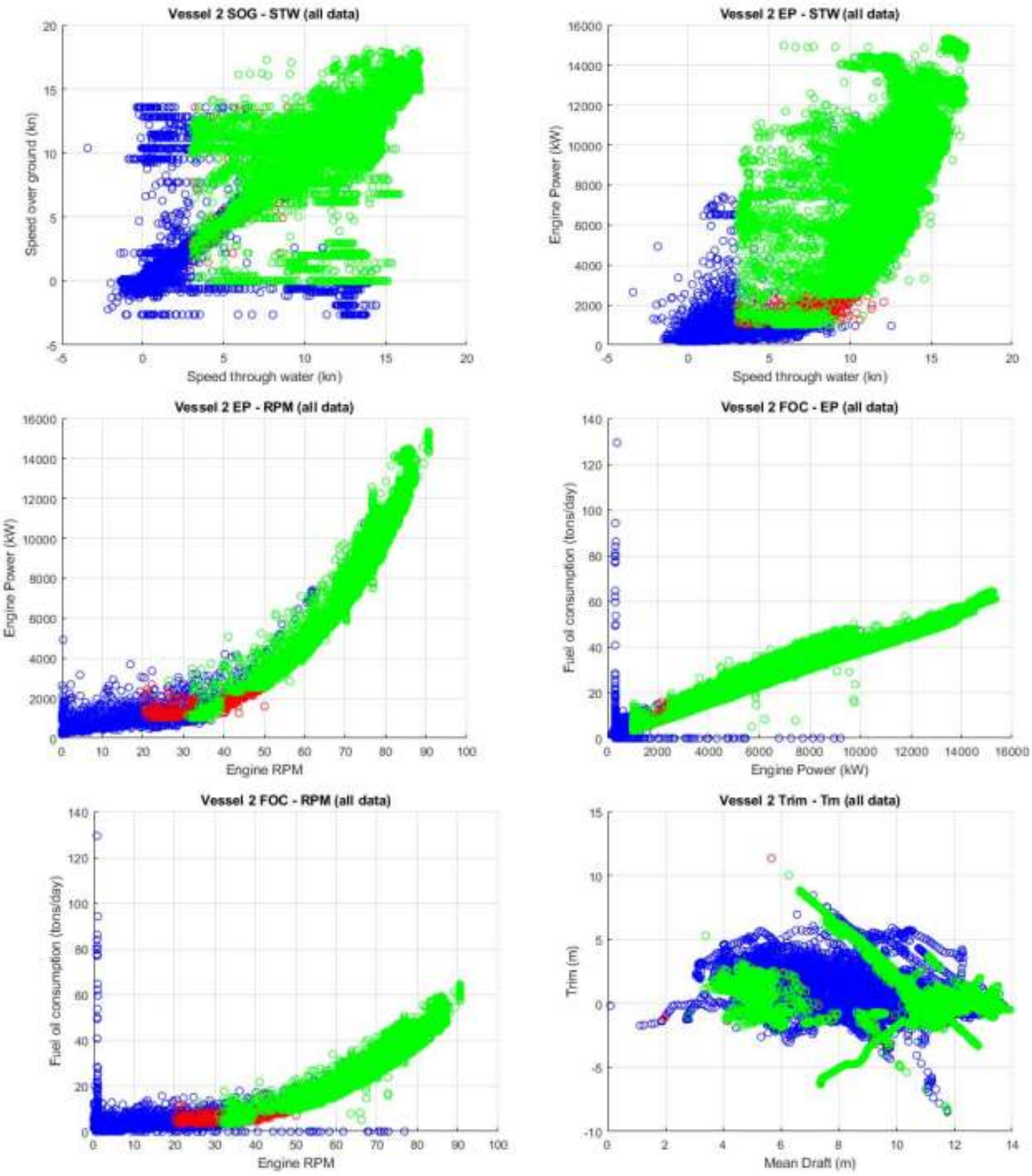

Figure 71: Filter EP_RPM – Vessel 2.

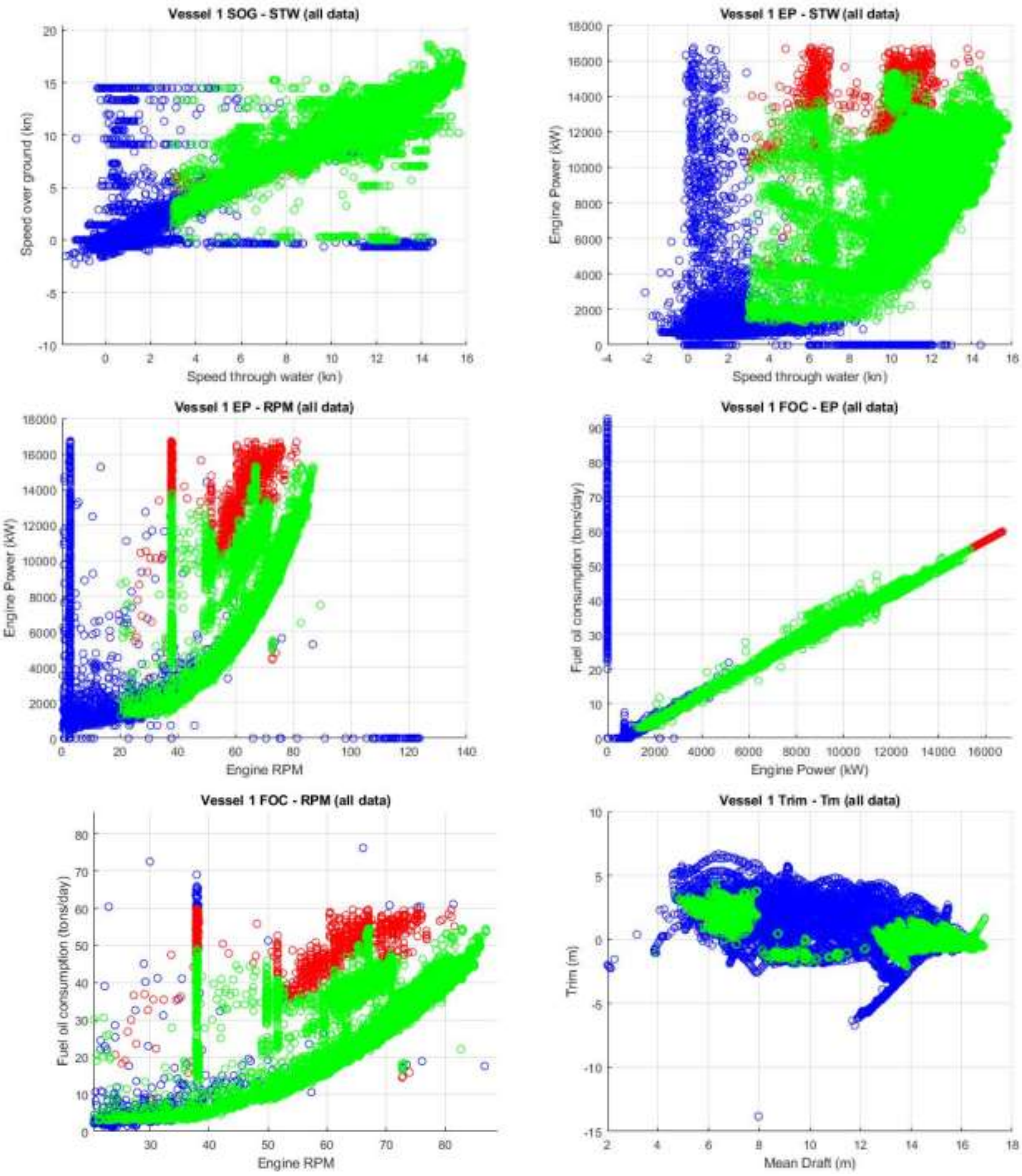

Figure 72: Filter RPM_EP – Vessel 1.

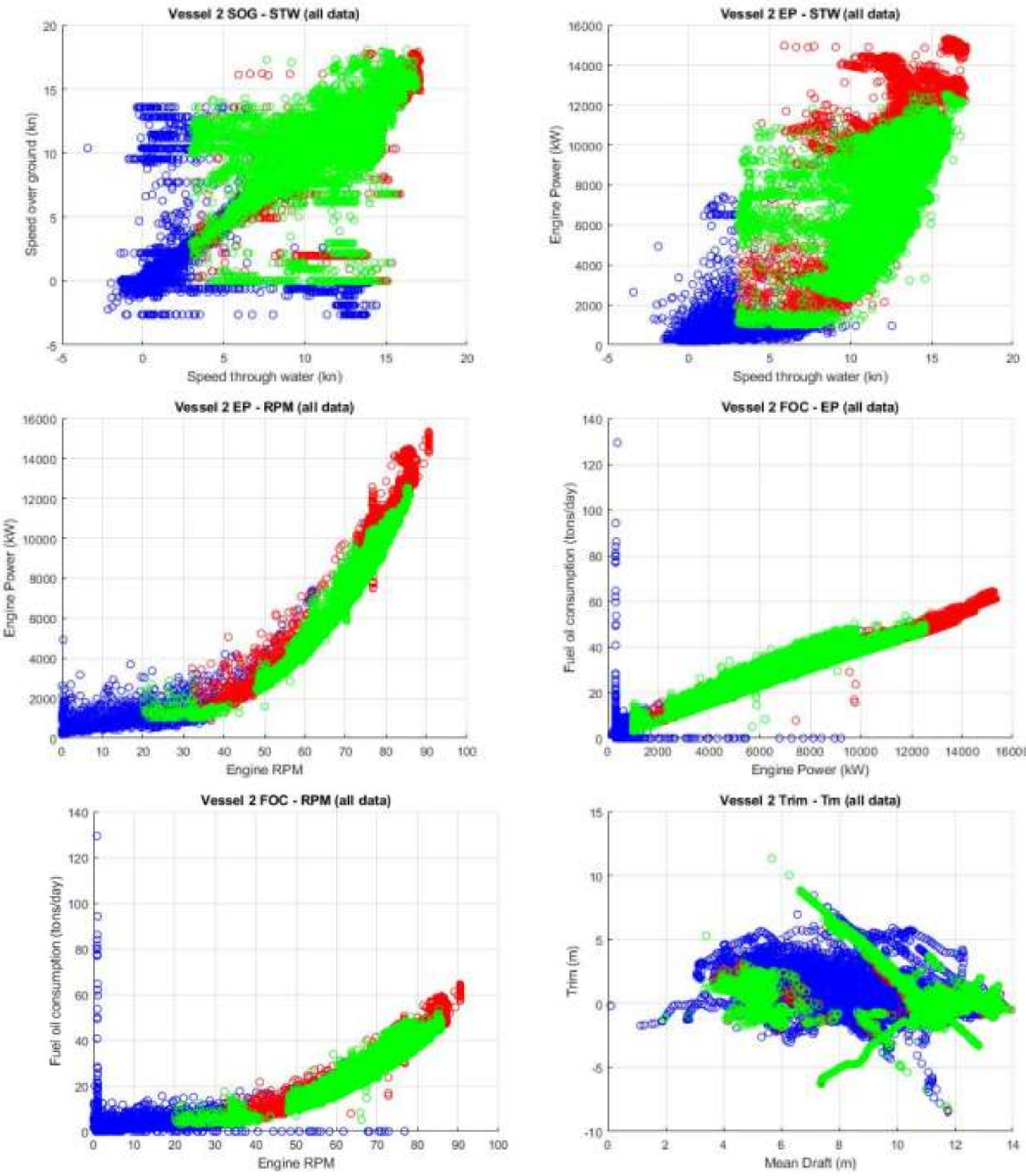

Figure 73: Filter RPM_EP – Vessel 2.

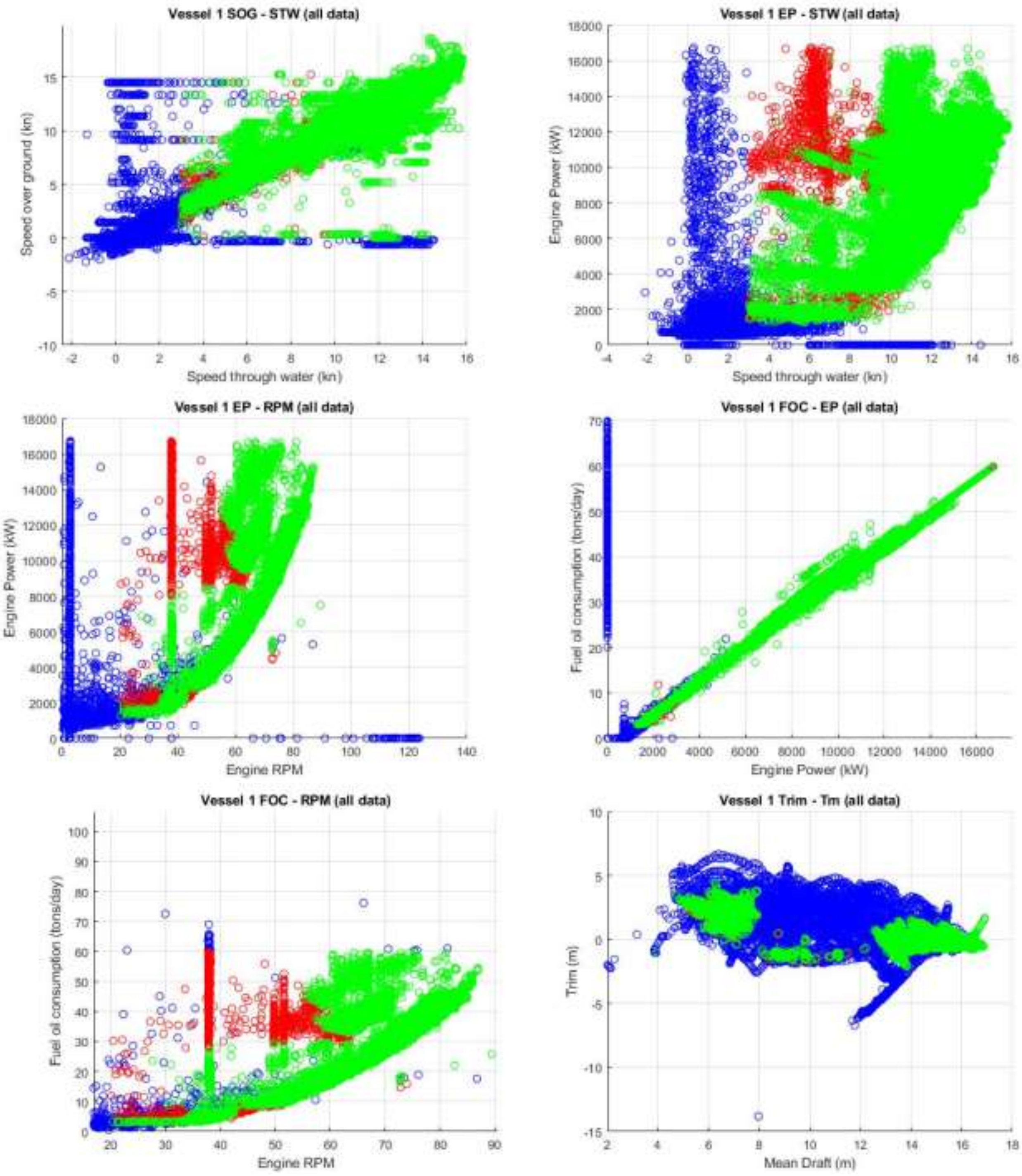

Figure 74: Filter FOC_RPM – Vessel 1.

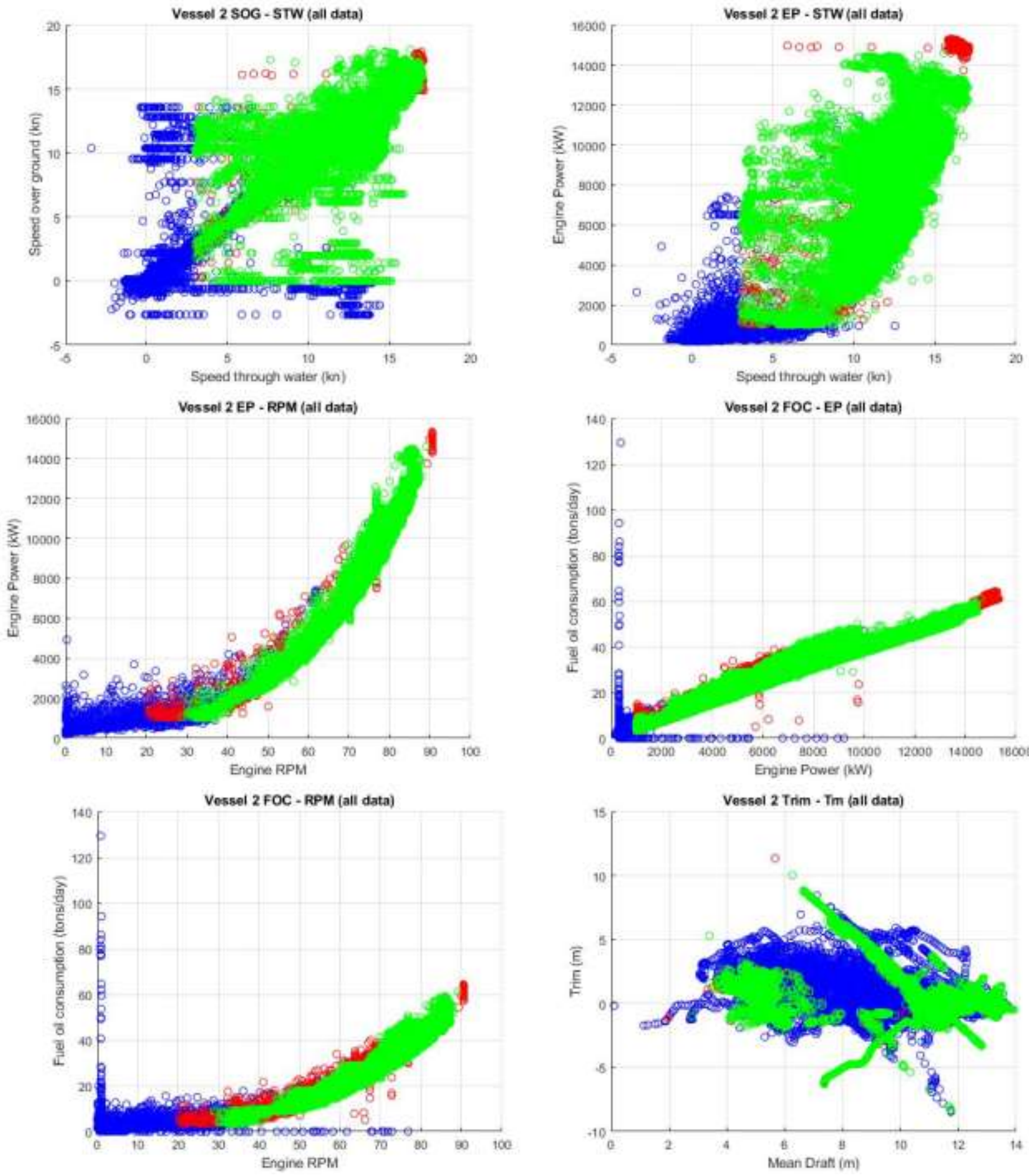

Figure 75: Filter FOC_RPM – Vessel 2.

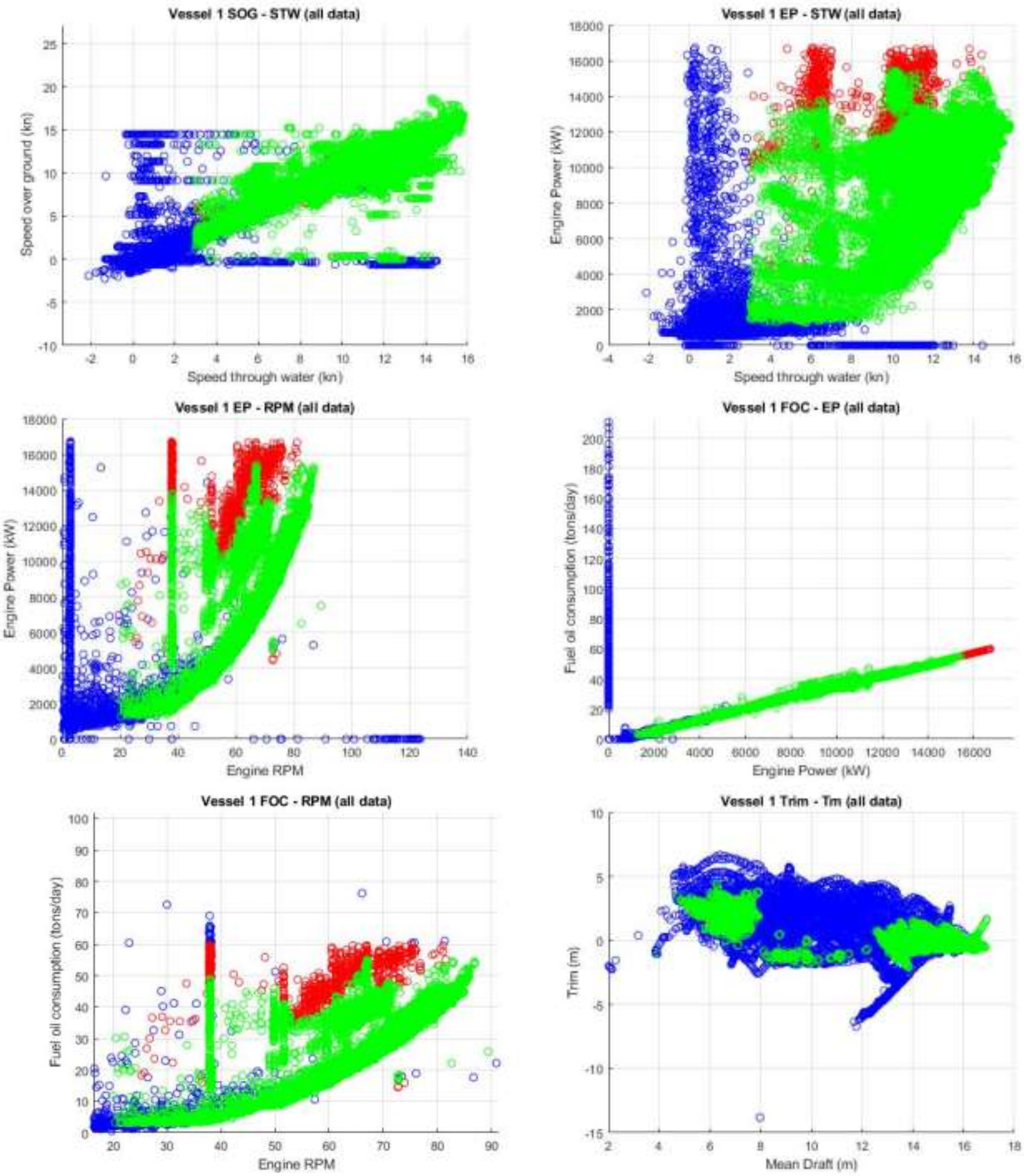

Figure 76: Filter RPM_FOC – Vessel 1.

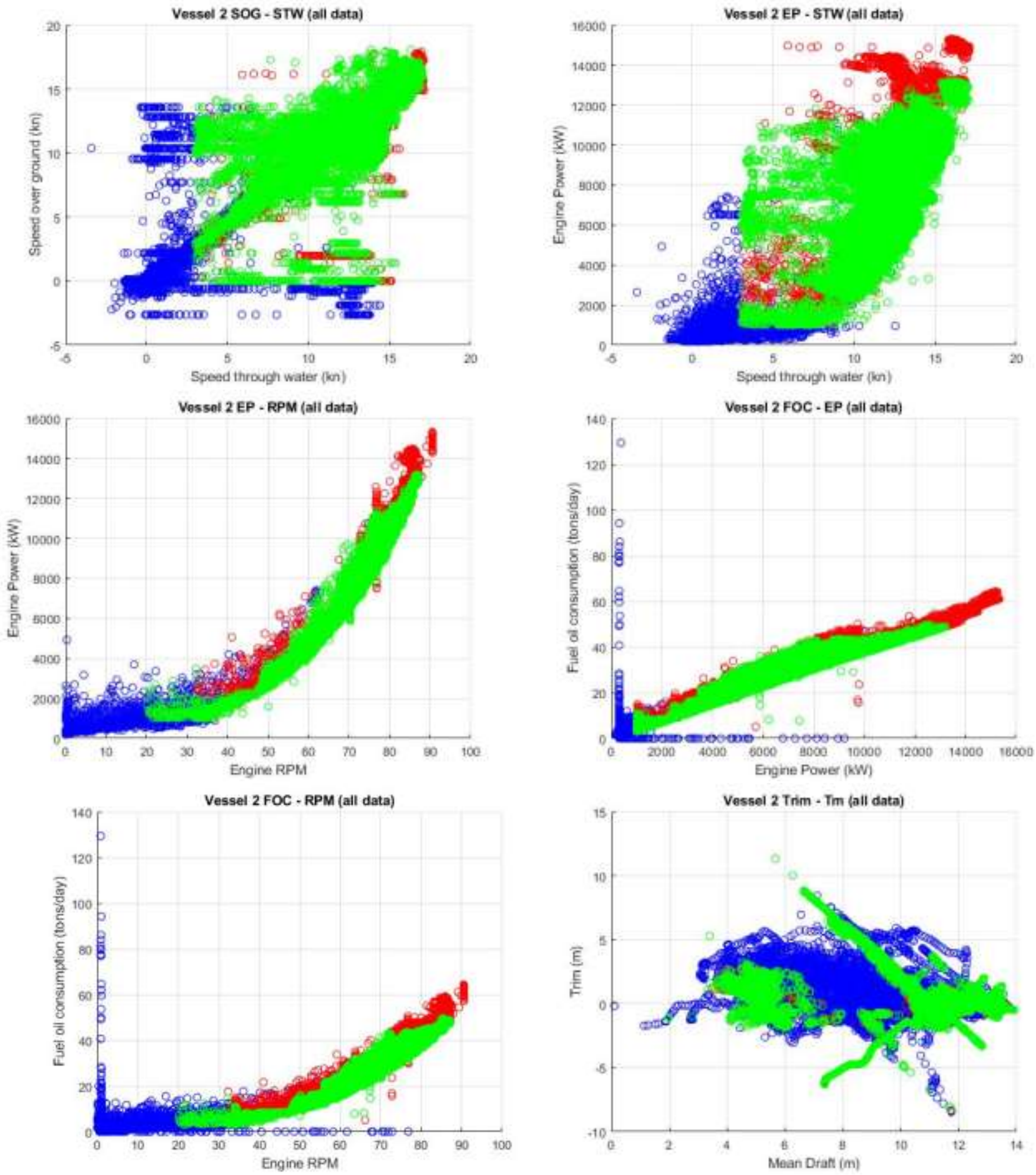

Figure 77: Filter RPM_FOC – Vessel 2.

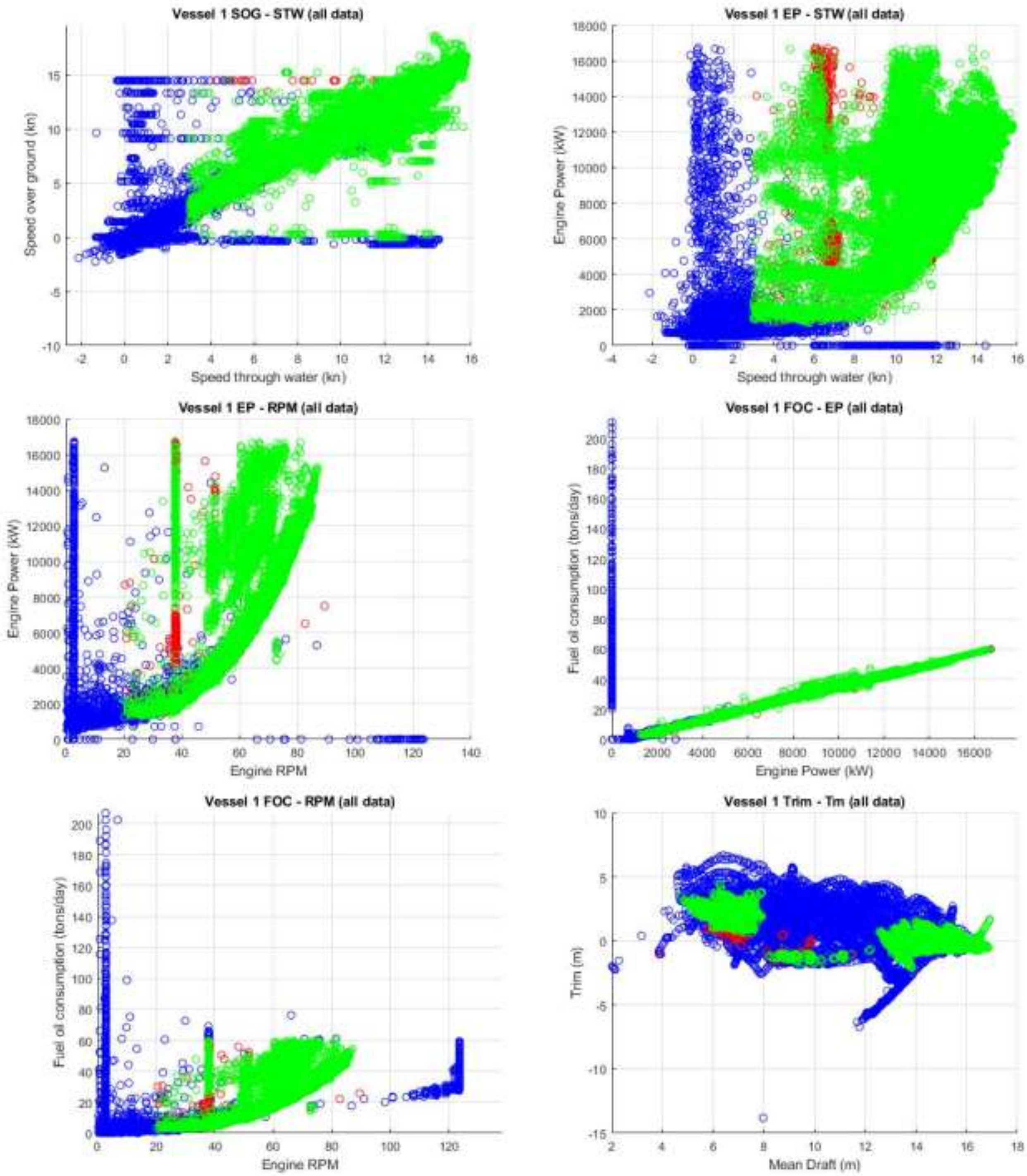

Figure 78: Filter TM_TRIM – Vessel 1.

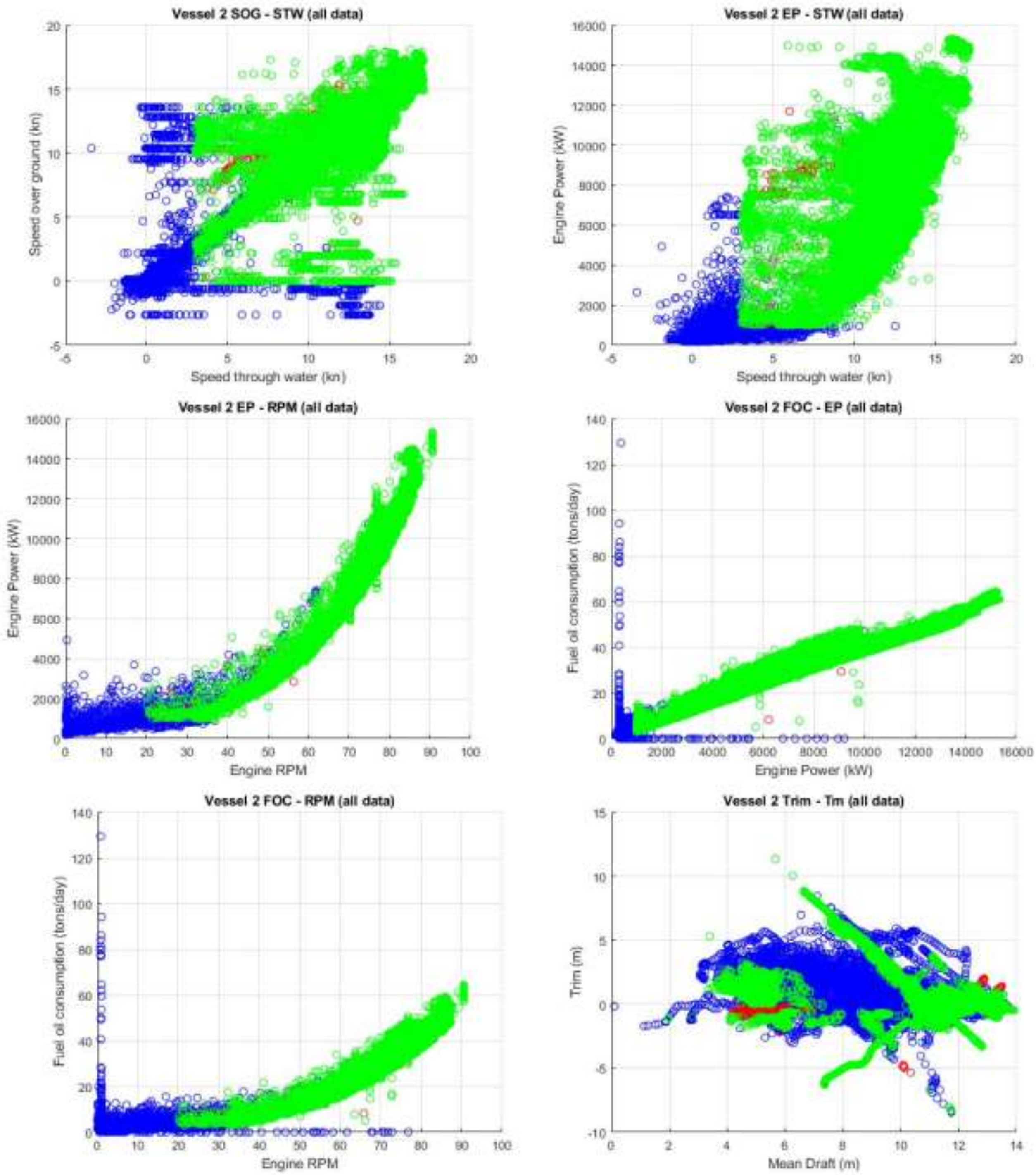

Figure 79: Filter TM_TRIM – Vessel 2.

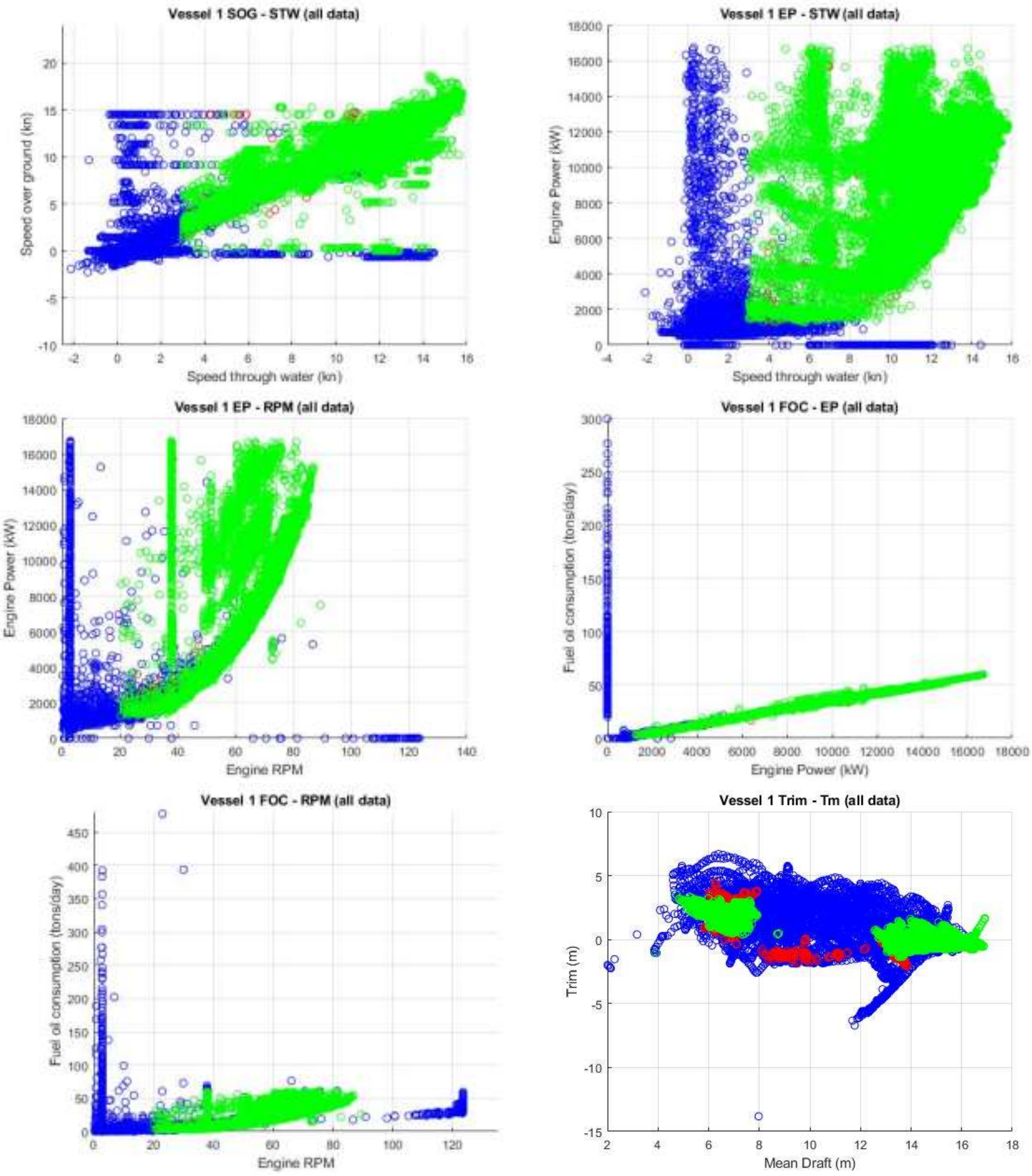

Figure 80: Filter TRIM_TM – Vessel 1.

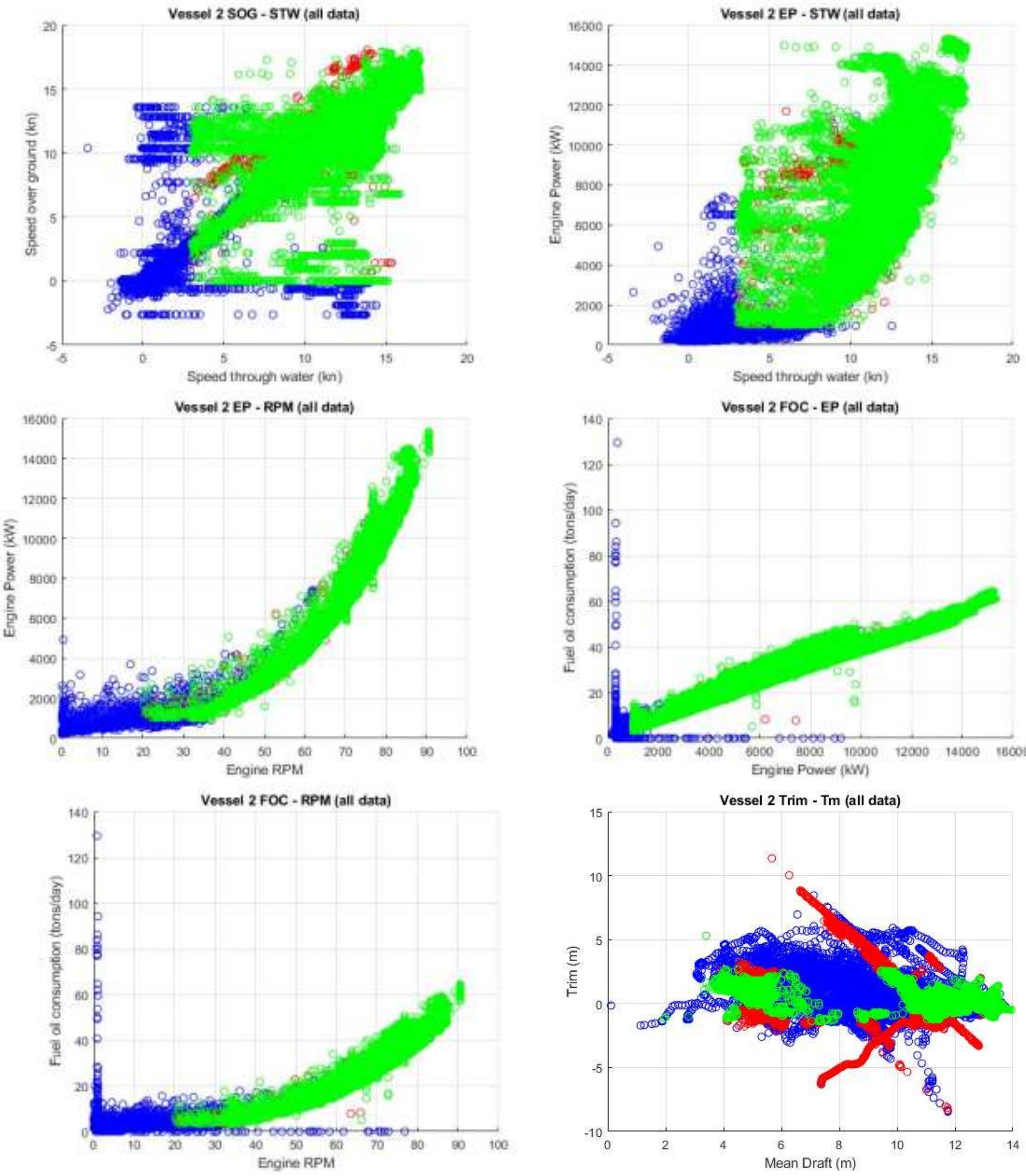

Figure 81: Filter TRIM_TM – Vessel 2.